H₂-IGCC Project Deliverable

Grant Agreement number	239349
Project acronym	H₂-IGCC
Project title	Low Emission Gas Turbine Technology for Hydrogen-rich Syngas
Funding Scheme	FP7-ENERGY-2008-TREN-1
Subproject	**2 Materials**
Work Package	**2.2 Performance of state-of-the-art materials/coatings in novel operating conditions**
Delivery number - name	**D 2.2.6**
Lead Beneficiary	
Dissemination level	**Limited**
Delivery month	**43**
Name, title and organisation of the scientific representative of the project's coordinator	Christer Bjorkqvist Managing Director, European Turbine Network (ETN) Tel: 00 32 2 646 1577 Fax: 00 32 2 646 15 78 E-mail: cb@etn-gasturbine.eu Project website address: www.h2-igcc.eu

Contractor	EU 7th Frame Programme

Subject   Mechanical characterisation of materials.

Contract   239349

Notes   Deliverable D 2.2.6

N. of pages   120   **N. of pages annexed** 0

Issue date   31/05/2013

Prepared   TGM – A. Cammi, S. Capelli, S. Concari

Laborelec – B. Ghys

Verified   TGM - F. Cernuschi

Approved   TGM – Luigi Mazzocchi

Table of contents

REVISIONS HISTORY

Revision number	Date	Protocol	List of modifications and/or modified paragraphs
00	31-5-2013	13002890	First issue

1 Introduction

Main target of H_2-IGCC project is to identify and develop gas turbine technology able to operate on undiluted H_2 rich fuel gas from a CO_2 capture process in an integrated gasification combined cycle plant configuration. In the frame of the whole project the SP2-Materials aim to demonstrate cost-effective materials and coatings technologies to overcome the component life-limiting problems of overheating and of hot corrosion resulting from the higher temperature and from residual contaminants in the syngas.

Overall, the materials challenge in using state-of-the-art gas turbine technology in the next generation of

IGCC plants (with and without CCS) is therefore focussed on solving the component life-limiting problems of overheating (in terms of mechanical performance and the need for improved thermal barrier coatings) in addition to the enhanced corrosion and erosion resulting from the higher temperatures and residual contaminants in the syngas.

Part of SP2-Materials activities are then focused on determining the degradation of existing materials under such operating conditions – covering oxidation, corrosion, erosion, thermal cycling (including interactions with mechanical properties) for combustors and all stages of blades and vanes and on identification of alternative advanced solutions for improved resistance. The overheating of turbine components as a result of the higher volumetric flow and higher water vapour content in combusted syngas has already presented a major challenge for the materials used in existing IGCC plants.

Over the last 20 years, gas turbine inlet temperatures and component operating temperatures have risen

to increase gas turbine efficiency (though the increase in metal temperatures has not been so large due to

sophisticated cooling technologies). As a result base alloys have been developed with progressively higher mechanical load capabilities, but at the cost of reduced corrosion resistance; through lowering the Cr content and by the addition of Al, Ti and refractory metals..

Al and Ti support the formation of γ', while refractory metal additions provide solid solution strengthening to the γ phase; both approaches increase the mechanical stability of the alloy, but result in a reduced protection against corrosion. As a result of these additions, the oxidation behaviour of the base material has changed from a chromia former to an alumina or mixed oxide former.

For increased fuel flexibility and the introduction of syngas derived fuels, the base alloys for the first rows of the high pressure turbine blades need to have high strength (Creep and fatigue resistance) plus high corrosion resistance as desirable properties, but with better protection than that provided by the formation of an alumina, or mixed oxide, scales as on current high strength superalloys, to resist against

corrosion.

It is generally accepted by gas turbine producers that the base alloy will be protected by additional coatings. State-of-the-art corrosion protection coatings for the first two stages of large utility gas turbines are MCrAlY coatings with high amount of Al and TBCs (usually yttria-stabilised zirconia, deposited by air plasma spray (APS) or electron beam physical vapour deposition (EB-PVD)). In the later gas turbine stages, which see lower flue gas temperatures, the blades and vanes just need to be protected against corrosion, and therefore these

components are chromized or protected with a chromium enriched and modified MCrAlY coating.

In this frame the SP2-Materials includes a specific workpackage (WP2.2) dedicated to evaluate the performance of state-of-the-art materials/coatings in novel operating conditions and a specific task (T2.2.5) for determination of mechanical properties.

This report summarises the activities performed for comparing virgin and aged coating/base material properties. The influence of coating/base metal degradation and composition on mechanical properties such as creep (performed at Laborelec) and thermo-mechanical fatigue (TMF) in air (performed at RSE) has been investigated on a selected number of combination substrate-coating systems. As concerns creep characterisation, the limitation usually existing for sampling ex-service material (limited quantity of material and strong limitation on geometry due to small thickness of component) suggested to make creep testing even through the small punch creep technique (SPCT performed at RSE), a technique applicable on actual service exposed components too. The conventional creep and small punch creep characterisation has been done as isothermal curves at maximum temperatures service. The thermomechanical fatigue tests has been conducted for the determination of a fatigue trend at different strain with a thermal cycle contribution representative of service-like condition based on the indication of turbomachinery manufacturer (Siemens).

2   Thermomechanical fatigue

Components exposed simultaneously to thermal and mechanical loads should be designed as safe components, taking care of fatigue damage induced by the variable (more or less regularly) stresses. In order to investigate the behaviours of materials subjected to combined thermal and mechanical loadings, the idealised conditions of a critical material element should be reproduced on a uniaxial laboratory test specimen. The test specimen is subjected, within its uniform section, to cyclic, theoretically uniform, externally imposed temperature and mechanical strain fields, simultaneously varied and controlled. Such a test is designated as strain-controlled "thermo-mechanical fatigue", commonly abbreviated as TMF. The specimen geometry and the set-up of the heating system are optimised with respect to a temperature field T which is as uniform as possible in the gauge section of the specimen at each instant of the cycle. The mechanical strain cycle is then realized by controlling the total strain, ε_{tot}, applied to the specimen in such a way that the thermal strain, ε_{th}, is compensated to achieve a given mechanical strain, $\varepsilon_m = \varepsilon_{tot} - \varepsilon_{th}$. The response of the specimen is measured in terms of the cyclic stress σ. Besides the cyclic material response the most important information to be gathered from a TMF test is the "TMF life" which is assessed in terms of the number of cycles to specimen failure. The decoupling of the temperature and mechanical strain, with an arbitrary phase shift between them, makes the TMF testing extremely versatile. At the same time, this additional degree of freedom generates a multitude of test combinations which should be considered, whilst only a limited number of combinations can be investigated in practice. The two basic shifts which have been investigated most frequently are in-phase cycling (no shift or 0°) where the maximum mechanical strain occurs at the maximum temperature of the cycle, and out-of-phase cycling (shift = 180°) where the mechanical strain maximum coincides with the temperature minimum while compression is applied at maximum temperature.

European Commission has funded a project within the 5th Framework Programme entitled "Thermo-mechanical Fatigue – The route to standardisation" (acronym: TMF-Standard) that produced a "Validated Code of Practice for Strain-Controlled THERMO-MECHANICAL FATIGUE TESTING"; this document has been used as reference document for experimental execution of TMF tests in H_2-IGCC T2.2.5.

Two different base materials, Rene 80 and PWA 1483, both coated with the same Sicoat 2464 have been tested on TMF as described later in details.

2.1 TMF test rig

RSE rig for thermo-mechanical fatigue tests is based on a 250 kN servo hydraulic machine made by MTS, controlled by a "Trio Sistemi e Misure srl" system; an Aetron induction furnace with coil for cylindrical shape allows specimen to be heated, while an electro valve blowing air improves cooling rates at low temperatures. A digital camera system, made by three Canon EOS 1100 D equipped with Canon EF 100 2.8 Macro USM and Sigma EM140 DGNA annular flash lights, enables crack surface monitoring in specimen gauge length from three different point of view, covering the whole sample. A picture of the complete rig is shown in Figure 1, while a still picture sample captured by one of the cameras is shown in Figure 2, where calibration thermocouple wires with 0.6 mm diameter are detectable.
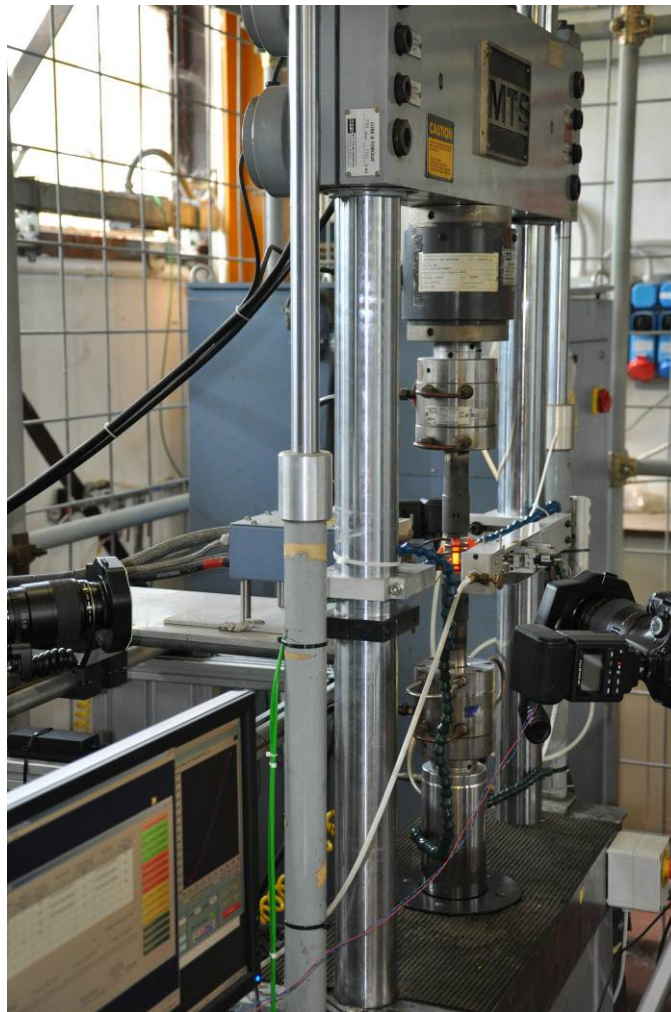

Figure 1 – RSE Thermo-Mechanical Fatigue Machine

Figure 2 –TMF specimen surface with ø 0.6 mm thermocouple wires

TMF tests are performed in agreement with "TMF Standard Code of Practice", published in 2006 by EC project THERMO-MECHANICAL FATIGUE – THE ROUTE TO STANDARDISATION a.k.a. TMF STANDARD, also following ASTM E2368–04 "Standard Practice for Strain Controlled Thermo-Mechanical Fatigue Testing" recommendations.

Test rig is based on hydraulic machine MTS 312.31, electronically and software revamped by "RT3" system provided by "Trio Sistemi e Misure S.r.l.", allowing a simultaneous mechanical (force, strain and displacement feedbacks) and thermal control (induction coil driven by one thermocouple, with a second one reading another specimen point). A strong synergy was adopted with the producer, in order to accomplish test standards and to optimize the testing strategy.

Figure 3 – Thermo-Mechanical test rig

TMF test is performed by simultaneously imposing a strain and thermal cycles, in order to evaluate material damage seen as stress drop from a reference cycle, defined as the one where material response seems to be stable.

Test standards set a preparatory sequence, because temperature is generally controlled in specimen peripheral zone in order to have a precise response in the centre, to avoid thermocouples' welding in the gauge length causing premature crack initiation; moreover during the test a mechanical strain pattern is imposed, so thermal strain has to be preliminarily determined.

First step, called "Thermal Set-up", is performed using a sample connected with two thermocouples, the first one welded in gauge length (central thermocouple, CT), and the other one welded near the junctions between the gauge length and the grips (peripheral thermocouple, PT). Temperature is controlled by CT while only thermal cycle is performed and stress is set to zero: PT can be correlated this way to CT readings during the whole TMF cycle.

Second step, called "Mechanical Set-up", is the real first one applied on each specimen from the batch, by which thermal cycle (set by PT) is correlated to thermal strain measured by extensometer, as even in this case stress is set to zero. Having performed the thermal set-up from one main specimen, mechanical set-up and the subsequent TMF test can be achieved only by welding a PT, whose temperature is strictly correlated to the needed one in the gauge length.

After the second step, TMF testing can be started: a thermal pattern in the gauge length is imposed feed-backing temperature in the peripheral zone, and a mechanical strain is imposed calculating the difference between extensometer readings (total strain) and thermal strain previously recorded in mechanical set-up.

Different kind of cycles can be performed, depending on the phase between thermal and mechanical cycles: "in phase" (0°), "out of phase" (180°), and "diamond" (90°). Just like low cycle fatigue testing, test ends when a crack causes premature specimen collapse, or a significant load drop occurs (e.g. 20 or 25% of stabilised maximum value).

Coated samples can be monitored by an automated photographic system controlling superficial cracks developing during TMF tests. No commercial system was found on market, in fact there was the needing of something monitoring the whole specimen and periodically acquiring photos; a solution by analogic VGA cameras was proposed, but low quality image output pushed to build a self-developed multi-camera system, using three 12 Megapixel Canon EOS 1100D set at 120° to cover every specimen angle, each one with macro lens and annular flash (see Figure 4 and an example of collected picture in Figure 5).
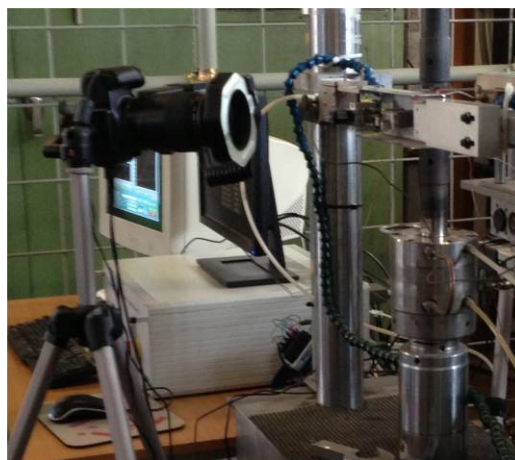

Figure 4 – Acquiring superficial cracks by camera system

Figure 5 – Example of cracks in detail shown by front camera

The management of programmed shooting was made possible thanks to the input of the manual remote control of each camera provided by the manufacturer: finding information on contacts' wirings, a National Instruments relay card (see Figure 6), switched by an internally developed software, allows the automated capture of still images (see Figure 7).
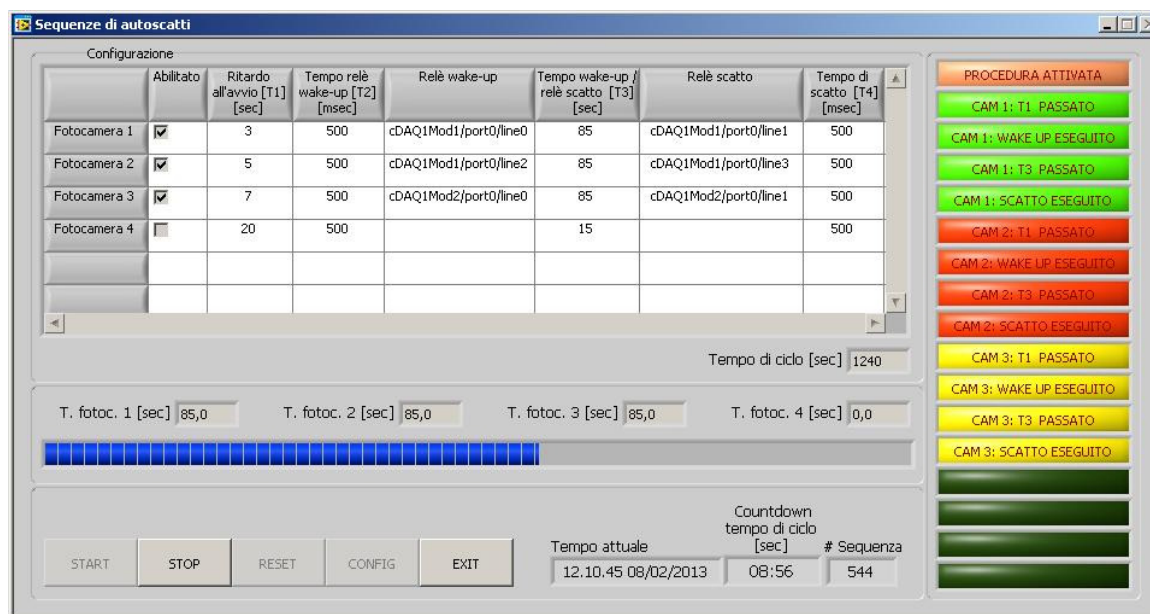

Figure 6 - National Instruments relay card

Figure 7 – Automated photo capture interface

Photos are taken in the "cold" phase of the cycle in order to get the superficial cracks, because specimens are very bright at high temperatures and geometry can't be properly distinguished.

A physical shield to the objectives was initially taken into account to protect the optical reflex system from the long-time exposition to radiation emitted by high temperature samples; any camera producer recommended to adopt such a protection on our concerns, but it was thought an excessive caution was taken in order to avoid warranty issues. Investigating the topic with camera experts, a polarizing filter on the objectives was instead mounted, and after many tests and trials no damage was found on the optics.

Each machine has been equipped with an annular flash balancing brightness in day and night conditions, so that cracks can be better highlighted.

Figure 8 – Annular flash

While the cameras are connected to a dedicated adapter, the annular flashes can only be powered by 4 batteries (4.8 ÷ 6 V); to overcome a reliability problem, an interface getting power from PC's USB ports was designed, getting 5 V voltage with a maximum 1 mA current, which is sufficient to provide power to the flashes. Performing one shot per cycle on the entire surface of the specimen, cracks development can be monitored, and also important information about the specimen surface damage can be acquired, especially for coated samples.

2.2 TMF specimens preparation

TMF tests scheduled at RSE in the frame of H₂IGCC project are related to two different base metals (Rene 80 and PWA 1483) both coated with standard bond coat of Sicoat 2464 for the "state-of–the-art" solutions. For both materials tests have been performed on specimens aged in air at 1000°C for 1000 h or aged at the same conditions with additions of 20% steam.

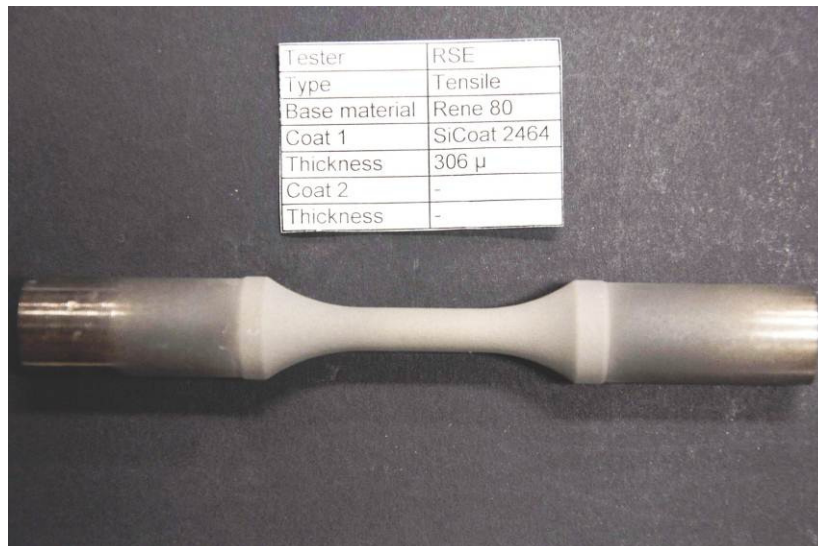An example of specimen after coating deposition is presented in Figure 9.

Figure 9 - TMF specimens after coating deposition

Specimens surface is then polished along the gauge length up to the final roughness R_a <0.2µm (according to standard requirements for fatigue testing), as showed in Figure 10.

Figure 10 - TMF specimen after polishing up to 0.2 Ra in gauge length

The reduction of bond coat thickness during polishing has been estimated by dimensional measurements of gauge length diameter at different positions before and after specimen preparation.

For the 6 specimens of coated Rene 80, the average reduction of coating thickness is 50 ± 4 µm; for the 6 specimens of coated PWA 1483 thickness reduction of coating is 33 ± 3 µm

Aspect of a specimen after ageing in air for 1000 hours at 1000 °C is shown in Figure 11, where the effect of oxidation is more evident in the uncoated grip heads (re-machined before testing) but can be detected in gauge length too.

Figure 11 - TMF specimen after ageing in air

Roughness measurement of oxidised gauge length surface has been performed on some specimens showing a significant variation along different lines around diameter. Averaged results are summarised in Table A and Table B for the two different base metal specimens tested in the project.

Table A - Roughness measurements Rene 80 coated specimens

Specimen Rene 80 + Sicoat 2464	Roughness Ra [µm]	
	Aged in air (1000h @1000°C)	Aged in air (1000 h @1000°C) + air with steam (1000h @1000°C, 20% H2O)
R262-4	0.31	
R262-5	nd	
R262-6	nd	
R262-1	0.39	0.50
R262-2	0.37	0.53
R262-3	0.38	0.64

Table B – Roughness measurements PWA 1483 coated specimens

Specimen PWA1483 + Sicoat 2464	Roughness Ra [µm]	
	Aged in air (1000h @1000°C)	Aged in air with steam (1000h @1000°C, 20% H2O)
R264-1	0,38	
R264-2	0,55	
R264-3	0,40	
R264-4		0,88
R264-5		1,05
R264-6		0,75

After ageing oxidation the specimens are then re-machined in grip heads without any further modification of gauge length surface.

2.3 Thermo mechanical fatigue tests

A set of tests has been performed on uncoated specimens of Rene 80 and PWA 1483 in order to define the optimal cycle duration representing the heaviest conditions of actual component compatible with a whole test duration reasonably performable in the scheduled period of H₂IGCC project activity. Results of base materials preliminary tests can be assumed also as reference data for comparison of results on correspondent coated specimens.

Cycle parameters have been defined basing on Siemens indication derived from large experience in turbine plant design and operational data.

2.3.1 Preliminary tests on uncoated Rene 80

A first test has been performed on uncoated Rene 80 specimen R263-6 (additional specimen to the list above reported initially planned for advanced coating application).

Selected test parameters correspond to an out of phase (OP) test type cycle with higher temperature (and thermal strain) combined to minimum mechanical strain.

Thermal cycle details are:
- Starting and minimum temperature 95°C
- Heating to maximum temperature (950°C) with heating rate 5°C/s (total time about 170 s)
- Holding time at maximum temperature 10 min
- Cooling to minimum temperature at cooling rate -5°C/s (total time about 170 s)
- Holding time at minimum temperature 5 min

The mechanical strain details are
- No mechanical strain at minimum temperature
- - 0.4 % mechanical strain (opposed to heating elongation) at maximum temperature
- Linear slope in cooling and heating phases (matching total time of temperature variation)

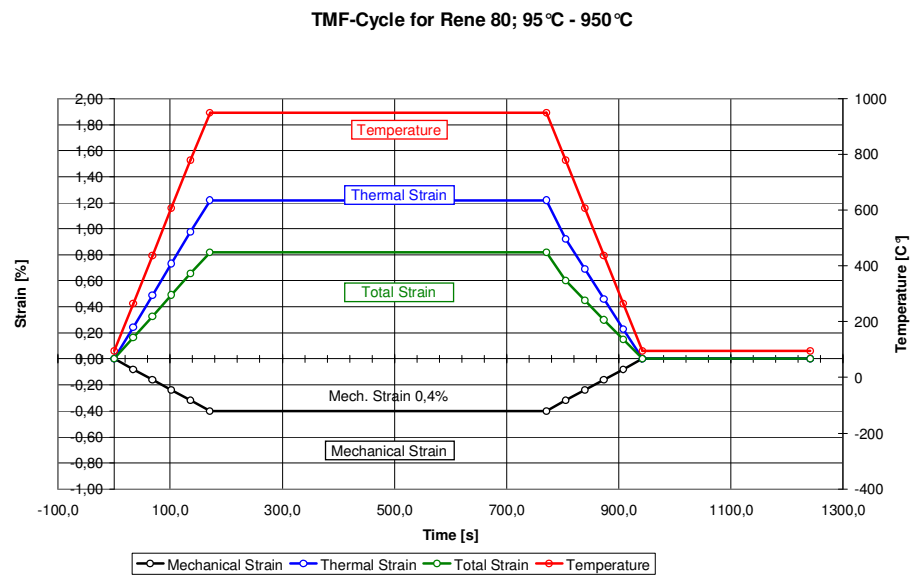The graphical aspect of test parameters is presented in Figure 12.

TMF-Cycle for Rene 80; 95 °C - 950 °C

Figure 12 – Graphical view of test parameters for uncoated Rene 80 specimen R263-6

The total time elapsed in every cycle is 1242 s (about 20 min).
Test has been performed up to 1284 cycles when failure occurred and the end criteria (load drop >25%) has been sudden matched.
The maximum and minimum stress applied at each cycle appear nearly constant after initial stabilisation phase up to the final cycle where a sudden drop occurred as shown in Figure 13.
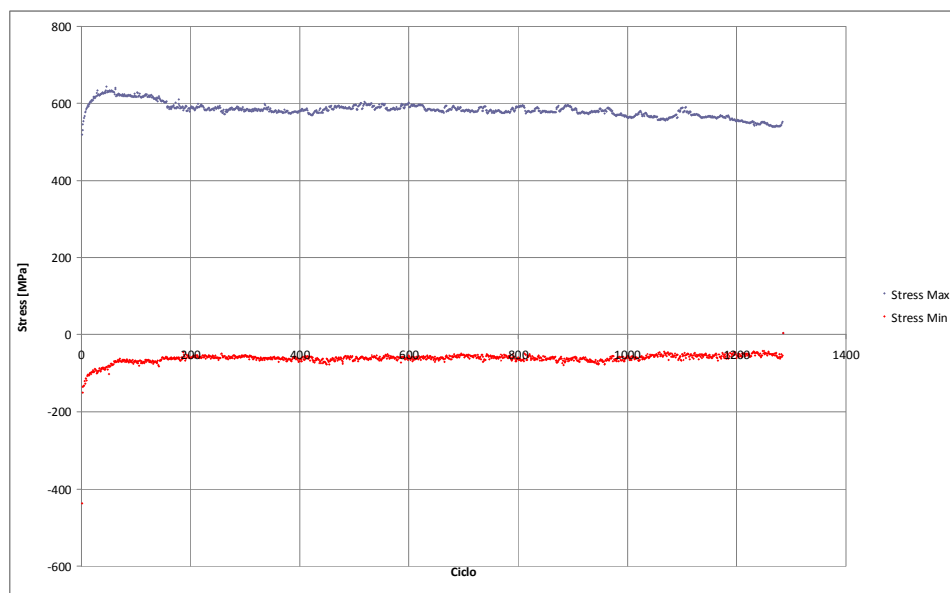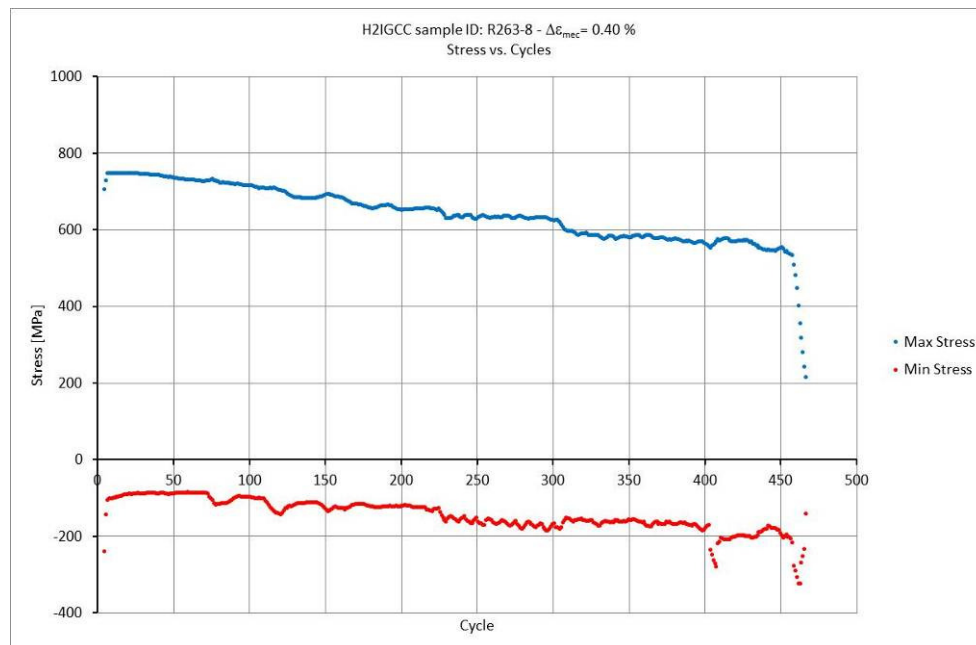

Figure 13 – Minimum and maximum stress at each cycle during R263-6 uncoated Rene 80 test

Figure 14 shows the hysteresis strain cycles during test comparing the initial condition (second cycle) and the half-life cycle. Some minor perturbations can be detected during cooling phases corresponding to intervention of additional air cooling for getting in line with required high cooling rate. Modification of air cooling system and valve opening program has been tested after this test in order to minimise strain cycle perturbations and results have been transferred to successive tests on coated specimens or repeated ones.
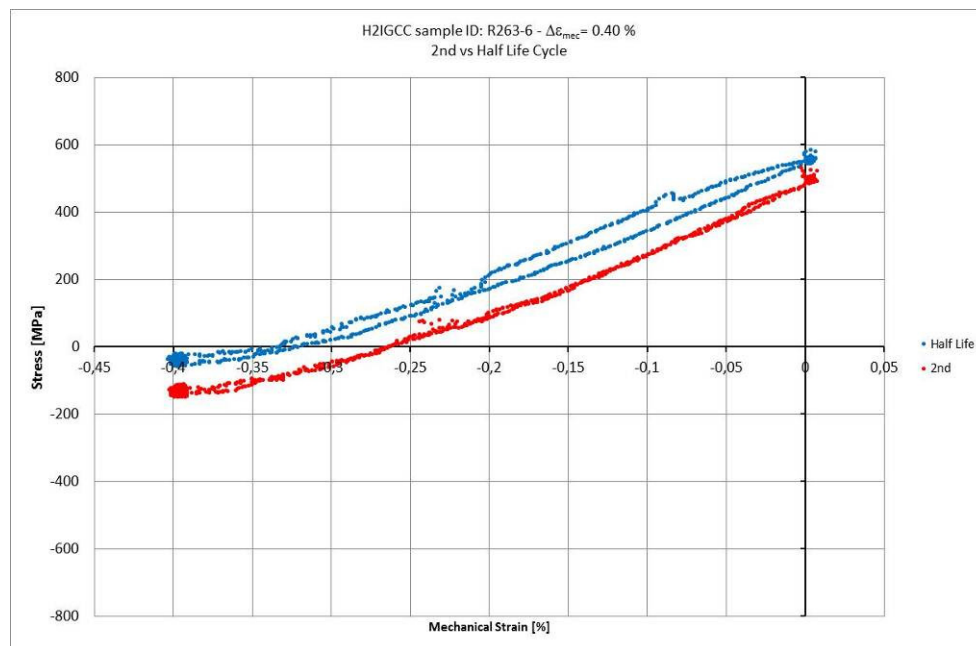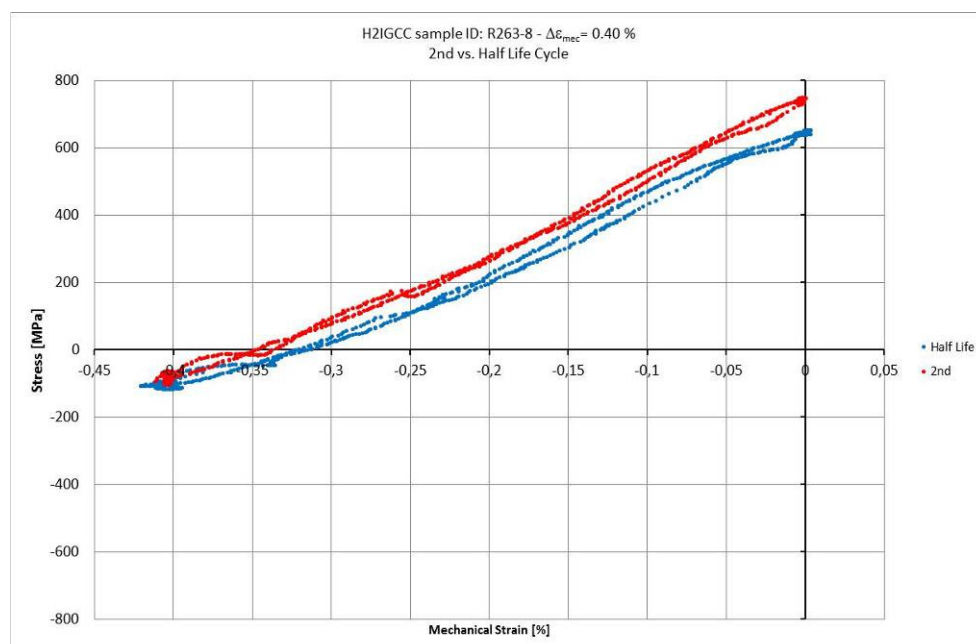
Figure 14 – Strain/stress hysteresis loop at second and half life cycles for R263-6 test

Detection of crack surface in gauge length is hindered by the oxidation of metal surface as shown in Figure 15. The surface oxidation starts to be detectable at 400 cycles and became very relevant after 1000 cycles.
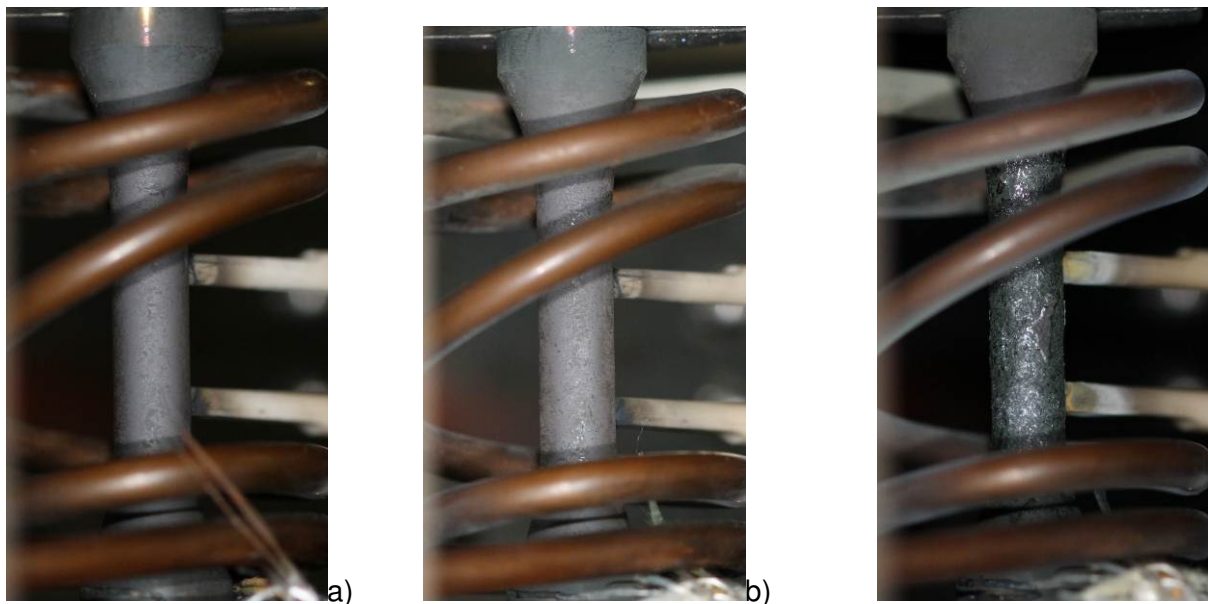
Figure 15 - Aspect of gauge length surface: a) at initial cycle, b) after 400 cycle with initial oxidation, c) close to final cycle with relevant oxidation

This test has been performed on a Rene 80 specimen machined from a plate with only a partial heat treatment applied compared to standard practice in manufacturing of Rene 80 components.

The hardness measured on this Rene 80 material is 328 ± 3 HV$_{30}$.

A second test has been performed on an additional Rene 80 specimen (R263-8 additional specimen not foreseen in the original test matrix), machined from a plate prepared by RSE with a complete standard heat treatment applied (including two final heat treatment steps similarly to

what occurs during coating application). Test has been performed applying the same thermal and mechanical cycle of previous one.

Test ended after 467 cycles when failure occurred, but the end criteria (load drop >25%) had been already matched at cycle 402.

The maximum and minimum stress applied at each cycle after an initial increase show a trend of regular decreasing with sudden drop in the final phase as shown in Figure 16.

Figure 16 – Minimum and maximum stress at each cycle during R263-8 uncoated Rene 80 completely heat treated

Figure 17 shows the hysteresis strain cycles during test comparing the initial condition (second cycle) and the half-life cycle..

Figure 17 – Strain/stress hysteresis loop at second and half life cycles for R263-8 test

Detection of crack surface in gauge length is hindered by the oxidation of metal surface as shown in previous case. The surface oxidation starts to be detectable at 400 cycles and became very relevant after 1000 cycles.

2.3.2 *Tests on coated Rene 80 aged in air*

Three specimens of Rene 80 coated with Sicoat 2464 (R262-4, R262-5 and R262-6) have been polished up to lower than 0.2 μm R_a roughness, then aged in air at 1000°C for 1000 h (see roughness value after ageing in Table A) and then tested in TMF rig.

First test has been performed on specimen R262-6 applying the same test parameter of uncoated Rene 80 specimen (R263-6) previously described:

- Starting and minimum temperature 95°C
- Heating to maximum temperature (950°C) with heating rate 5°C/s
- Holding time at maximum temperature 10 min
- Cooling to minimum temperature at cooling rate -5°C/s
- Holding time at minimum temperature 5 min
- No mechanical strain at minimum temperature
- -0.4 % mechanical strain at maximum temperature
- Linear slope for strain variation (from 0 to - 0.4% and vice versa) in cooling and heating phases

Test went to sudden rupture with load drop exceeding 25% after 665 cycles.

The maximum and minimum (applied at each cycle) stresses during test are graphically presented in Figure 18.
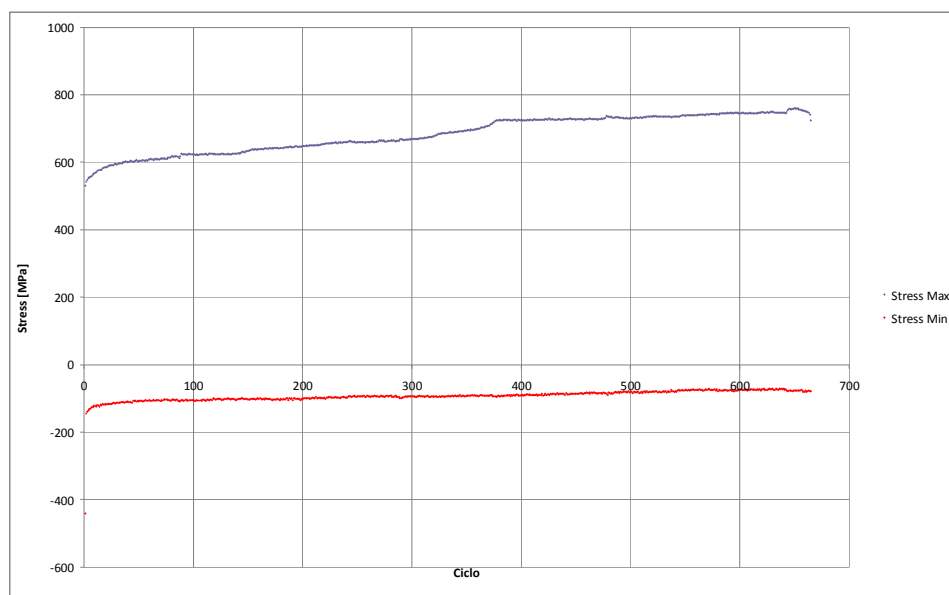
Figure 18 – Minimum and maximum stress at each cycle during R262-6 coated Rene 80 aged in air tested with 0.4 % mechanical strain

Figure 19 shows the hysteresis strain cycles comparing initial phase (second cycle) and half-life cycle.
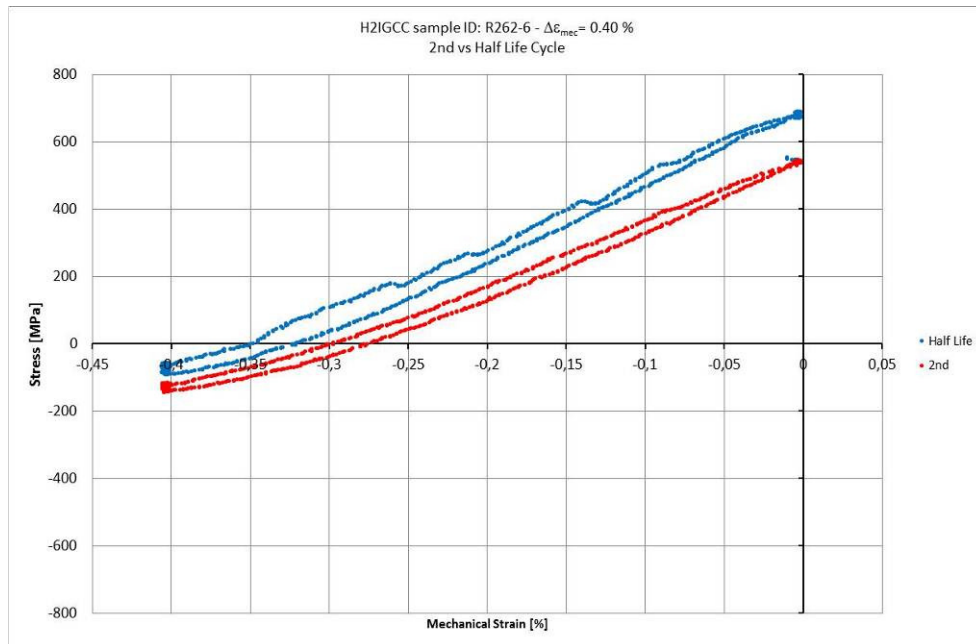
Figure 19 – Strain/stress hysteresis loop at second and half life cycles for R262-6 test (coated Rene 80)

The first surface cracks in gauge length can be detected in between cycle 250 and 290, while the crack leading to failure can be detected after cycle 500. Figure 20 and Figure 21 show a sequence of some significant pictures with crack surface formation and growth during test.
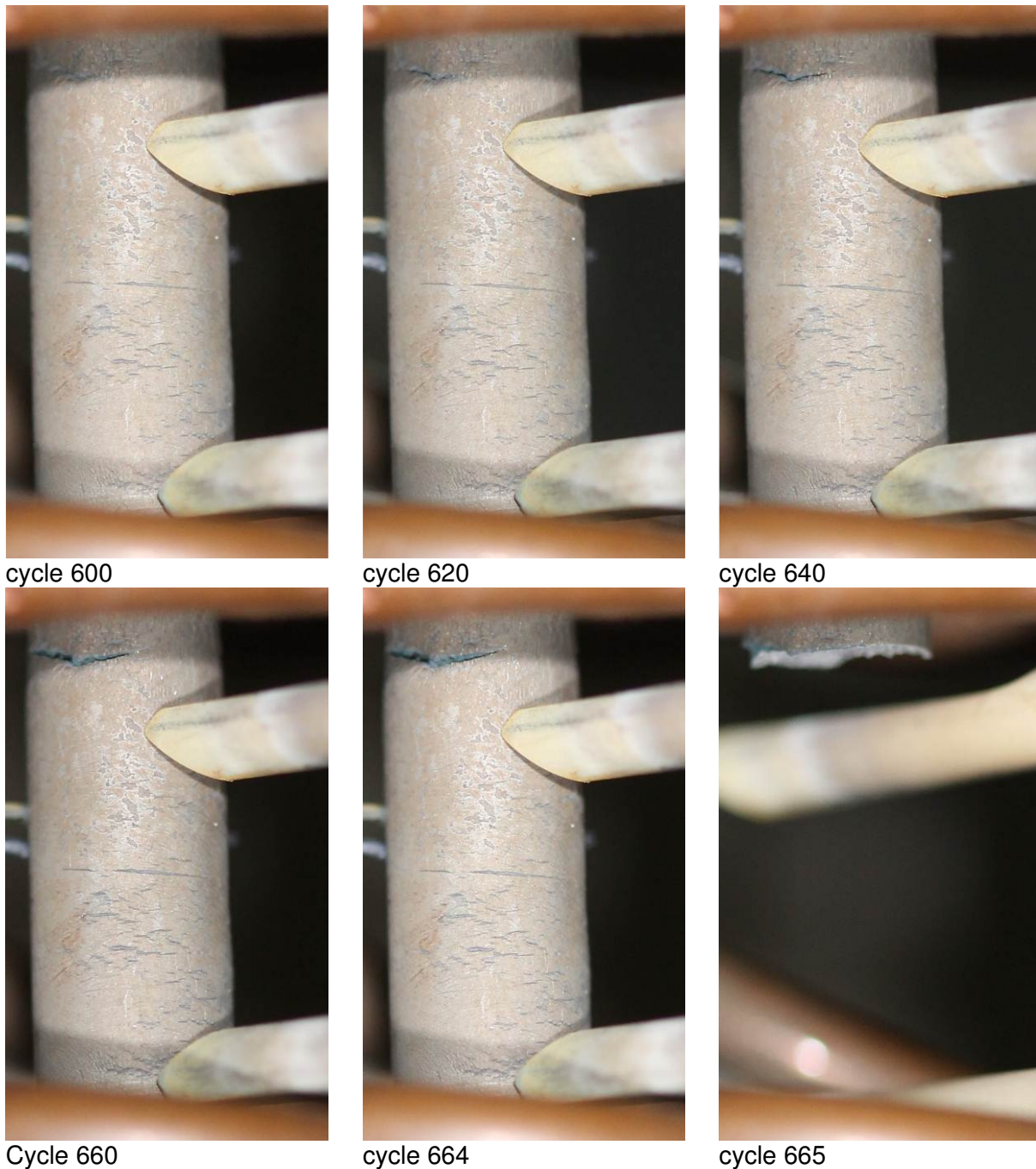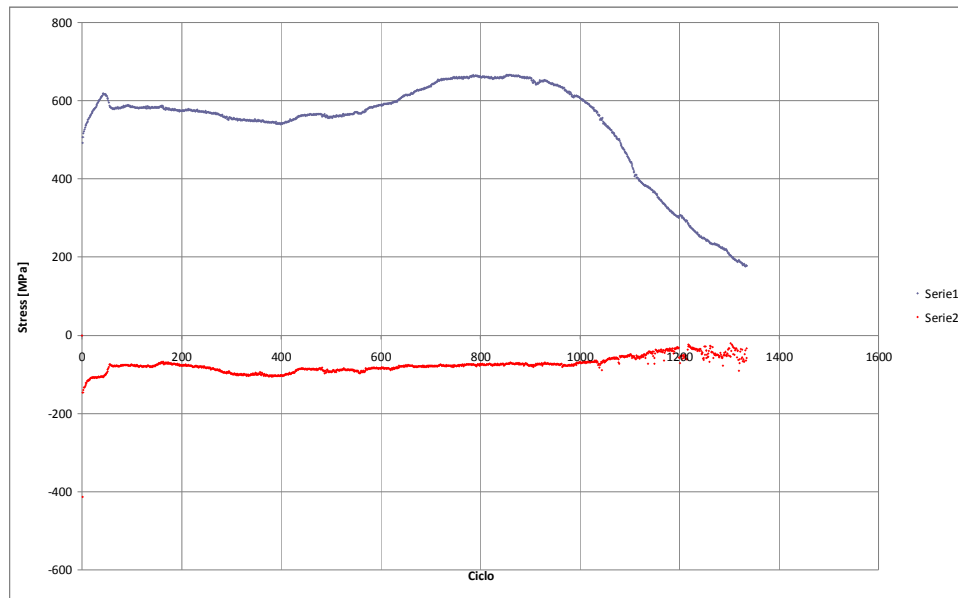
cycle 1

cycle 250

cycle 280

cycle 450

cycle 500

cycle 550
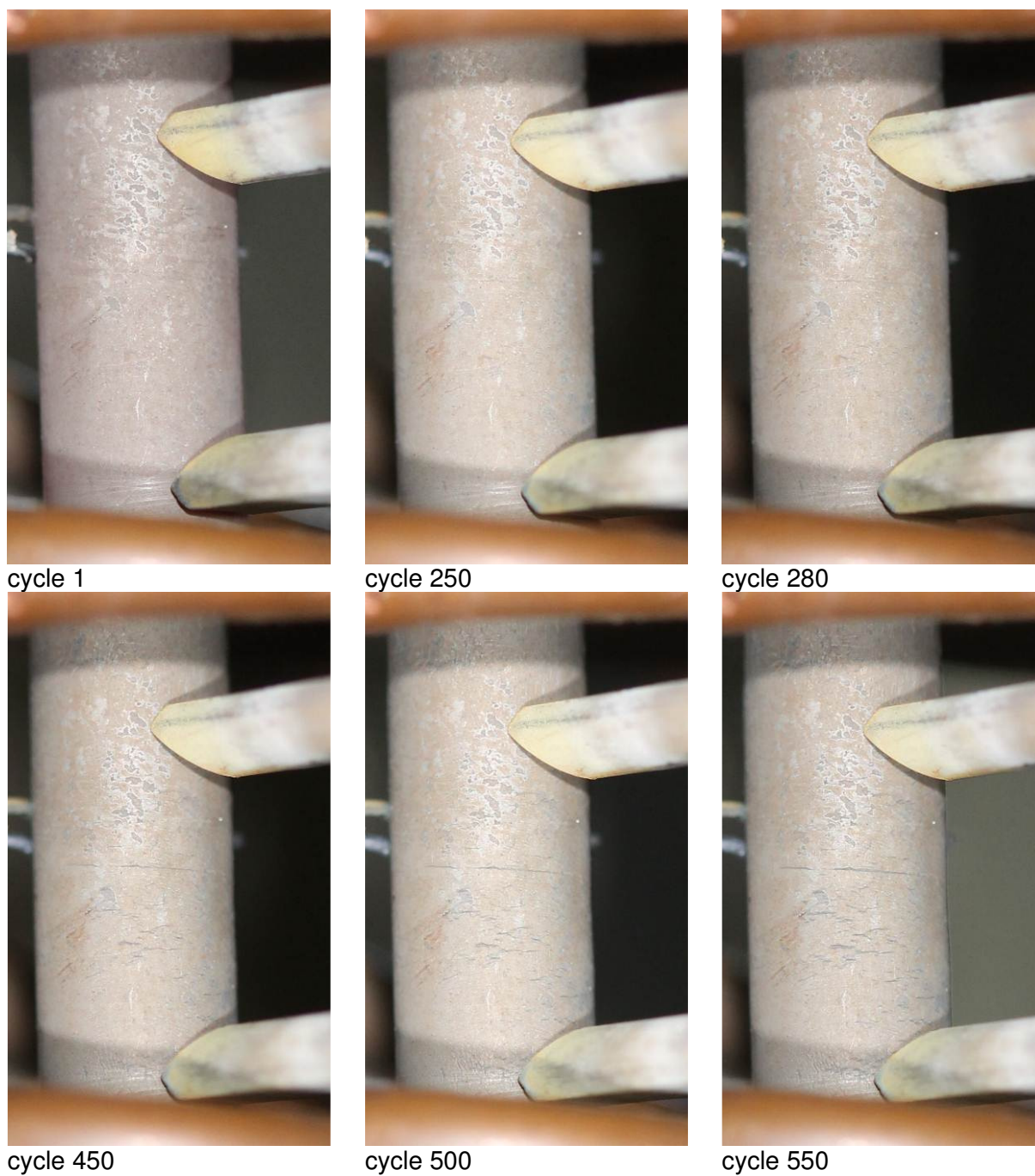
Figure 20 – Pictures taken at different cycles showing the formation and growth of some surface crack in the central part of gauge length for specimen R262-6 (coated Rene 80)

cycle 600

cycle 620

cycle 640

Cycle 660

cycle 664

cycle 665

Figure 21 – Pictures taken at different cycles showing the growth of surface crack leading to final failure in the upper part of gauge length for specimen R262-6 (coated Rene 80)

A second test has been performed on specimen R262-5 (always Rene 80 coated with SiCoat 2464 and aged in air 1000 h at 1000°C) applying the same parameters of R262-6, except a reduced mechanical strain (reduced to - 0.35%). This test showed the formation of several cracks on specimen coated surface with a progressive increase of drop load. Test has been stopped after 1335 cycles matching a boundary limit for security of the machine on drop load. Post-test estimation assuming as end of life criteria (25% drop of maximum stress) showed this condition has been reached after 1079 cycles. First crack on gauge length surface can be detected in the range between cycle 570 and 630. The maximum and minimum (applied at each cycle) stress trend during test is shown in Figure 22.
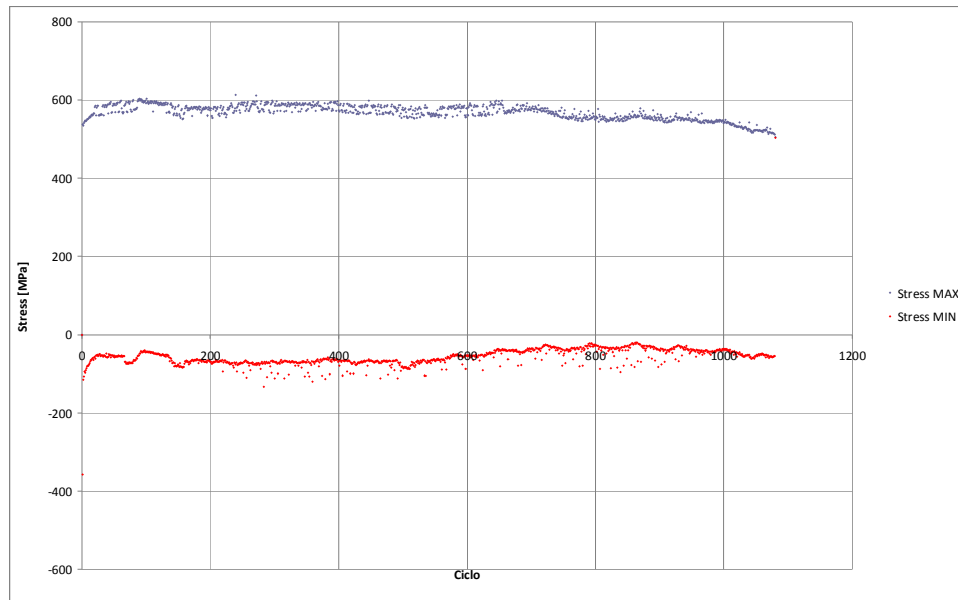
Figure 22 – Minimum and maximum stress at each cycle during R262-5 coated Rene 80 aged in air tested with 0.35 % mechanical strain

The hysteresis strain cycles comparing initial phase (second cycle) and half life cycle is shown in Figure 23.
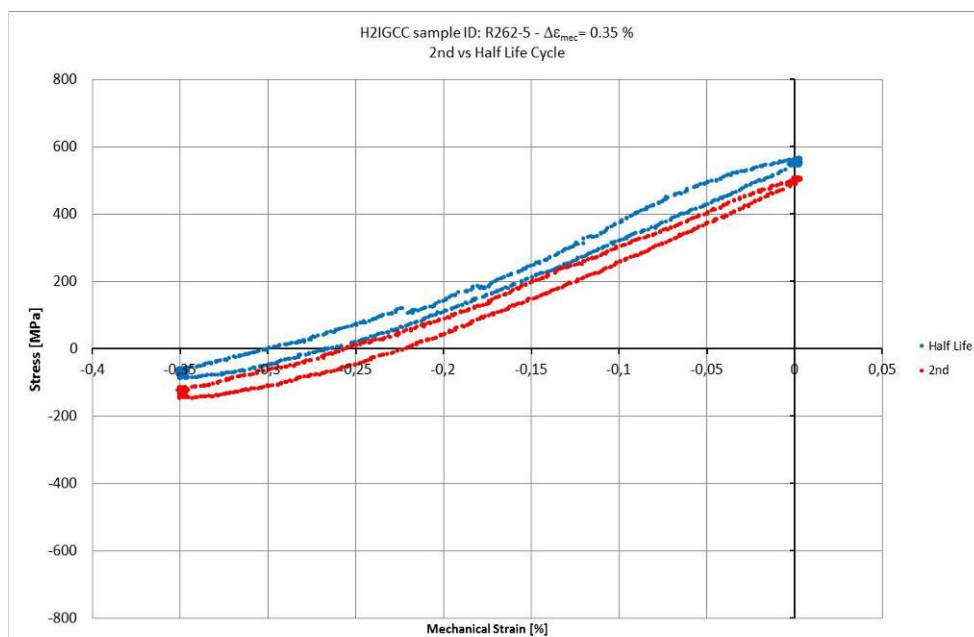
Figure 23 – Stress/strain hysteresis loop at second and half-life cycles for test on specimen R262-5

A third test has been started on specimen R262-4 (always Rene 80 coated with SiCoat 2464 and aged in air for 1000 h at 1000°C) repeating the test on R262-5 with programmed stop after 1079 cycles (the number of cycles where end life criteria was matched in previous test) unless a quicker matching of end criteria on load drop would be obtained. Test has been completed with detection of several cracks in gauge length; the first crack can be detected in the range between cycle 250 and 300. The maximum and minimum (applied at each cycle) stress trend during test is shown in Figure 24. At the end of cycle 1079 (pre-defined stop) the drop load of maximum stress was approximately 18% showing a condition close to usual end criteria (25% drop load) and

allowing to obtain a specimen for metallographic investigation representative of end-life criteria without any additional material degradation.

A sequence of some significant pictures acquired during test at significant steps for crack surface formation and growth is presented in Figure 25.
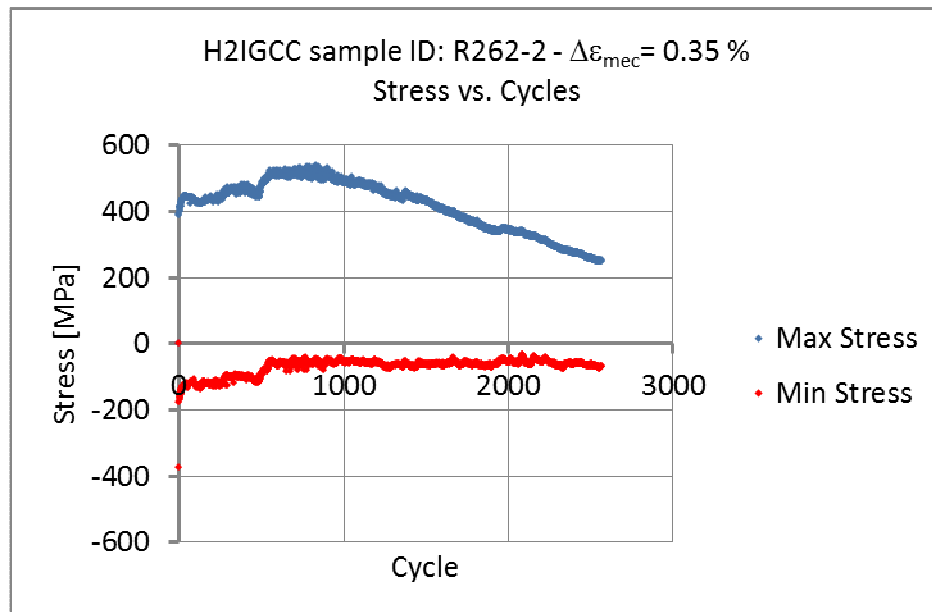

Figure 24 – Minimum and maximum stress at each cycle during R262-4 coated Rene 80 aged in air tested with 0.35 % mechanical strain and stopped at cycle 1079

Cycle 2   cycle 250   cycle 300
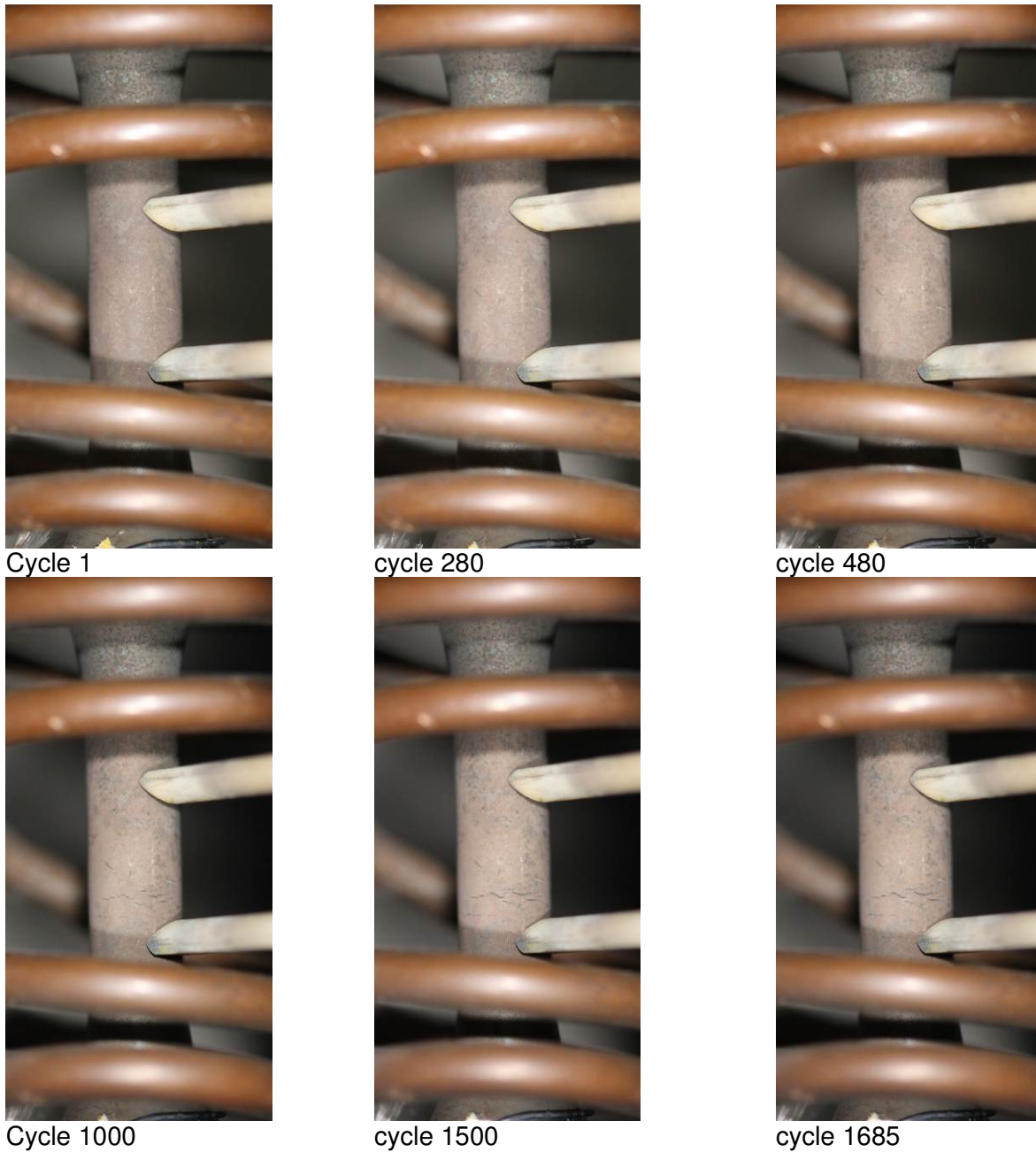
Cycle 600   Cycle 900   cycle 1079
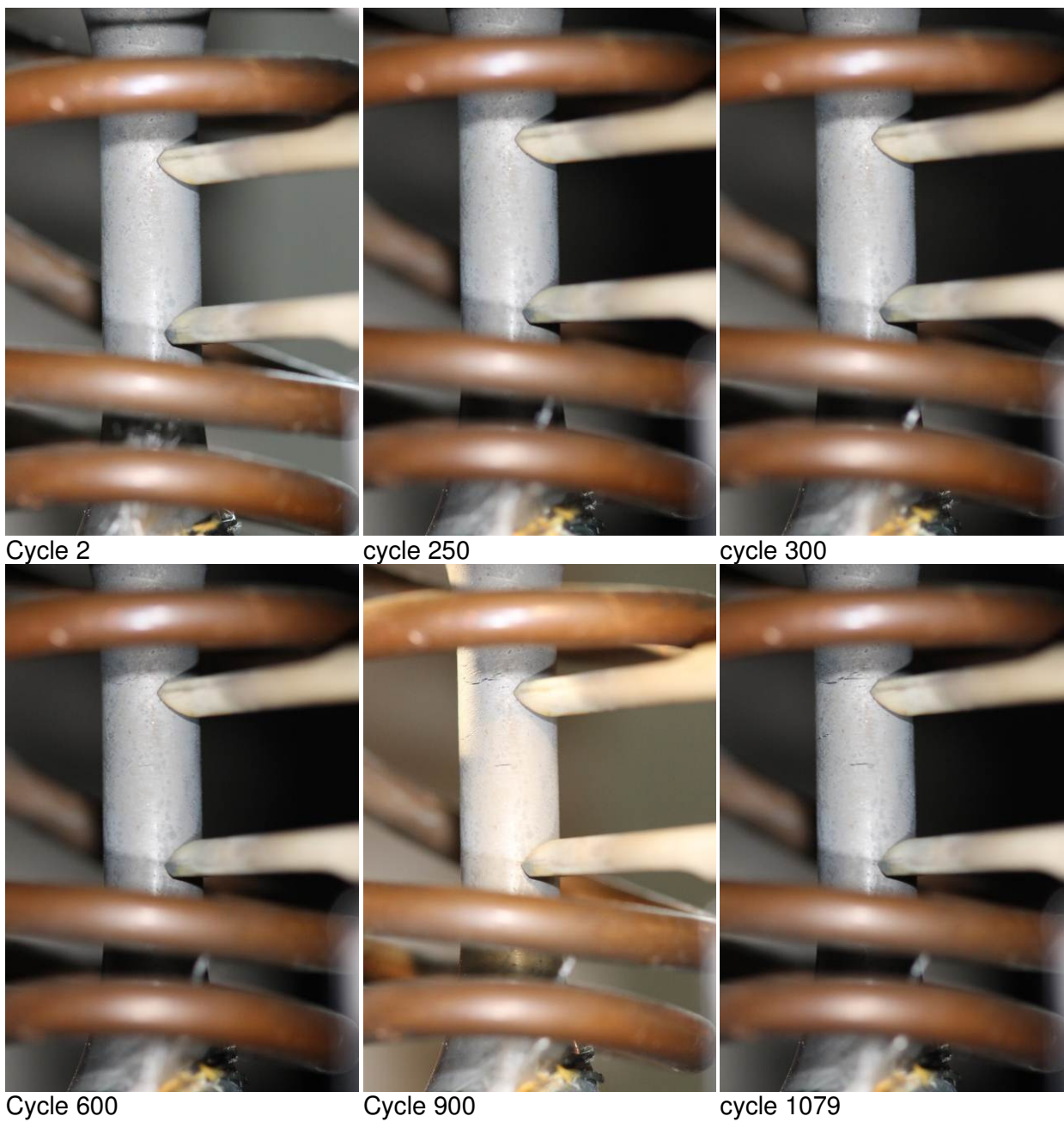
Figure 25 - Pictures taken at different cycles showing the growth of surface crack in gauge length for specimen R262-4 (coated Rene 80)

Results of TMF tests performed on coated Rene 80 aged in air are summarised in Table C.

Table C – Summary of TMF test on coated Rene 80 aged in air

Specimen	Material	Mech strain	First detectable crack	End cycle	Stress Max/min Half life	Note
R262-6	Rene 80 + SiCoat 2464 Aged in air 1000 h at 1000°C	- 0.4% at T max 0% at T min	~250 cycle (first detectable crack) ~500 cycle (initial detection of failure crack)	665 (failure)	686 Mpa -92 MPa	
R262-5		- 0.35% at T max 0% at T min	~600 cycle	Unfailed Stopped at cycle 1335 Drop load 25% at cycle 1079	565 MPa -88 MPa	
R262-4		- 0.35% at T max 0% at T min	~270 cycle	Unfailed Stopped at cycle 1079 (Drop load 18%)	581 MPa -73 MPa	Predefined stop cycle

2.3.3 Tests on coated Rene 80 aged in air+steam

Three specimens of Rene 80 coated with Sicoat 2464 (R262-1, R262-2 and R262-3) have been polished up to lower than 0.2 μm R_a roughness, then firstly aged in air at 1000°C for 1000 h and successively aged in air with 20% humidity at 1000°C for 1000 h (see roughness value after ageing in previous Table A).

Two of the three specimens have then been tested applying the same conditions of R262-6 and R262-5 (coated Rene 80 aged in air), that means the same thermal cycle represented in Figure 12 combined with a mechanical strain - 0.4 % (specimen R262-1) or - 0,35% (specimen R262-2).

The TMF test on specimen R262-2 has been stopped after 2566 cycles, but post-test analysis showed a 25% drop load end criteria matched at cycle 1685. No failure occurred at the specimen; first detectable surface crack appeared at approximately 480 cycles while some surface defects were detectable even before at cycle 250-280.

The maximum and minimum (applied at each cycle) stress trend during test is shown in Figure 26.
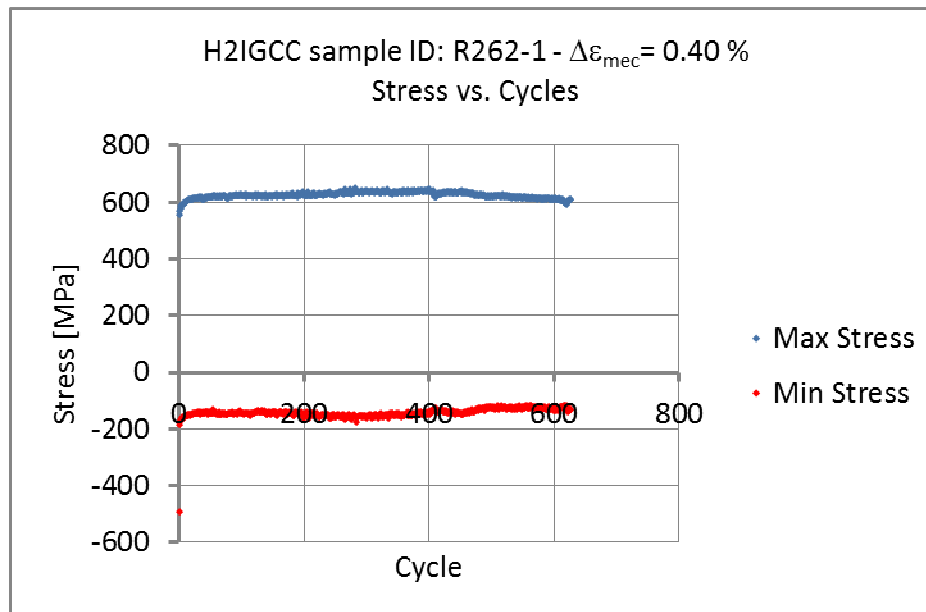
Figure 26 – Minimum and maximum stress at each cycle during R262-2 coated Rene 80 aged in air+steam tested with 0.35 % mechanical strain

The hysteresis strain cycles comparing initial phase (second cycle) and half life cycle is shown in Figure 27
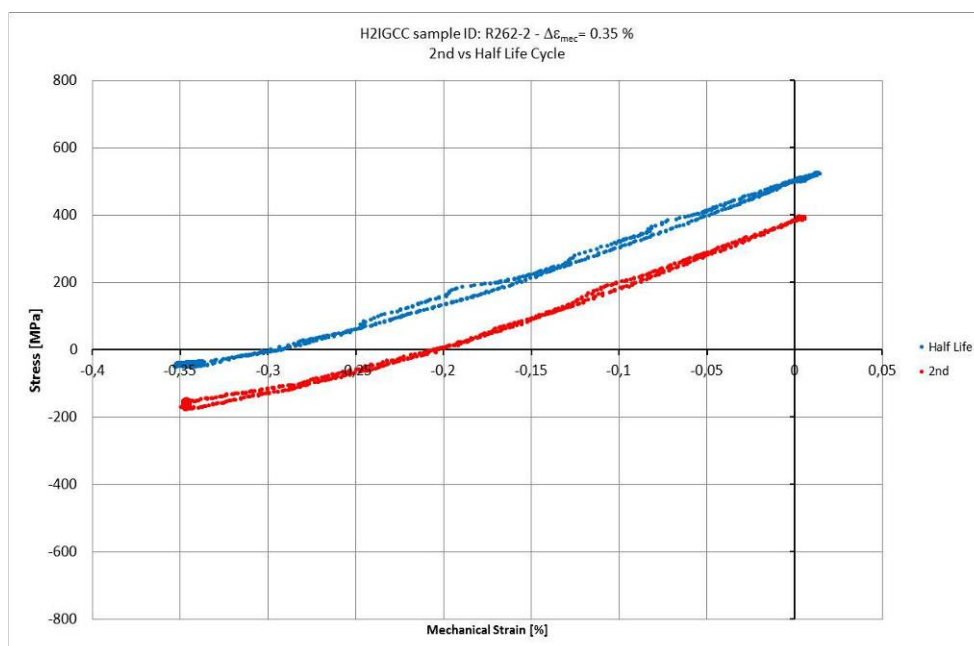
Figure 27 - Stress/strain hysteresis loop at second and half-life cycles for test on specimen R262-2

Pictures representative of surface crack evolution acquired during test are presented in Figure 28 .

Figure 28 - Pictures taken at different cycles showing the growth of surface crack in gauge length for specimen R262-2 (coated Rene 80)

The TMF test on specimen R262-1 ended at cycle 627 with a sudden failure of the specimen. The failure was located in the gauge length of the specimen but in an area where it was not possible to observe crack formation and growth (optically hidden to cameras by heating coils), the first detectable surface crack can be observed on gauge length surface approximately after 350 cycles while some surface defects are present even at cycle 250. Figure 29 shows the trend, during test, of maximum and minimum stress at each TMF cycle.

Figure 29 – Minimum and maximum stress at each cycle during R262-1 coated Rene 80 aged in air+steam tested with 0.40 % mechanical strain

The hysteresis strain cycles comparing initial phase (second cycle) and half life cycle is shown in Figure 30.
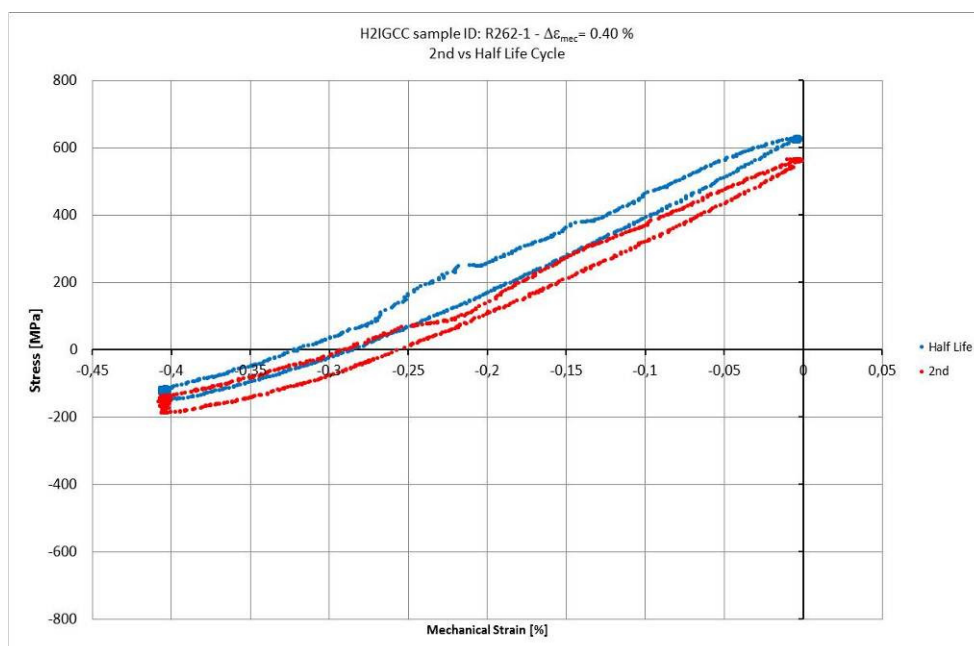
Figure 30 - Stress/strain hysteresis loop at second and half-life cycles for test on specimen R262-1

The images of some surface cracks evolution during test are collected in Figure 31 representing some relevant step of damage evolution.

Cycle 1

cycle 250

cycle 350

Cycle 500

cycle 627

cycle 628

Figure 31 - Pictures taken at different cycles showing the growth of surface crack in gauge length for specimen R262-1 (coated Rene 80)

Table D summarizes the TMF tests matrix for coated Rene 80 aged in air and steam.

Table D – Summary of TMF test on coated Rene 80 aged in air+steam

Specimen	Material	Mech strain	First detectable crack	End cycle	Stress Max/min Half life	Note
R262-2	Rene 80 + SiCoat 2464 Aged in air 1000 h at 1000°C +	- 0.35% at T max 0% at T min	~480 cycle (some surface defects detectable at	Unfailed Stopped at cycle 2566 Drop load 25% at	523 MPa -52 MPa	

	aged in air with 20% humidity 1000 h at 1000 °C		cycle 250-280)	cycle 1685		
R262-1		- 0.4% at T max 0% at T min	~350 cycle (some surface defects detectable at cycle 250)	627 (failure)	630 MPa -150 MPa	
R262-3				Not tested		Used for metallography

2.3.4 *Preliminary tests on uncoated PWA 1483*

A first test has been performed on uncoated PWA 1483 specimen R265-6 with selected test parameters corresponding to an out of phase (OP) test type cycle with higher temperature (and thermal strain) combined to minimum mechanical strain.

Thermal cycle details are:

- Starting and minimum temperature 95 °C
- Heating to maximum temperature (950 °C) in 1000 s (heating rate about 0.85 °C/s)
- Holding time at maximum temperature 10 min
- Cooling to minimum temperature in 1100 s (cooling rate about - 0.78 °C/s)
- Holding time at minimum temperature 5 min

The mechanical strain details are

- No mechanical strain at minimum temperature
- -0.6 % mechanical strain at maximum temperature
- Linear slope in cooling and heating phases

The graphical aspect of test parameters is presented in Figure 32.
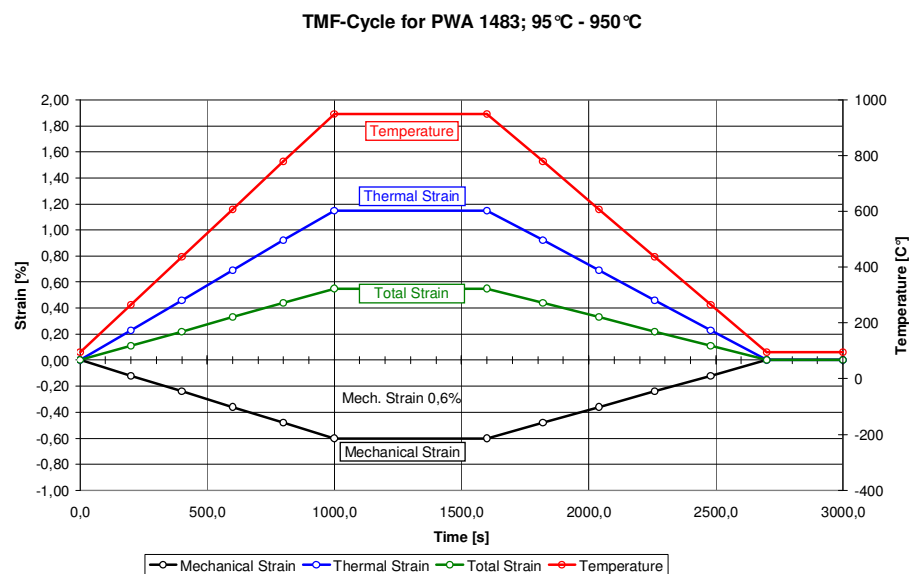
Figure 32 – Graphical view of test parameters for uncoated PWA 1483 specimen R265-6

The total time elapsed in every cycle is 3000 s (50 min).

Test has been performed up to more than 900 cycles with regular trend of minimum and maximum load (at each cycle) increasing and approximately constant stress range (max load – min load) as shown in Figure 33.

PWA 1483 TMF 0.6% mech strain
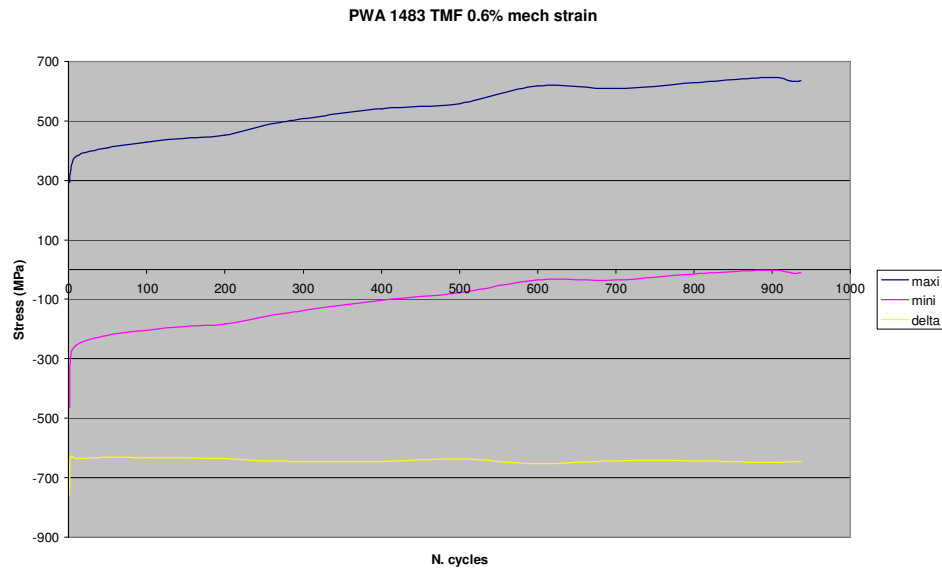
Figure 33 - Trend of max and minimum load applied at each cycle n R265-6 TMF test

Figure 34 shows the hysteresis strain shifting toward higher loads during test for some reference cycle during test.

TMF on PWA 1483 uncoated
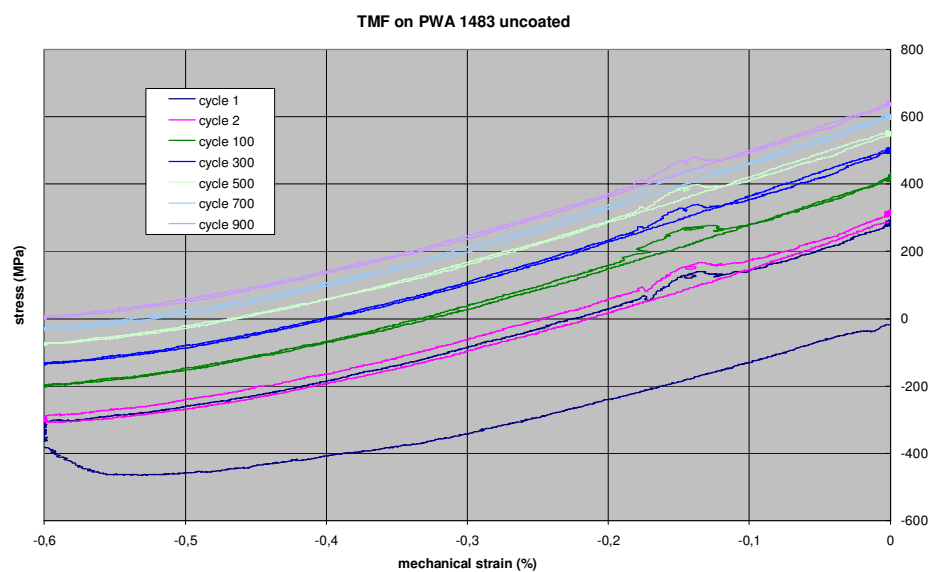
Figure 34 – Trend of shifting for hysteresis strain during the first 900 cycles of R265-6 test

At cycle 938 an unexpected failure of thermocouple (spot welded to the specimen) caused an irregularity on applied strain forcing to test interruption. Strain data at cycle 938 is presented in Figure 35.
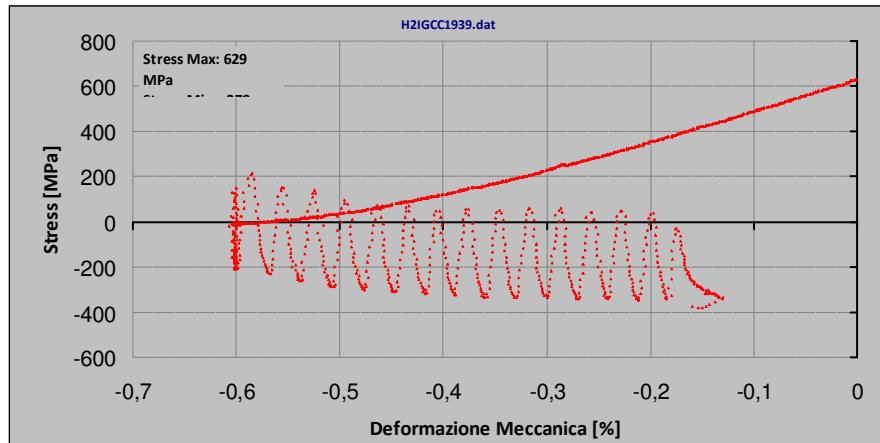
Figure 35 - Irregular strain cycle 938 due to thermocouple failure and forcing to test interruption

Some trials of test restart according to TMF-Standard Code of practice recommendations have been performed unsuccessfully.
No evidence of surface crack was detected during test.

An additional specimen (R265-9) of uncoated PWA 1483 has been machined and the test has been performed with the cycle used for Rene 80 (see Figure 12) but the same problem of thermocouple weld failure occurred after 945 cycles leading to invalid test.

2.3.5 *Tests on coated PWA 1483 aged in air*

Applying the same test conditions used for coated Rene 80 (graphically described in Figure 12), a first test has been performed on a specimen of coated PWA 1483 (R264-1) aged 1000 h in air at 1000°C. The test has been performed with a - 0.4% mechanical strain. The test has been stopped after 2160 cycle without failure. Post-test examination showed that end criteria (25% drop load from maximum value) can be observed at cycle 1458. Trend of minimum and maximum stress at each cycle is presented in Figure 36.
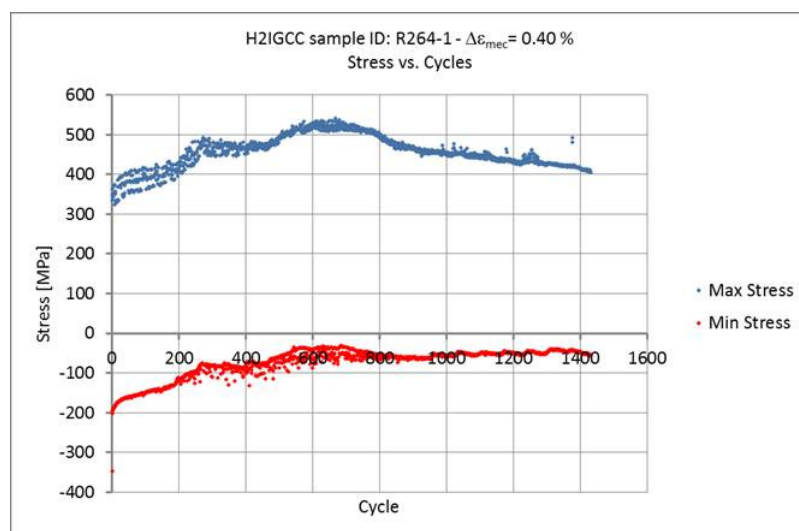
Figure 36 - Trend of max and minimum load applied at each cycle n R264-1 TMF test

The hysteresis strain cycles comparing initial phase (second cycle) and half life cycle is shown in Figure 37.
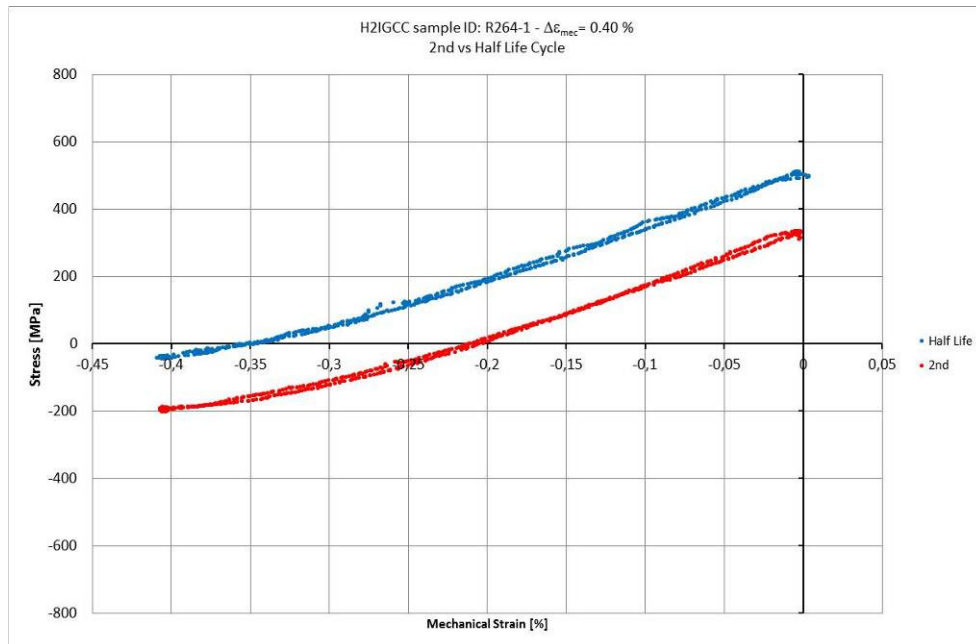
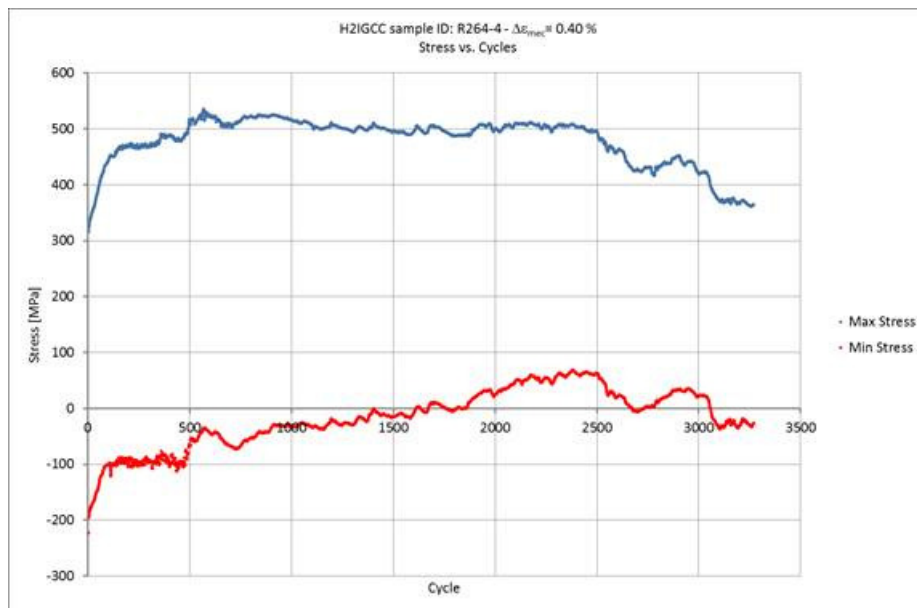**Figure 37 - Stress/strain hysteresis loop at second and half-life cycles for test on specimen R264-1**

The images of crack surface evolution during test are collected in Figure 38 representing some relevant step of damage evolution. First crack growing on gauge length surface can be detected after approximately 350 cycle; this crack can be considered as the evolution of a pre-test defect maybe related to machining and oxidation phases.
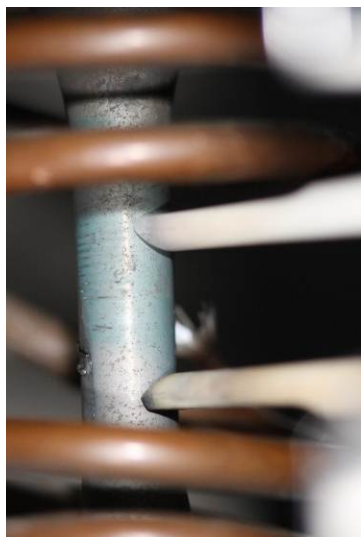
Cycle 2

cycle 200
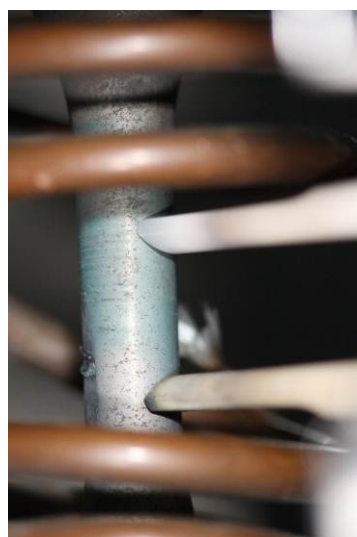
cycle 350

Cycle 400
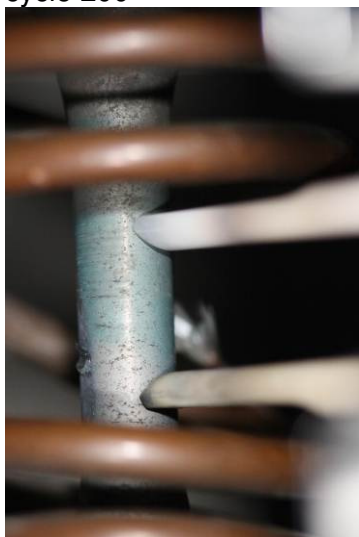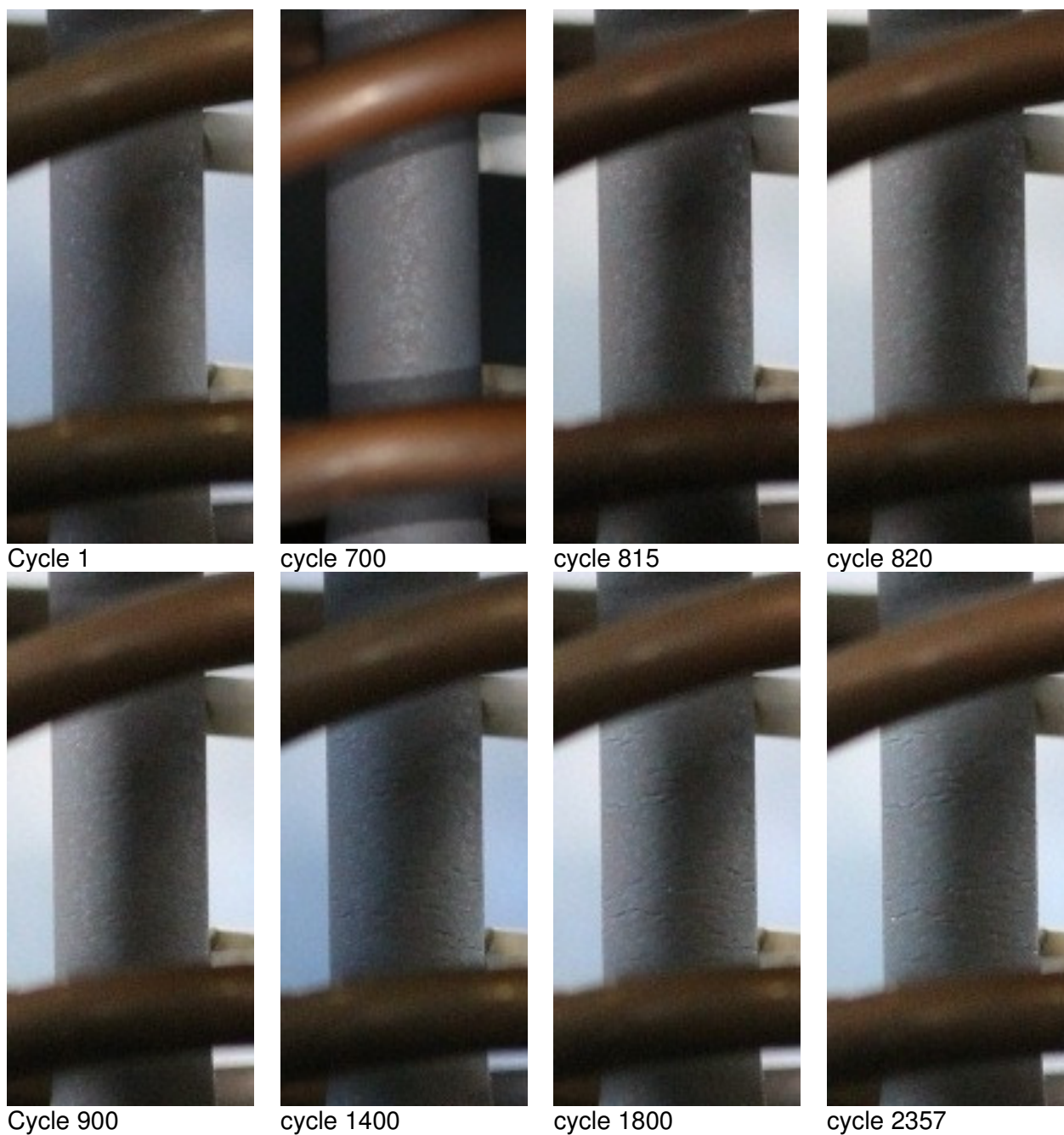
cycle 800

cycle 1100
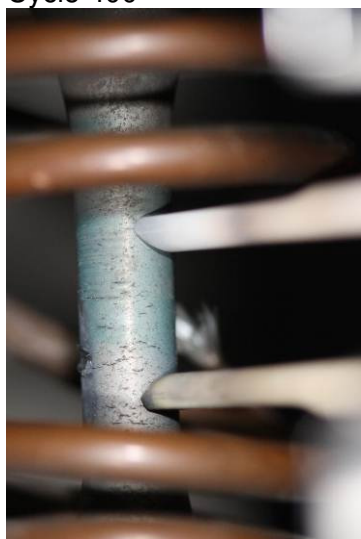
Cycle 1200

cycle 1300
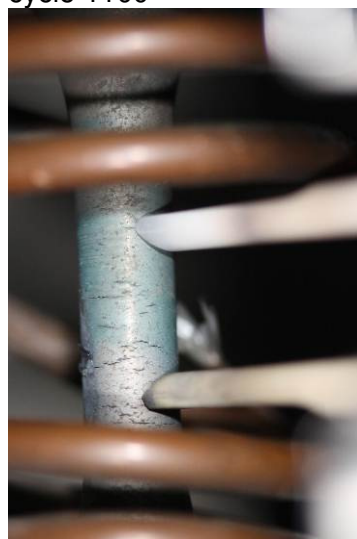
cycle 1431

Figure 38 - Pictures taken at different cycles showing the growth of surface crack in gauge length for specimen R262-1 (coated PWA 1483 aged air)

2.3.6 *Tests on coated PWA 1483 aged in air+ steam*

The same test matrix of coated PWA 1483 aged in air, has been applied to specimens of coated PWA 1483 aged in air with a 20% steam content, exposed 1000 h at 1000 °C.

The first test (R264-4) has been performed combining the same thermal cycle with a mechanical strain -0.4% at the maximum temperature. Test has been stopped after 3272 cycles without failure of the specimen. The end of life criteria (25% drop load) has been matched at cycle 2357 in terms of drop for the delta stress (difference among maximum and minimum stress at each cycle) while the drop on the maximum stress at each cycle has been matched at cycle 3057. Trend of minimum and maximum stress at each cycle is presented in Figure 39, while in Figure 40 the trend of delta stress is reported.

The hysteresis strain cycles comparing initial phase (second cycle) and half life cycle is shown in Figure 41.

Figure 39 - Trend of max and minimum load applied at each cycle n R264-4 TMF test
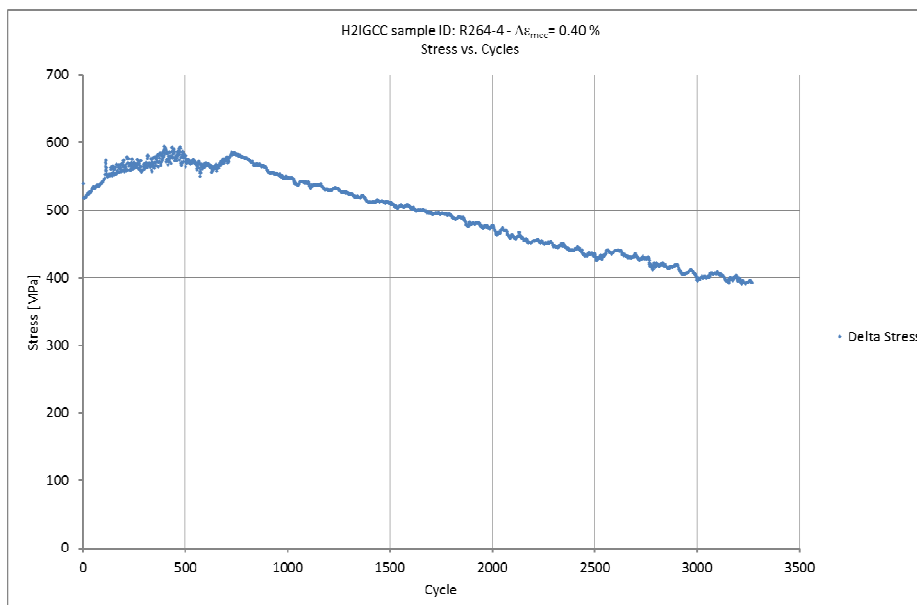
Figure 40 – Trend of delta stress (stress max – stress min at each cycle) for 264-4 TMF test
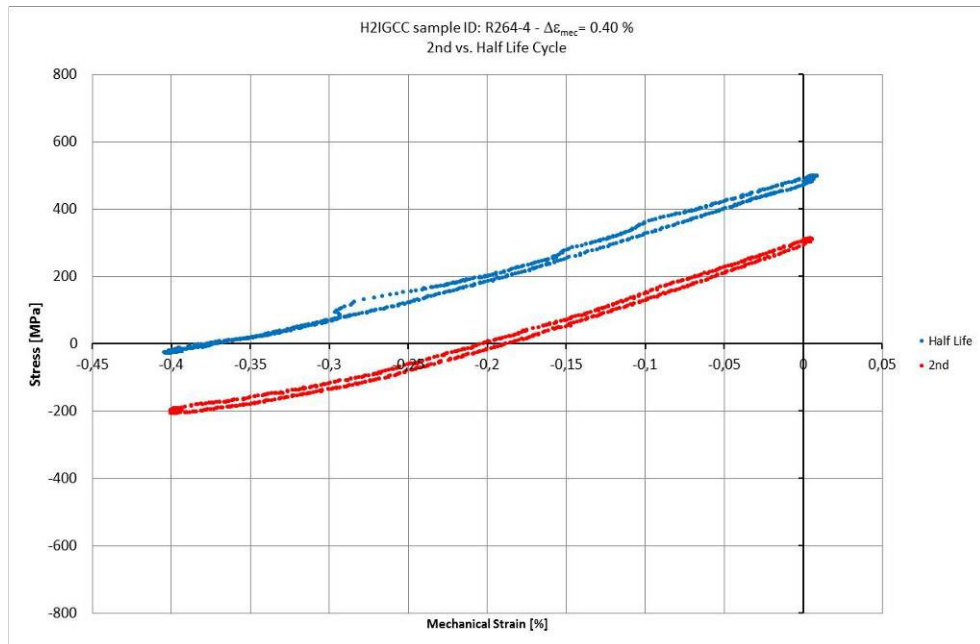
Figure 41 - Stress/strain hysteresis loop at second and half-life cycles for test on specimen R262-4

First cracks surface in gauge length can be detected after about 820 cycles as very limited penetration in coating material. Pictures of most significant steps in crack development are summarised in Figure 42.

Cycle 1   cycle 700   cycle 815   cycle 820

Cycle 900   cycle 1400   cycle 1800   cycle 2357

Figure 42 - Pictures taken at different cycles showing the growth of surface crack in gauge length for specimen R262-4 (coated PWA 1483 aged air+ steam)

2.4 Metallography related to TMF tests

2.4.1 Uncoated Rene 80

2.4.1.1 R263-6 preliminary test on partially heat treated Rene 80

Specimen went to rupture after 1284 cycles without any relevant variation in max and min stress applied at each cycle as previously shown in Figure 13. The aspect of broken specimen disassembled from TMF test machine is presented in Figure 43.

Figure 43 – R263-6 broken specimen after 1284 cycles in TMF test

Fracture surface aspect observed on SEM at low magnification is reported in Figure 44.
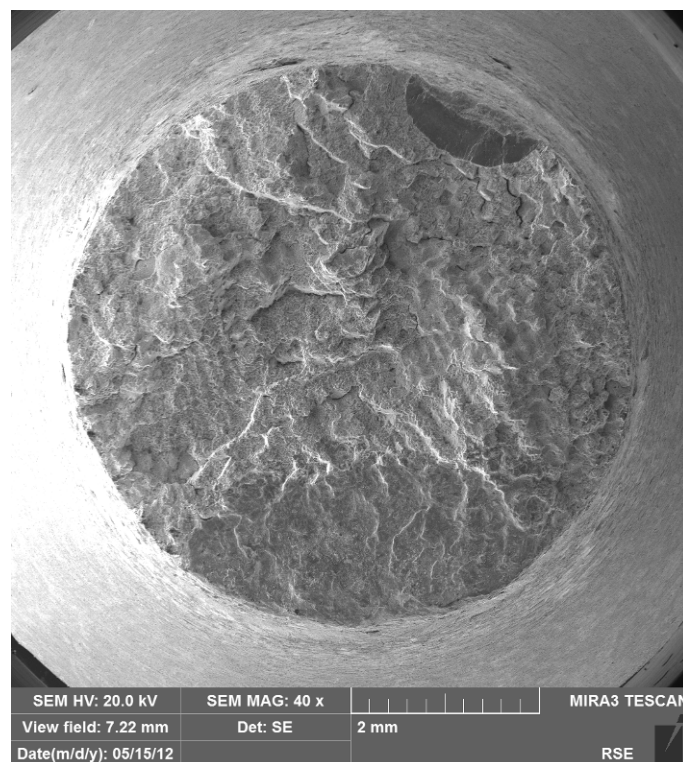
Figure 44 – Fracture surface of specimen 263-6

Two separated areas of crack initiation and growth can be observed, easily detectable due to surface oxidation and smoother aspect. Details at large magnification of the two areas are presented in Figure 45.
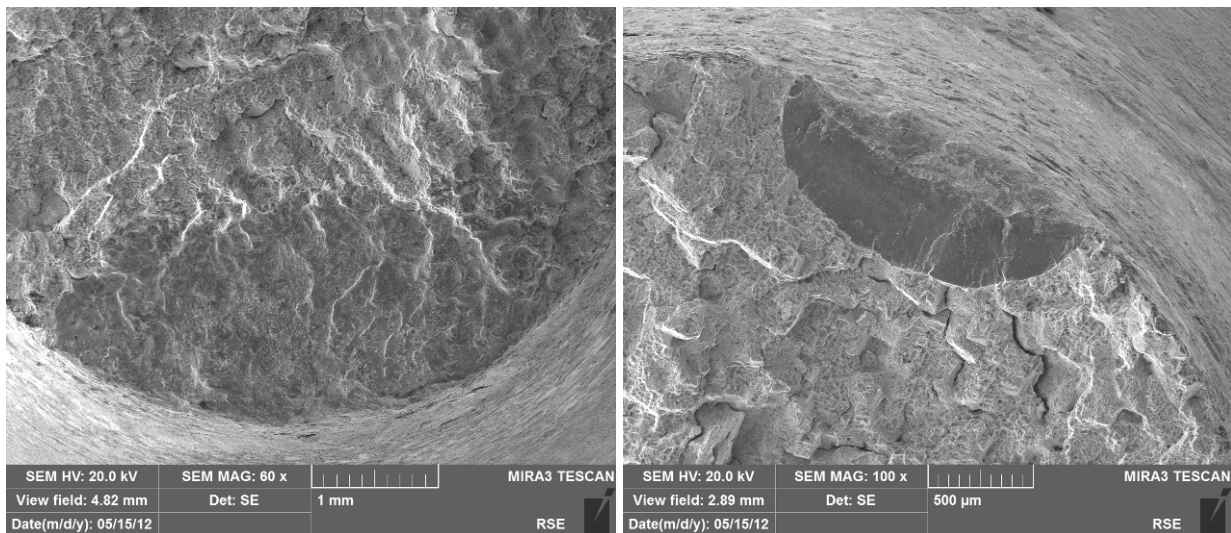
Figure 45 – View of the two separated areas with crack initiation and growth on fracture surface (R263-6)

One of the two pieces of broken specimen has then been sectioned transversally to fracture surface plane along a diameter centered on the bigger area of crack initiation and growth. The macrographs of metallographic specimen are shown in Figure 46; some other cracks parallel to fracture surface can be observed with different dimensions.

a)   b)   c)
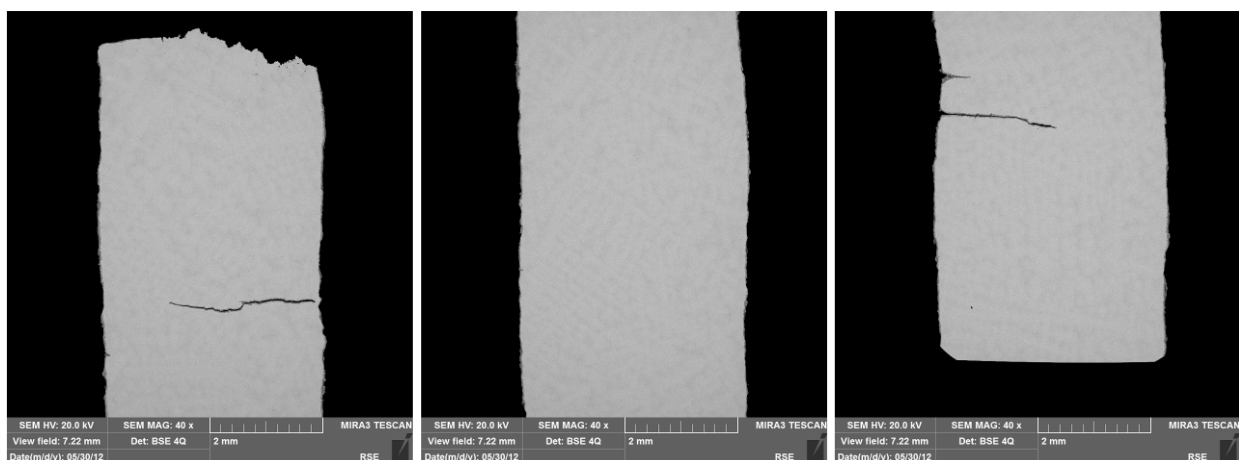
Figure 46 – Micrographs of metallographic specimen from R263-6: a) fracture surface on the upper with crack initiation and growth on the left, b) central part of the specimen, c) lower part of the specimen close to transition area toward end connection of the specimen

The fracture surface appear to be smooth and oxidised in the initiation and fatigue growth area (see Figure 47a) while it is more fragmented (grain and dendrite detachment) in the remaining part of the fracture (see Figure 47b).
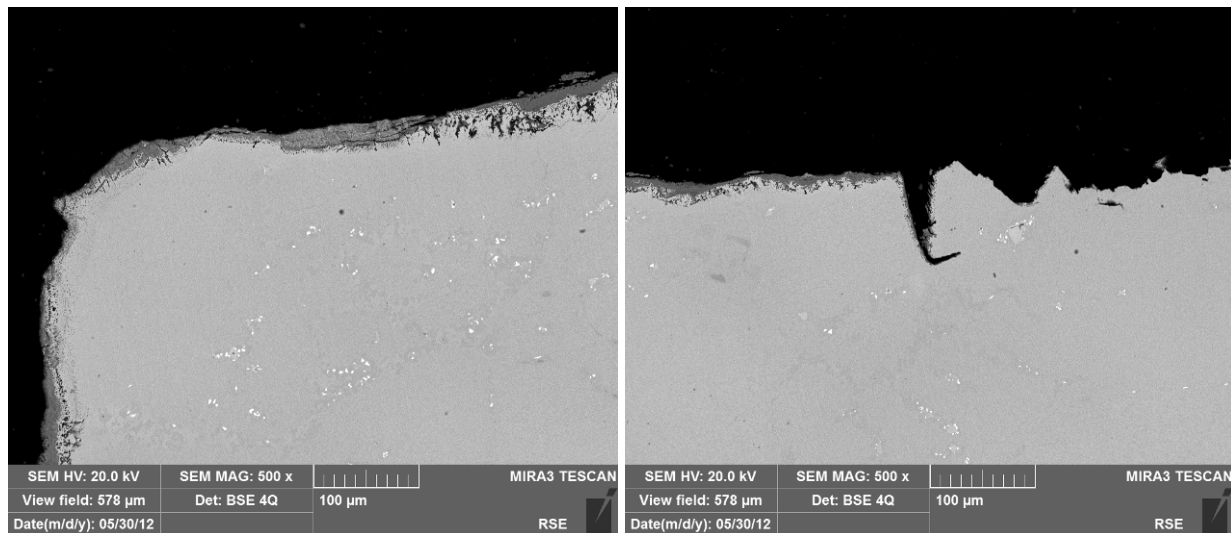
Figure 47 – Fracture surface on metallographic specimen from R263-6: a) crack initiation and growth with oxidation b) transition from oxidised surface to final tear with more fragmented aspect

The aspect of the other cracks detected in metallographic specimen aside of fracture surface but included in the gauge length of the specimen is presented in Figure 48, Figure 49 and Figure 50. Some of these secondary cracks appear to be significantly developed and oxidised.
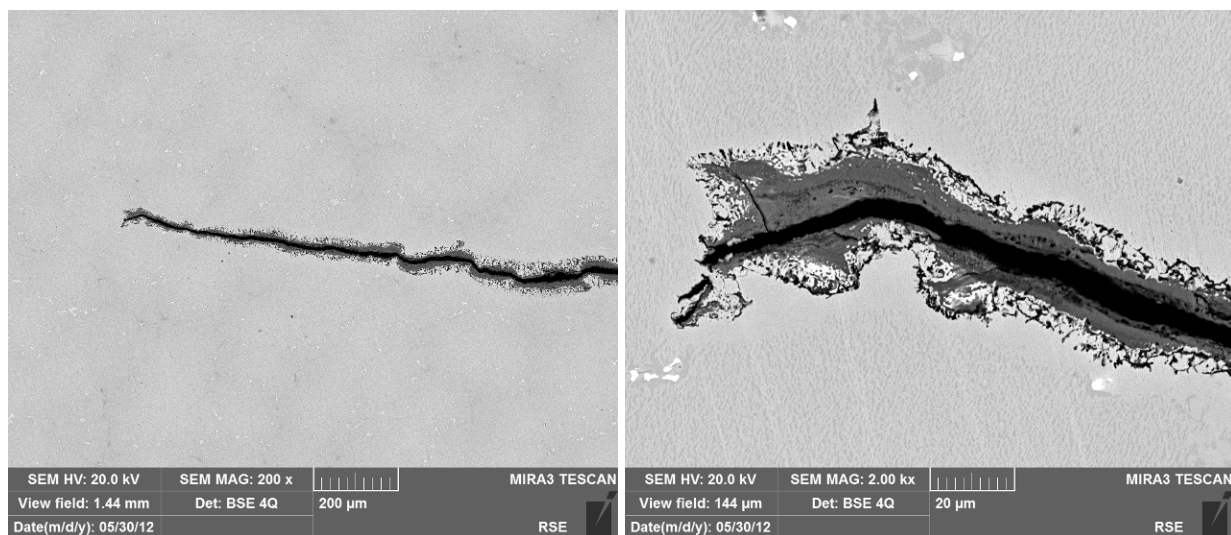
Figure 48 – Aspect of a secondary crack and detail of crack tip (R263-6)
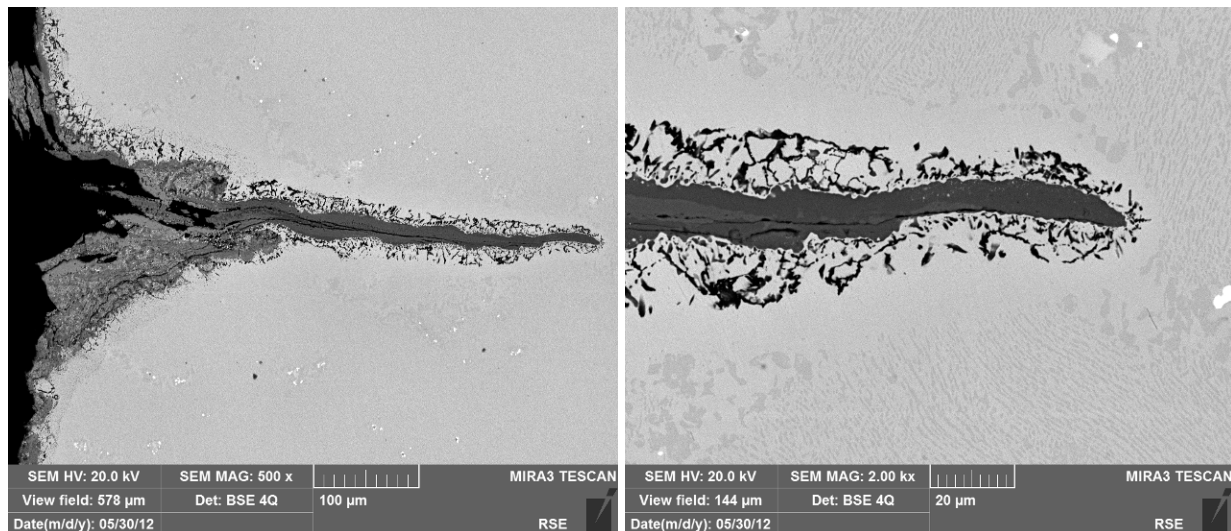
Figure 49 – Aspect of a secondary crack and detail of crack tip (R263-6)
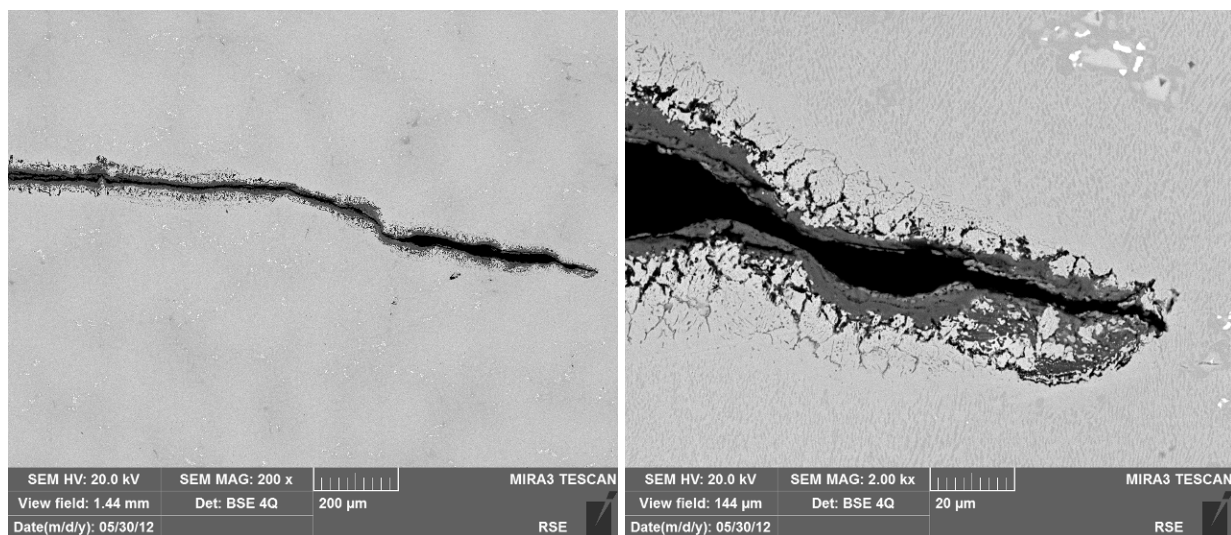
Figure 50 – Aspect of a secondary crack and detail of crack tip (R263-6)

2.4.2 Rene 80 with SiCoat 2464 specimens aged in air

As previously described, the three specimens after coating application, have been aged in air at 1000°C for 1000 hours and then tested without any other polishing of gauge length surface.

2.4.2.1 R262-6 specimen

This specimen has been tested with the application of thermal cycle described in Figure 12 and a compressive mechanical strain (- 0.4%) at maximum temperature. Specimen went to failure after 665 cycle. The first cracks can be detected on gauge length after about 200 cycles, the crack leading to final failure can be detected later at about 500 cycles.

The aspect of broken specimen disassembled from TMF test machine is presented in Figure 51.

Figure 51 – R262-6 broken specimen after 665 cycles in TMF test

Fracture surfaces aspect of the two pieces of specimen observed at low magnification is reported in Figure 52.
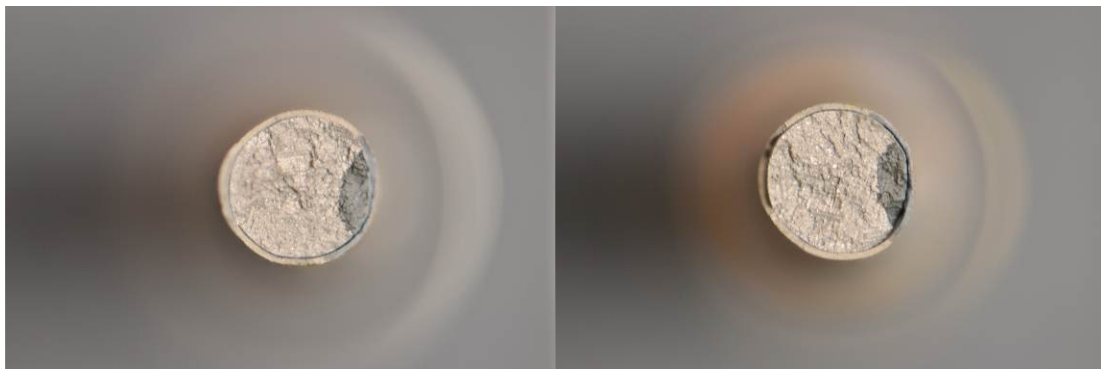
Figure 52 – Aspect of fracture surfaces on the two parts of broken specimen R262-6

The aspect of one of the two faces observed on SEM is presented in Figure 53, where the crack initiation area is located in the lower part of the picture. Details of the crack initiation area are presented in Figure 54. The aspect of bond coat fracture surface in the crack initiation area is presented in Figure 55.
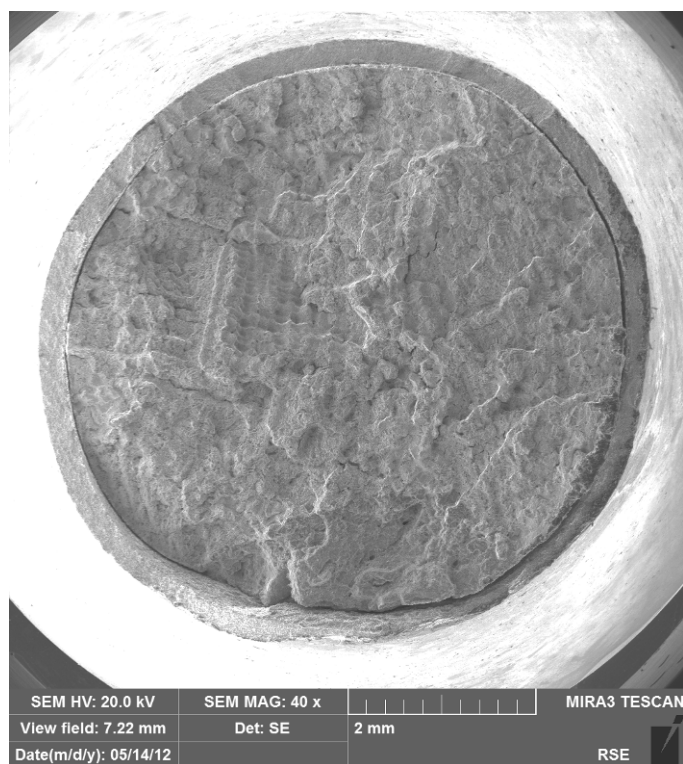
Figure 53 – Fracture surface of broken specimen R262-6
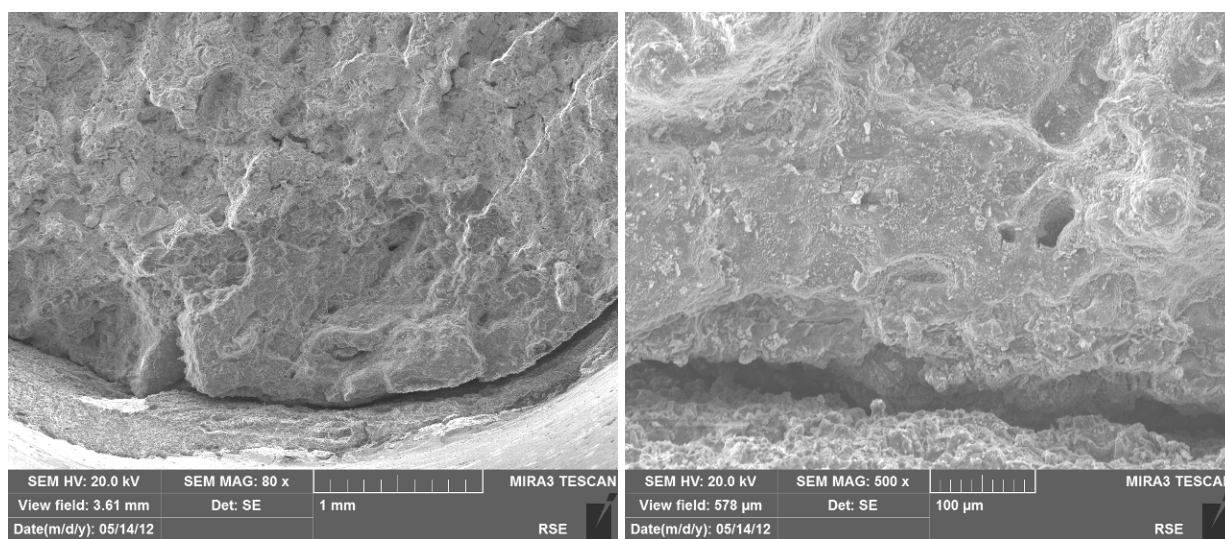
Figure 54 – SEM observation at different magnification of crack initiation area on fracture surface (R262-6)
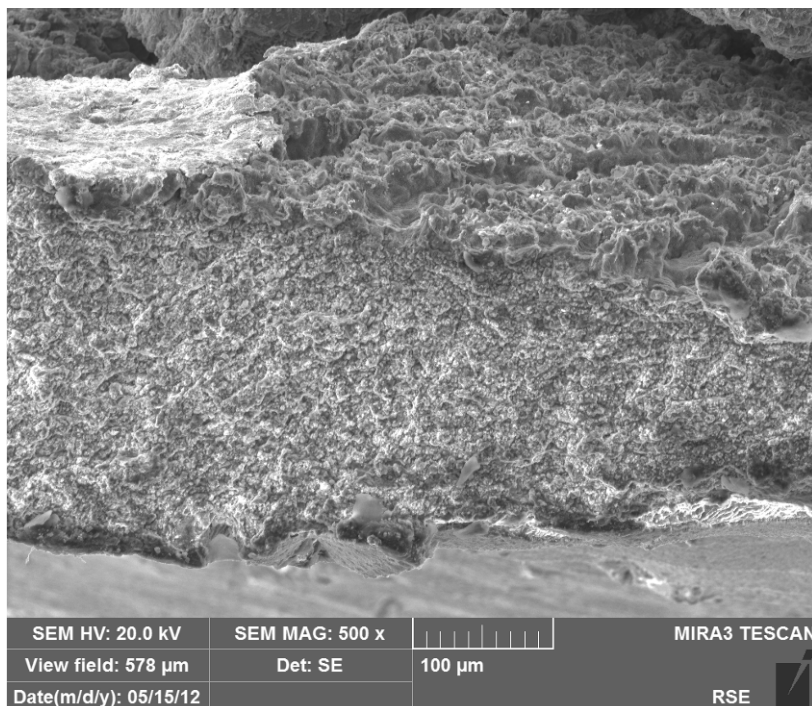
Figure 55 – Aspect of bond coat in crack initiation area of fracture surface (R262-6)

By sectioning the fragment of broken specimen transversally to fracture surface in the area of crack initiation a metallographic specimen has been prepared. The macro view of this metallographic specimen is shown in Figure 56.
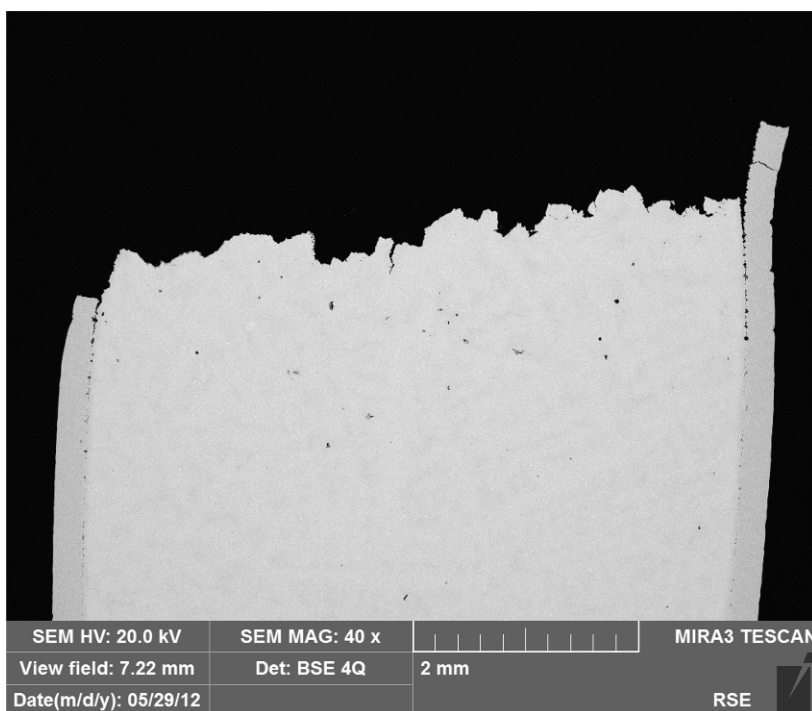
Figure 56 – Macro view of metallographic specimen transversal to fracture surface (R262-6)

The crack initiation area appears smoother than the other part of fracture and partially covered by a thin oxide layer as shown in Figure 57.
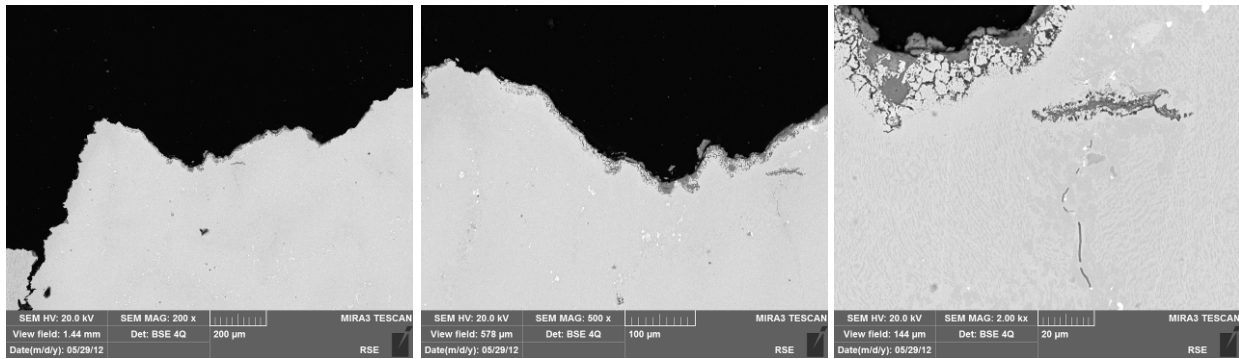
Figure 57 - Zoom on fracture surface in the crack initiation area (R262-6)

Some additional cracks limited to bond coat and some detachments of bond coat from base material can be observed in the same metallographic specimen at a certain distance from fracture surface, as shown in Figure 58.
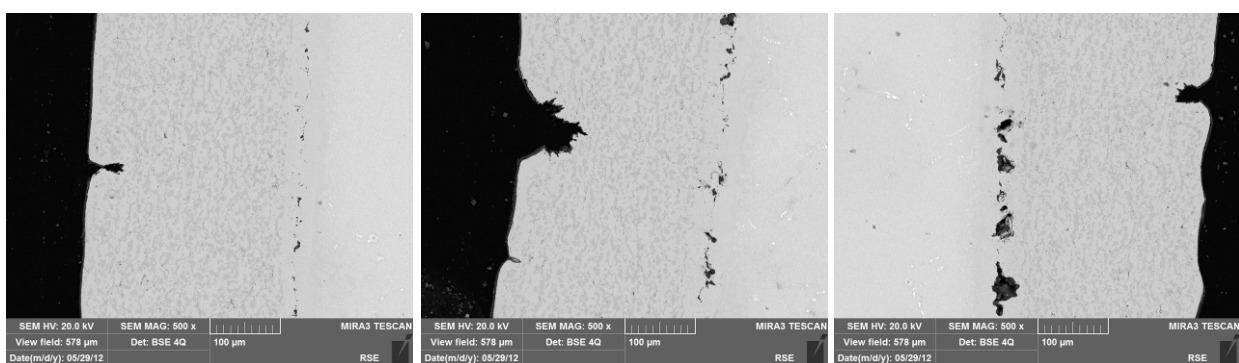
Figure 58 – Aspect of other cracks in bond coat or detachment of bond coat from base metal (R262-6)

2.4.2.2 R262-5 specimen

Test has been stopped at cycle 1335 without a complete failure of the specimen, unless many cracks were observed on gauge length surface since cycle 570; the end life criteria (25% drop load) was matched after 1079 cycles.

The presence of several cracks in gauge length has been confirmed by examination at SEM of specimen disassembled from TMF machine; some examples of crack surface with different levels of opening and extension are shown in Figure 59.
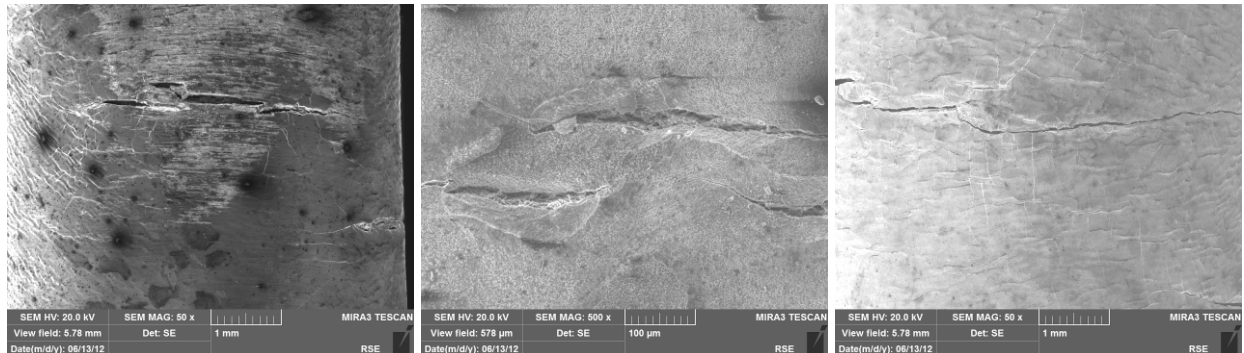
Figure 59 – Some examples of surface crack in gauge length of specimen R262-5

By sectioning longitudinally the specimen, some of the cracks can be observed in metallographic specimens showing different situations, as demonstrated in Figure 60. More or less developed situations of bond coat detachment from base metal can be detected also in some areas where there is no evidence of radial cracks, as shown in Figure 61. The detachment of bond coat with T-cracks formation appears to be influenced also by an original not optimised adhesion of coating to base metal, as better demonstrated in the following chapter about metallographic investigation of a not-tested specimen.
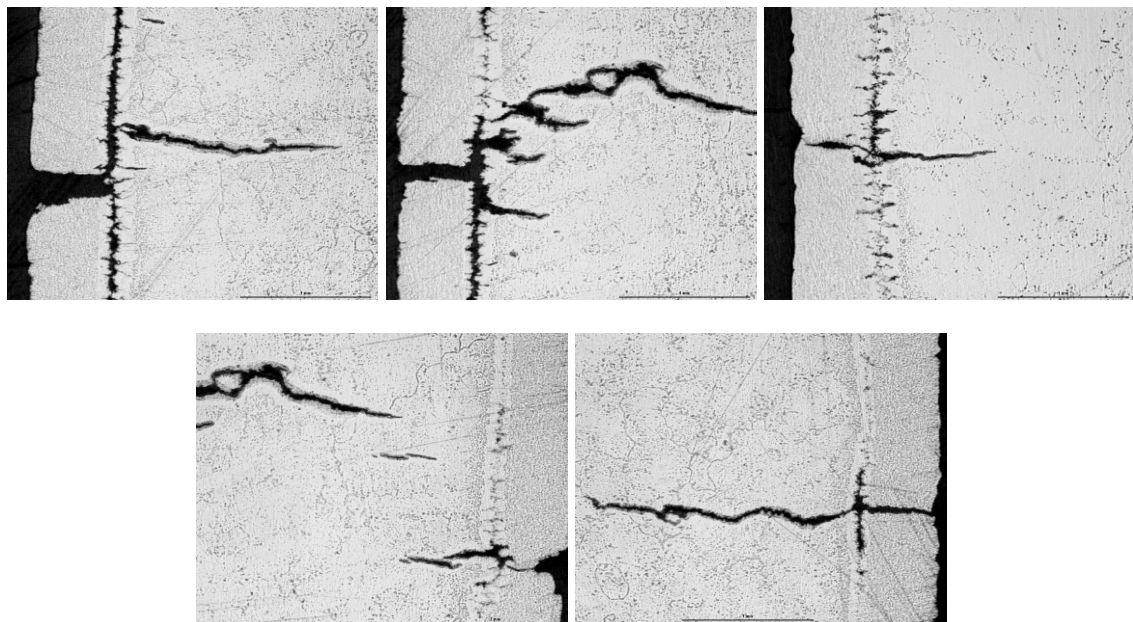
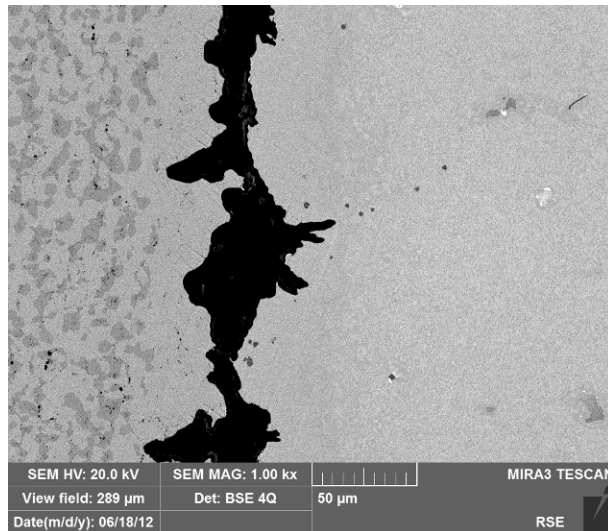**Figure 60 – Some cracks observed in metallographic specimen from R262-5**

Figure 61 – Different situation of bond coat detachment in some areas without radial cracks (R262-5)

2.4.2.3 R262-4 specimen

This specimen has been tested with the same conditions of the specimen R262-5, but setting the stop of the test at cycle 1079 (where R262-5 matched the end of life criteria).

The specimen at the end of the test shows a significant number of cracks more or less developed transversally to specimen axis (see Figure 62).
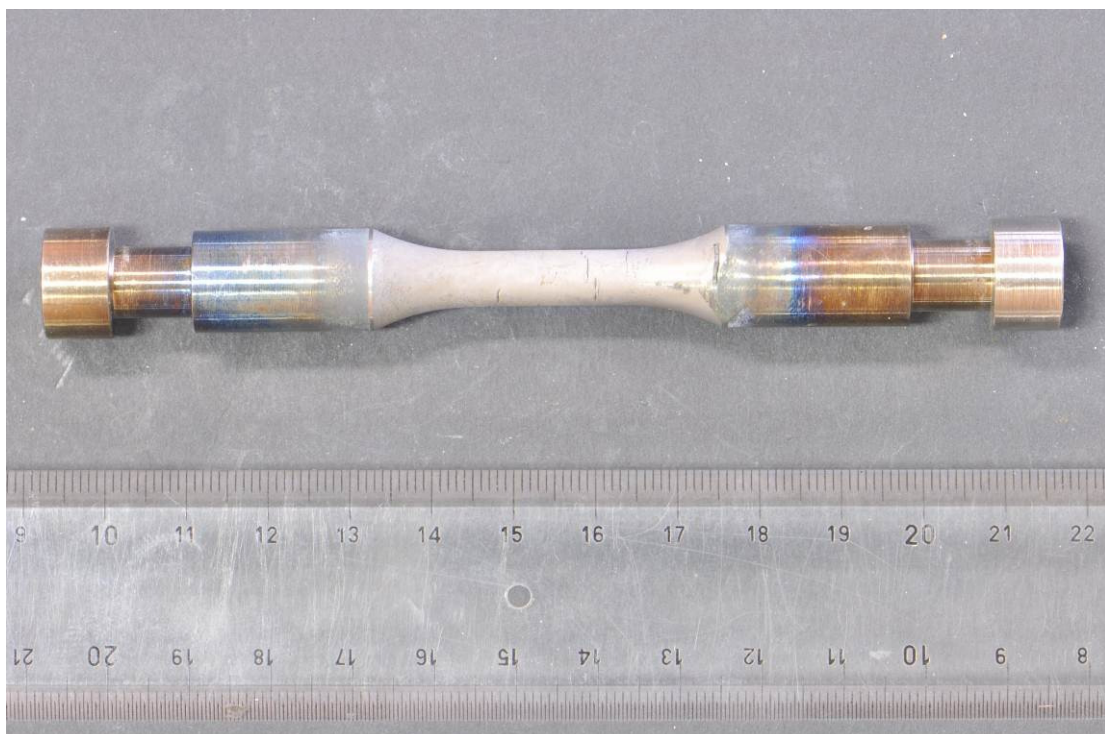

Figure 62 – Aspect of specimen R262-4 at the end of TMF test

Details on some cracks aspect can be observed in Figure 63.
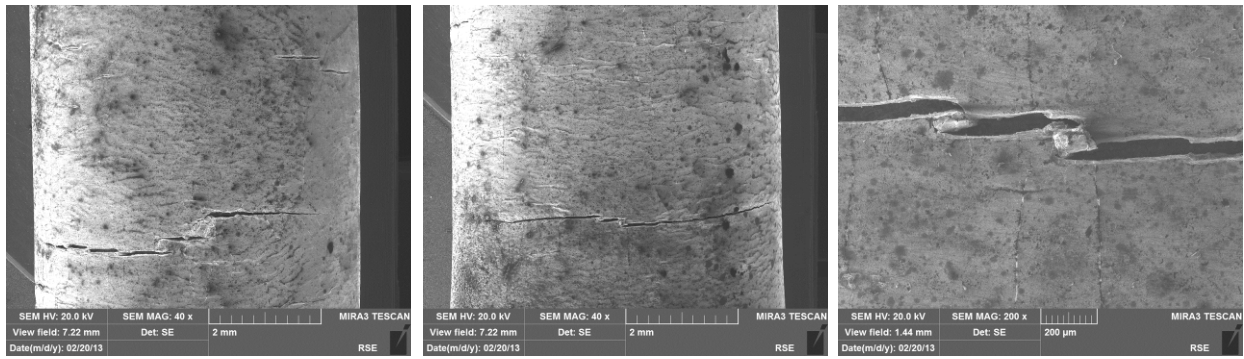
Figure 63 – Cracks on the surface of specimen R262-4 at the end of the TMF test

The metallographic specimen prepared by longitudinal sectioning of tested specimen, in the center of biggest crack, show the presence of different crack growths; cracks extended to coating and base metal, cracks limited to coating, detachments of the coating from base metal, and small defects at the interface between coating and base metal (see Figure 64)
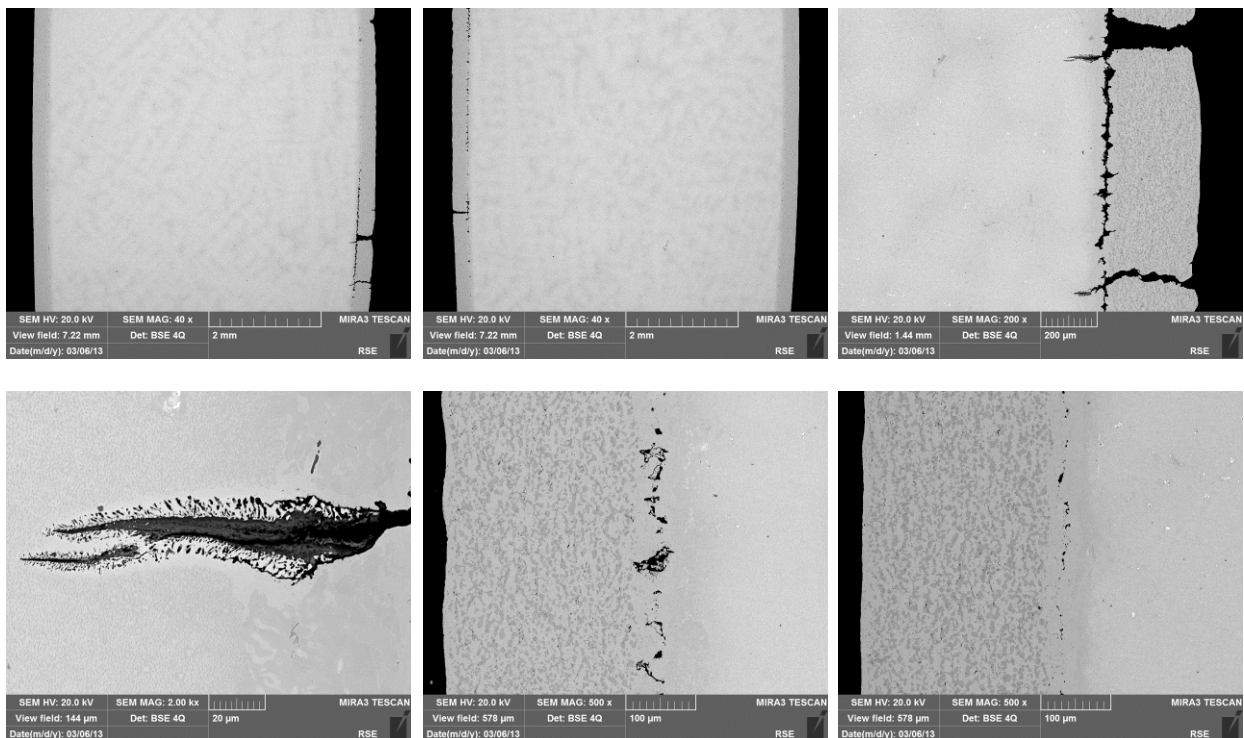

Figure 64 – The aspect of different cracks observed on metallographic section of specimen R262-4

The aspect of γ' (strengthening phase in base metal) on tested specimen is presented in Figure 65 showing some localized rafting and coarsening of cuboidal phase, compared to the situation observed in aged but not tested base metal presented in Figure 66. The micrographs presented in Figure 65 and every documentation of γ' aspect later presented in this document are reported with orientation corresponding the loading axis in mechanical tests with vertical axis of pictures.
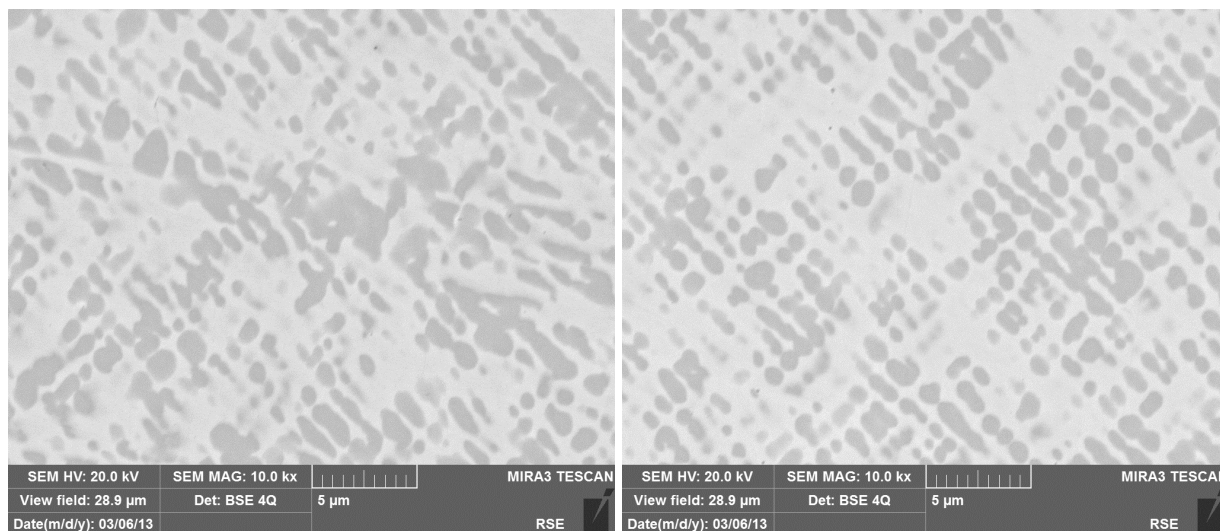
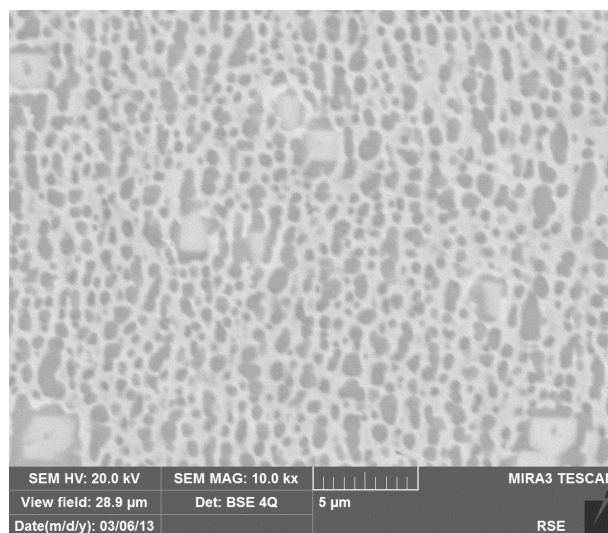**Figure 65 – Aspect of γ' in base metal of specimen R262-4 after test**

Figure 66 – Aspect of γ' in base metal of specimen R262-3 (specimen not tested)

2.4.3 Rene 80 with SiCoat 2464 specimens aged in air and steam

2.4.3.1 Specimen R262-2

This specimen has been tested with the same conditions of the specimen R262-5 that was aged in air without additional steam. Both specimens have been tested on TMF rig without failure. The specimen aged in air with steam matched the end criteria after 1685 cycle with a higher number of cycle compared to the specimen aged in air without additional steam. The test of specimen R262-2 have been stopped after 2566 cycles.

Tested specimen shows the presence of some cracks, more or less developed transversally to specimen axis (see Figure 67).

Figure 67 – Aspect of specimen R262-2 at the end of TMF test

Images taken on SEM with different magnification of some cracks are collected in Figure 68.
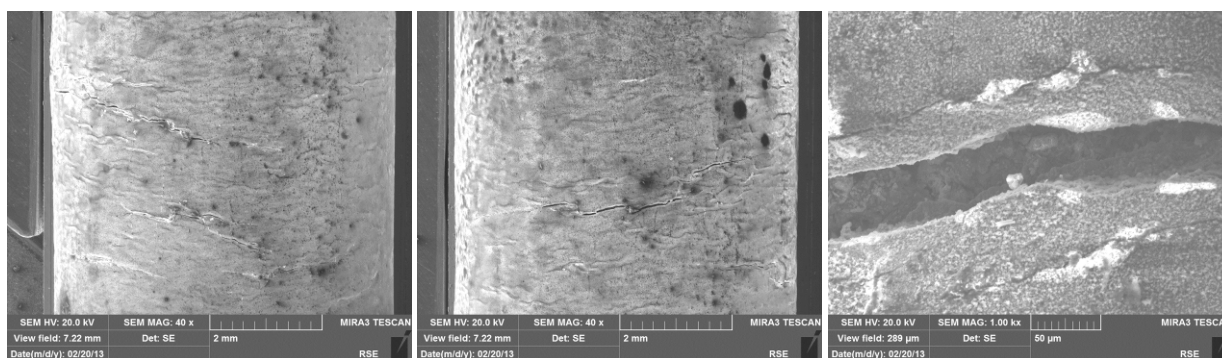

Figure 68 – Cracks on the surface of specimen R262-2 at the end of the TMF test

The biggest crack extends near to half section of the specimen, as it can be seen in Figure 69, where some other cracks limited to bondcoat or extended to base metal are shown too.

The aspect of γ' of this tested specimen is presented in Figure 70 showing some localized rafting and coarsening of cuboidal phase.
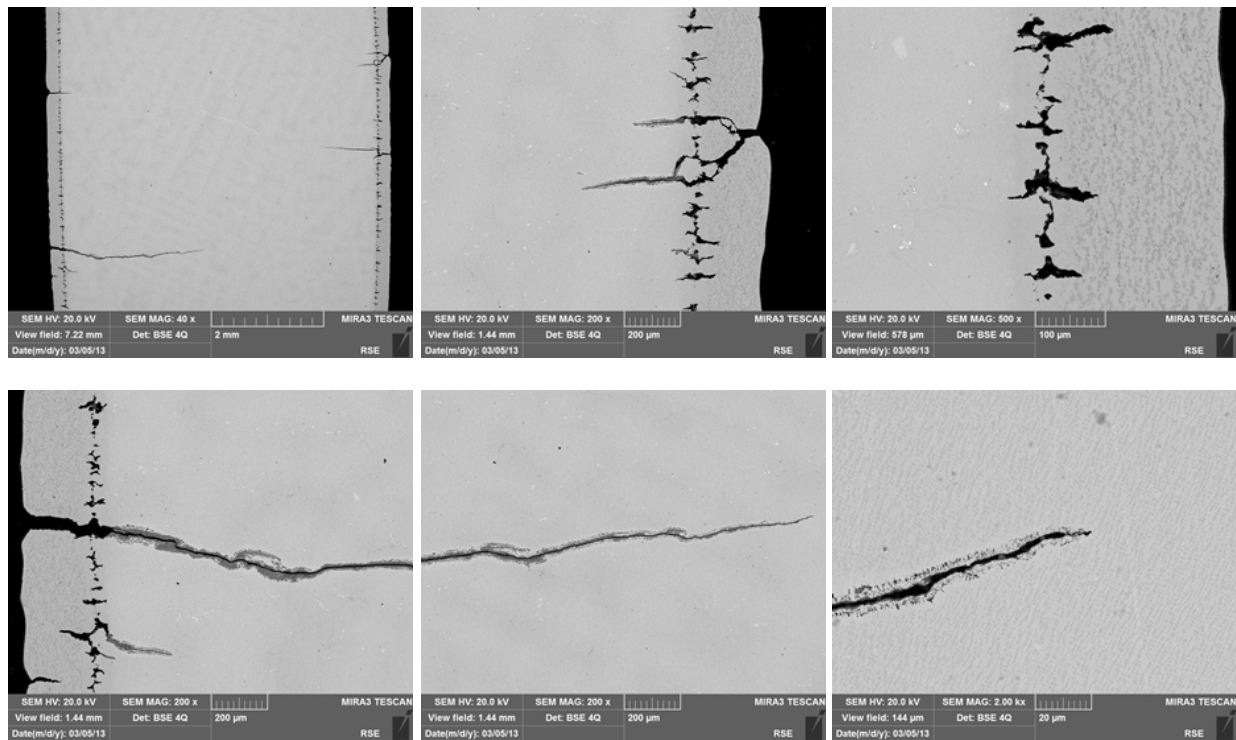
Figure 69 - The aspect of different cracks observed on metallographic section of specimen R262-2 with detailed zoom images of the biggest crack developed close to half section of the specimen
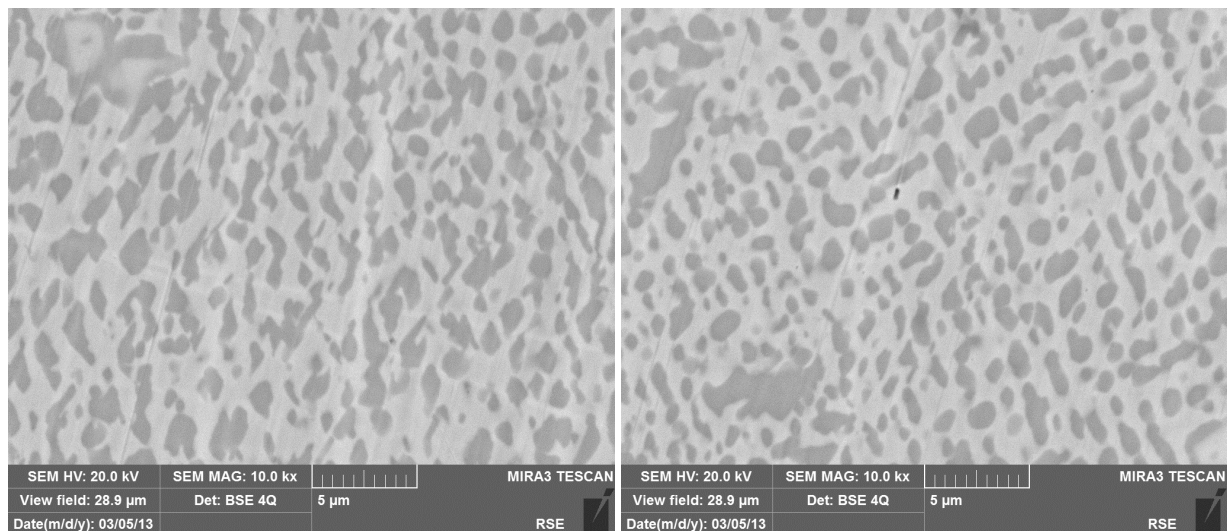

Figure 70 – Aspect of γ' in base metal of specimen R262-2 after test

2.4.3.2   Specimen R262-1

This specimen has been tested with the same conditions of the specimen R262-6 that was aged in air without additional steam. Both specimens went to rupture during test. This specimen aged in air with steam failed at cycle 627 (shorter life than equivalent condition specimen aged in air without additional steam).

The aspect of broken specimen disassembled from TMF test machine is presented in Figure 51. Fracture surfaces aspect of the two pieces of specimen observed at low magnification is reported in Figure 52.
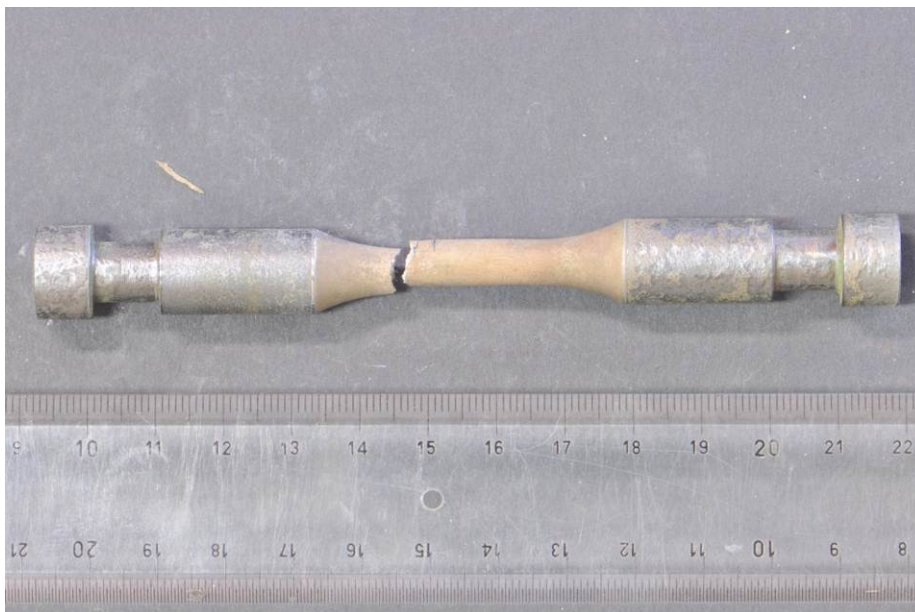
Figure 71 – R262-1 broken specimen after 627 cycles in TMF test
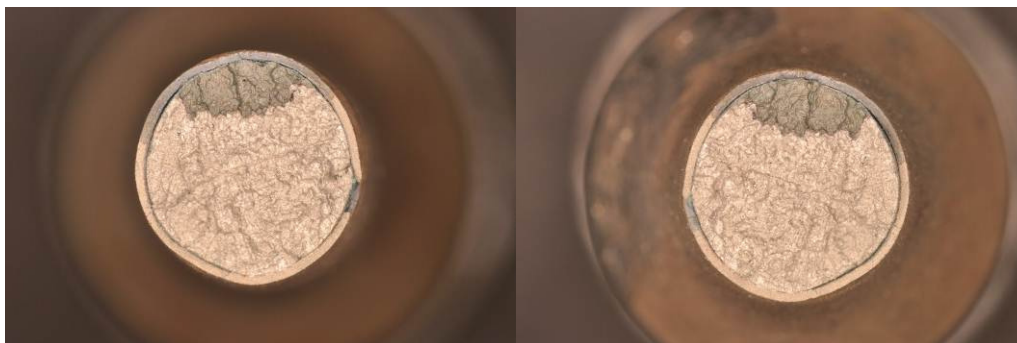

Figure 72 -Aspect of fracture surfaces on the two parts of broken specimen R262-1

The aspect of one of the two faces observed on SEM is presented in Figure 73, where the crack initiation area is located in the lower part of the picture. Details of the crack initiation area are presented in Figure 74.
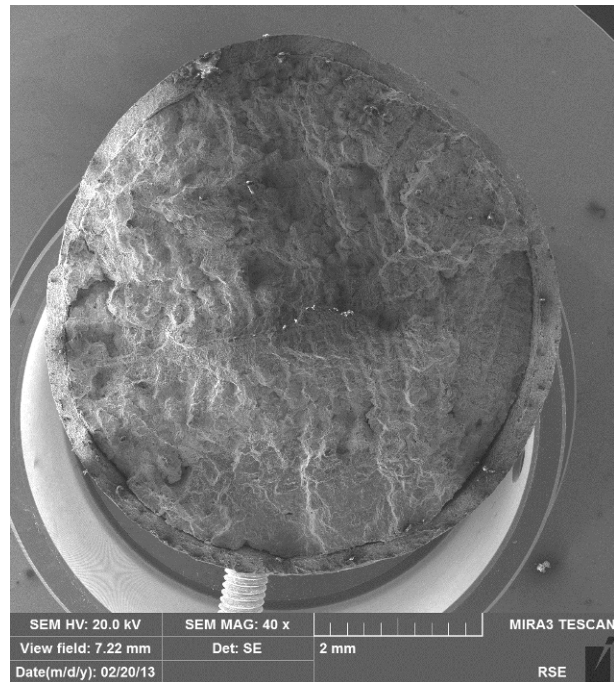
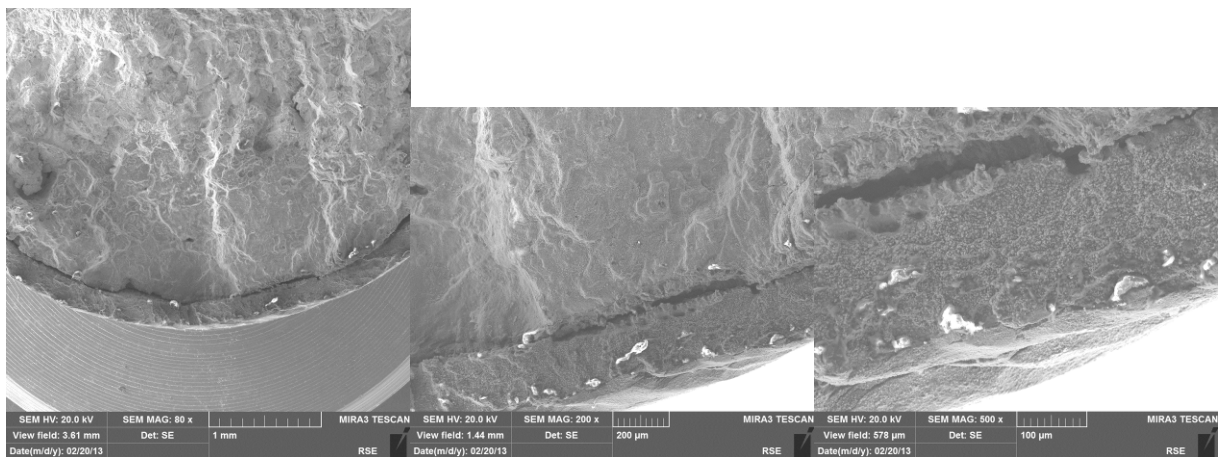**Figure 73 – Fracture surface of broken specimen R262-1**

Figure 74 – SEM observation at different magnification of crack initiation area on fracture surface (R262-1)

A second large crack close to fracture surface, but not related to, is documented in Figure 75 with pictures taken on SEM at different magnifications.
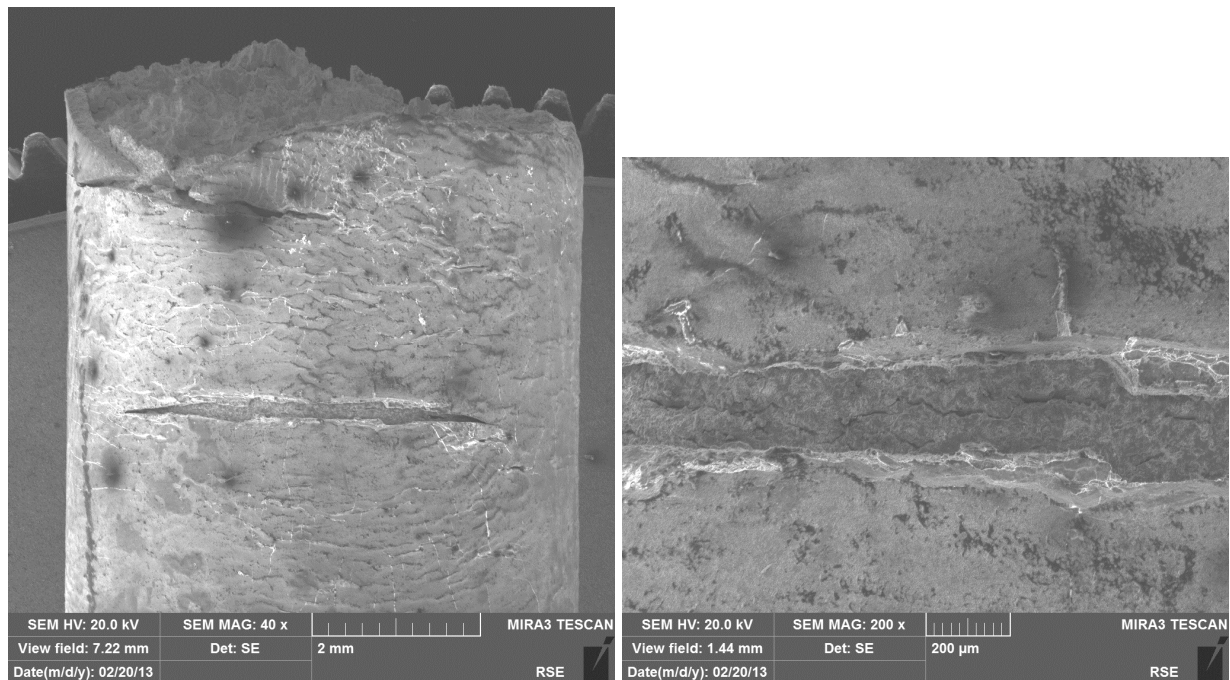
Figure 75 – Secondary crack developed on gauge length surface close to fracture in specimen R262-1

By sectioning the fragment of broken specimen transversally to fracture surface in the area of crack initiation a metallographic specimen has been prepared. The macro view of this metallographic specimen is shown in Figure 76.
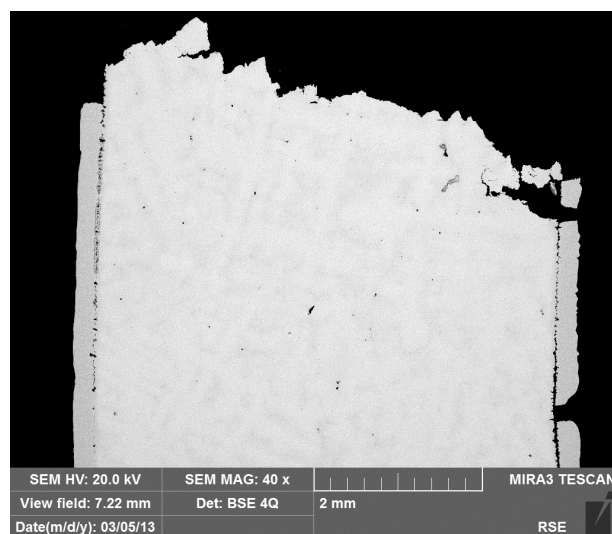

Figure 76 – Macro view of metallographic specimen prepared by R262-1 tested on TMF

Figure 77 show detailed micrograph of crack initiation area on fracture surface and of the secondary crack close to fracture surface that appears to be limited to bond coating and not extended to base metal,
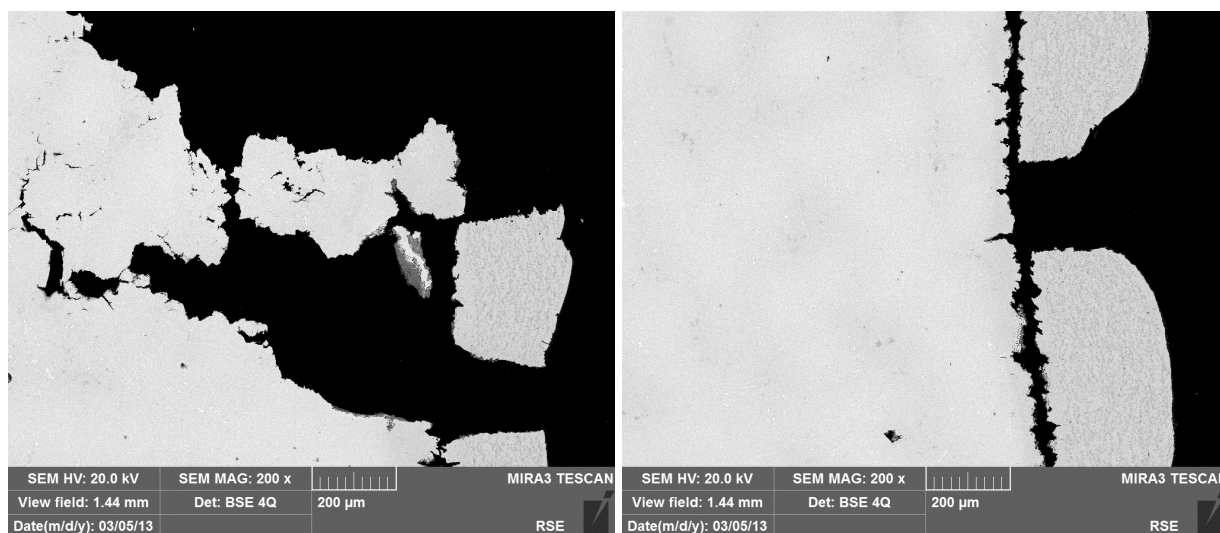
Figure 77 – Details of fracture surface crack initiation area (on the left) and secondary crack close to fracture surface (on the right)

The aspect of γ' on this tested specimen is presented in Figure 78 showing some localized rafting and coarsening of cuboidal phase.
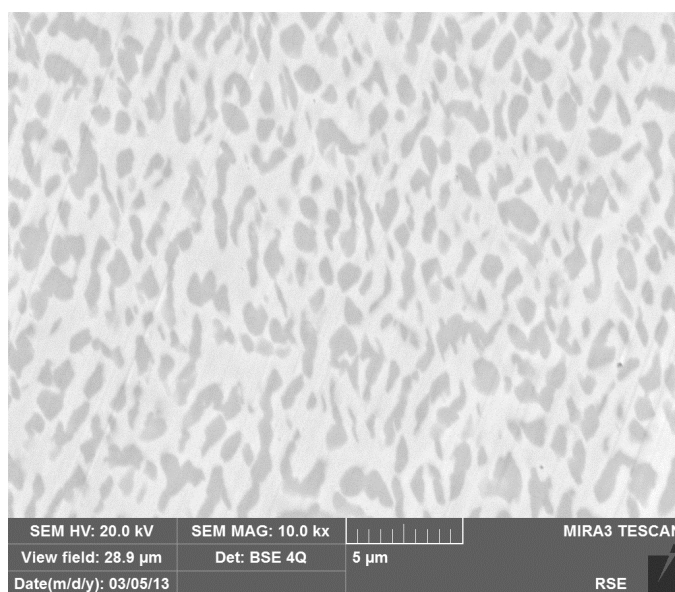

Figure 78 – Aspect of γ' in base metal of specimen R262-1 after test

2.4.3.3   Specimen R262-3

This specimen has been aged in air with 20% steam but not tested in order to detect if some defects at the interface of base metal with bond coat are present prior to TMF tests. The aspect of specimen at the end of the ageing is reproduced in Figure 79. The macro view of metallographic specimen prepared by longitudinal sectioning of the specimen is presented in Figure 80. Small defects and precipitates at the interface among base metal and bond coat can be detected, as demonstrated in Figure 81. The same picture shows also the presence of two depleted areas (layers with approximate thickness of 15-20 μm) on both sides of coating/base metal interface. On the base metal side this precipitates depletion corresponds to dissolution of γ' phase, while in the bond coat it's due to dissolution of β phase; both phenomenon essentially related to Al migration and precipitation as oxide. The aspect of γ' phase internally to base metal with a partial coarsening of the cuboid has already been presented (as comparative image) in

Figure 66, additional pictures taken from different positions of metallographic section are reported in Figure 82.

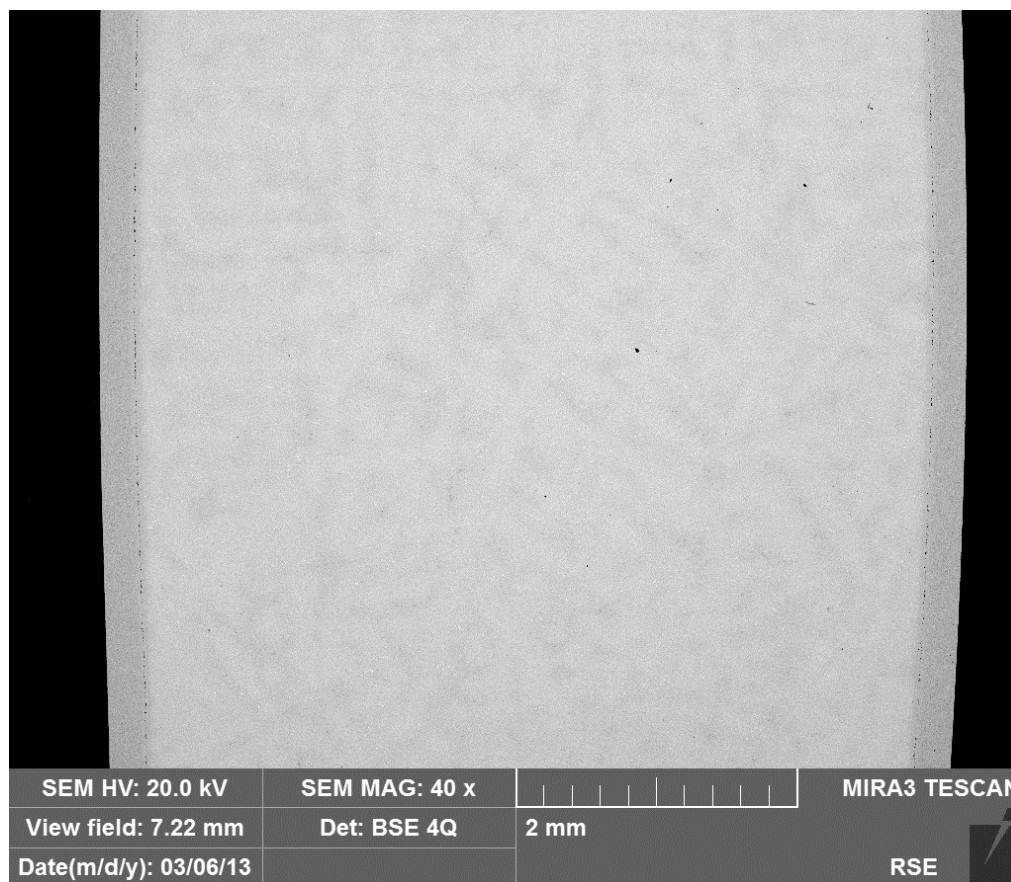**Figure 79 – Aspect of specimen R262-3 after ageing in air with 20% steam**

Figure 80 – Macro view of metallographic specimen obtained by longitudinal sectioning of specimen R262-3
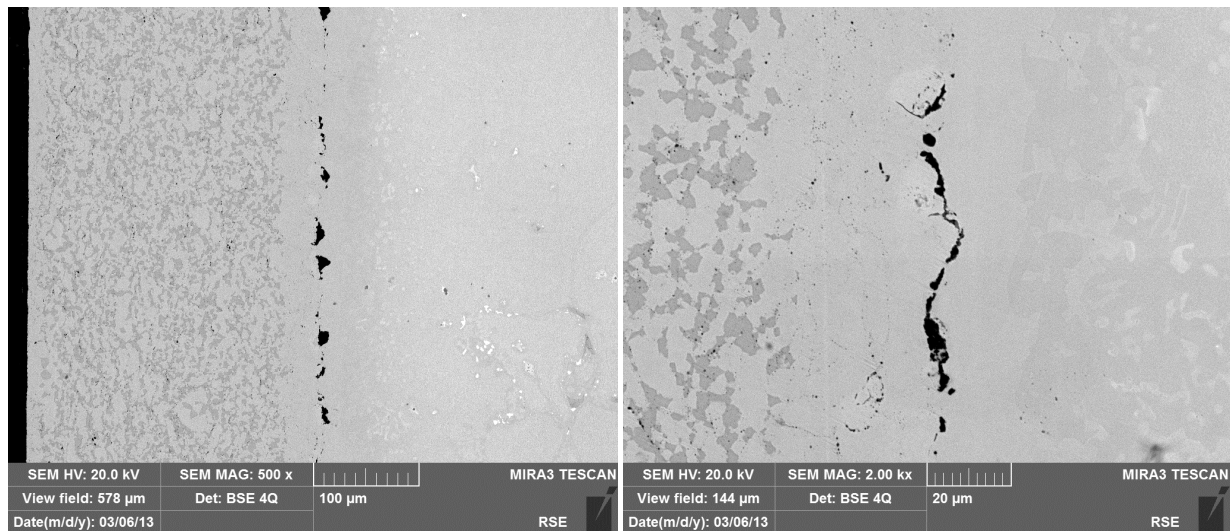
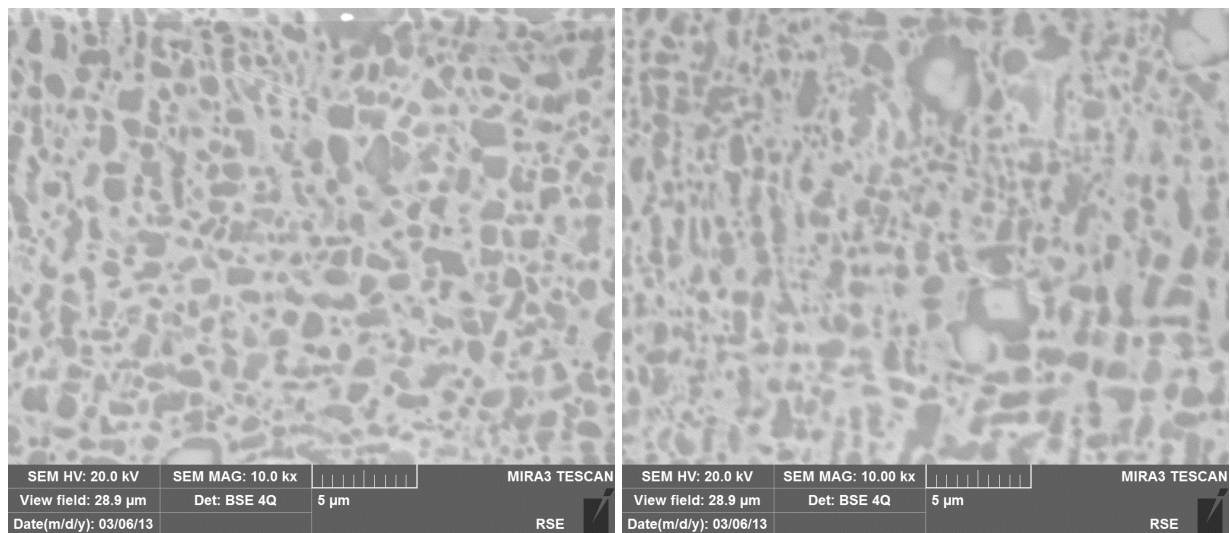**Figure 81 – Defects at the interface among base metal and bond coat in specimen R262-3**

Figure 82 – Aspect of γ' in different positions of specimen R262-3 aged in air with 20% steam

The precipitates and precipitates at the interface presented in Figure 83 can be characterised by the EDS spectra presented in the following figures and referred to labelled areas.

Figure 83 – Precipitates and defect at the interface between bond coat and base metal of specimen R262-3
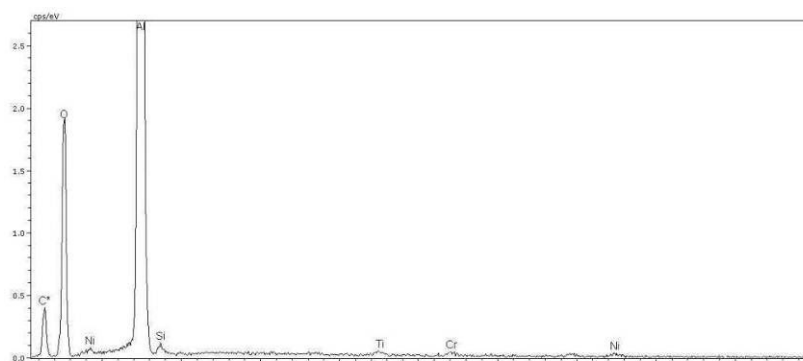
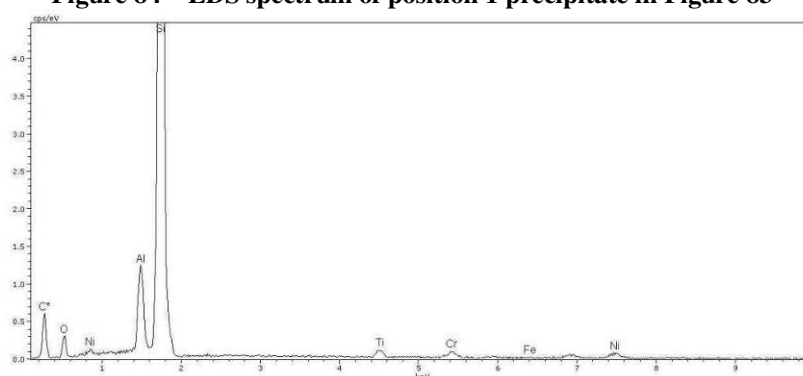**Figure 84 – EDS spectrum of position 1 precipitate in Figure 83**

Figure 85 – EDS spectrum of position 2 precipitate in Figure 83
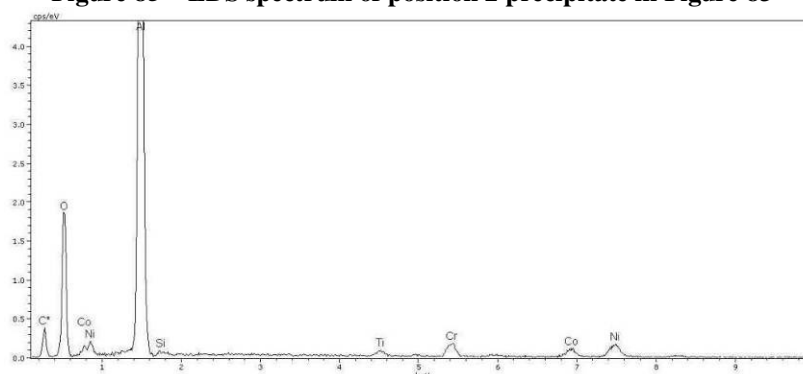

Figure 86 – EDS spectrum of position 3 defect in Figure 83

The materials evolution at the interface between bond coat and base metal can be observed also by the EDS-line analysis presented in Figure 87. Dark particles at the interface are mainly detected as aluminium oxide, there is no evidence of products including nitrogen; these particles appear to be residual of grit blasting materials used in coating application preliminary surface finishing.
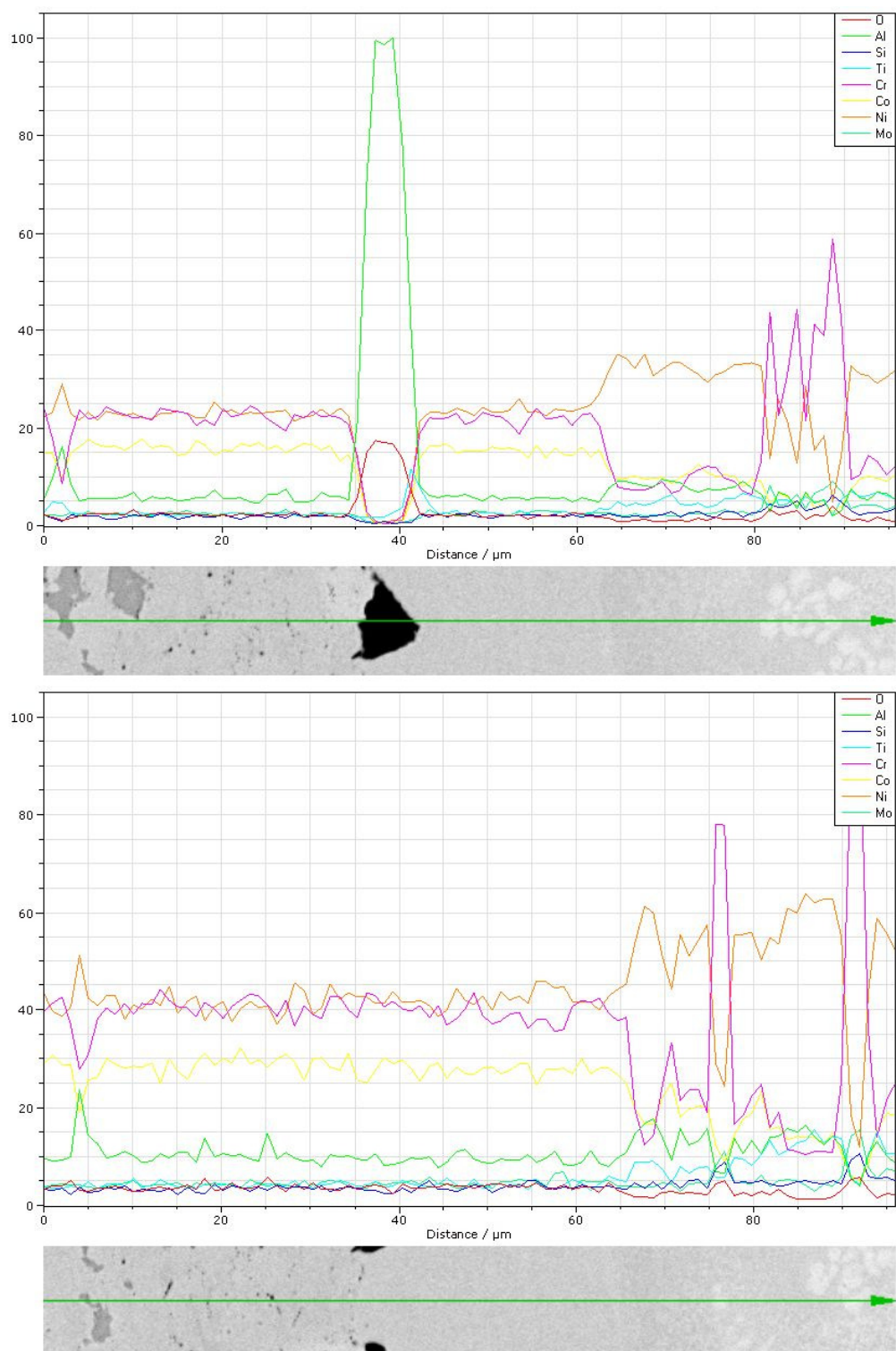
Figure 87- EDS-line analysis with chemical elements detectable at the interface between base metal and bond coat for specimen R262-3

2.4.4   Uncoated PWA 1483

2.4.4.1   R265-6 preliminary test

The specimen has been tested with thermal cycle condition described in Figure 32.

After test interruption, due to thermocouple weld detachment and unsuccessful restart trials, the specimen R265-6 has been observed on SEM some small cracks on gauge length have been detected. An example of observed cracks is reproduced in Figure 88. All cracks are oriented transversally to specimen axis, average length of the cracks is about 0.5 mm with a narrow opening.
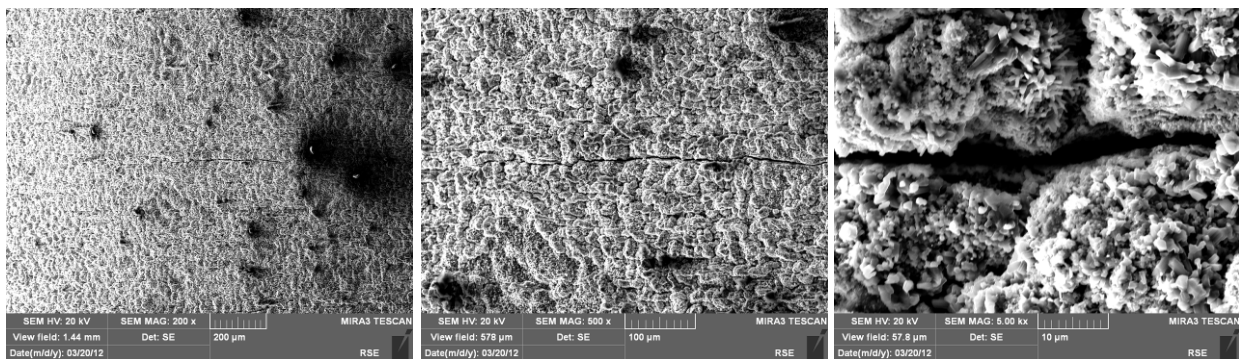

Figure 88 – Example of a SEM observed surface crack at different magnification (R265-6)

The specimen has then been sectioned transversally to cracks orientation showing a limited oxidation on external surface and a crack penetration lower than 0.1 mm as shown in Figure 89.
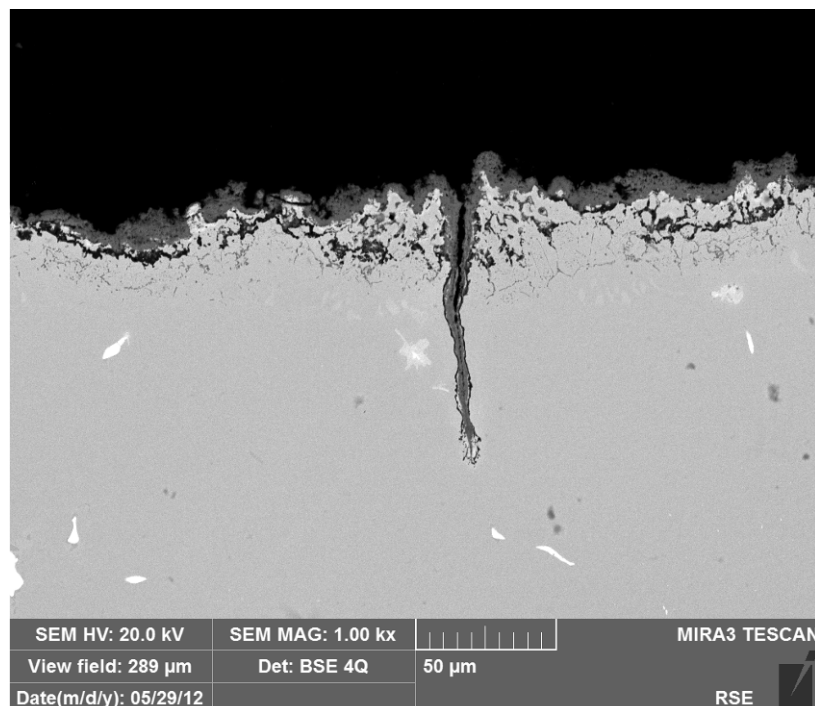

Figure 89 – SEM BSE micrograph of crack in gauge length with limited oxidation on external surface (R265-6)

Metallographic specimen prepared by the sectioning of TMF tests show also the presence of some defect included in base metal PWA 1483 as reproduced in Figure 90.
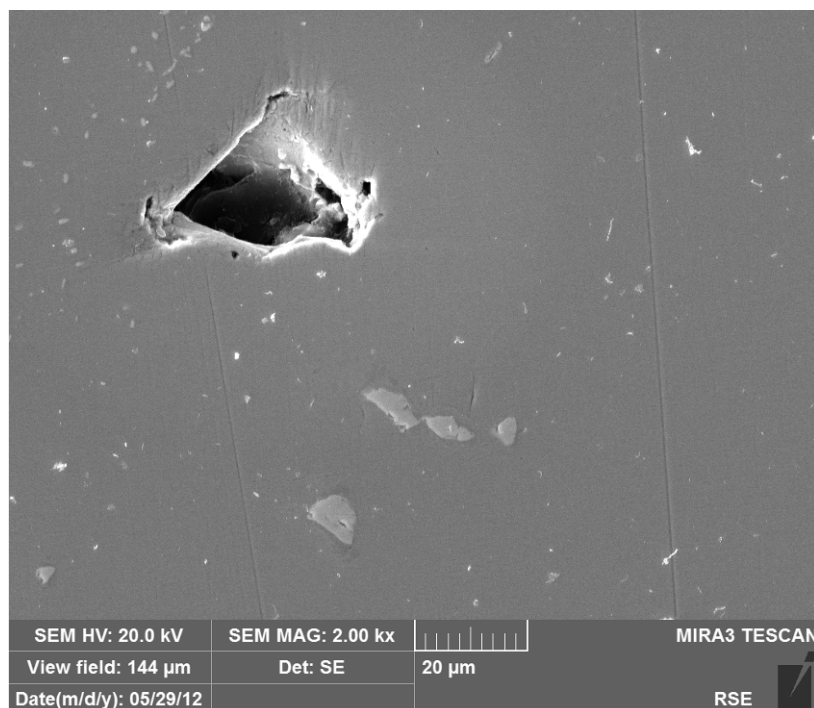
Figure 90 – Presence of a defect in base metal PWA 1483 detected on SEM (R265-6)

2.4.5   PWA 1483 with SiCoat 2464 specimens aged in air

Three specimens with PWA 1483 base metal after Sicoat application have been aged in air at 1000°C for 1000 hours and then tested without any other polishing of gauge length surface.

2.4.5.1   Specimen R264-1

This specimen has been tested with the application of thermal cycle described in Figure 12 and a compressive mechanical strain (- 0.4%) at maximum temperature. Test has been stopped at cycle 2160 without a complete failure of the specimen, unless many cracks were observed on gauge length surface since cycle 350; the end life criteria (25% drop load) was matched after 1458 cycles

The presence of several cracks in gauge length has been confirmed by examination at SEM of specimen disassembled from TMF machine; some examples of crack surface with different level of opening and extension are shown in Figure 91.
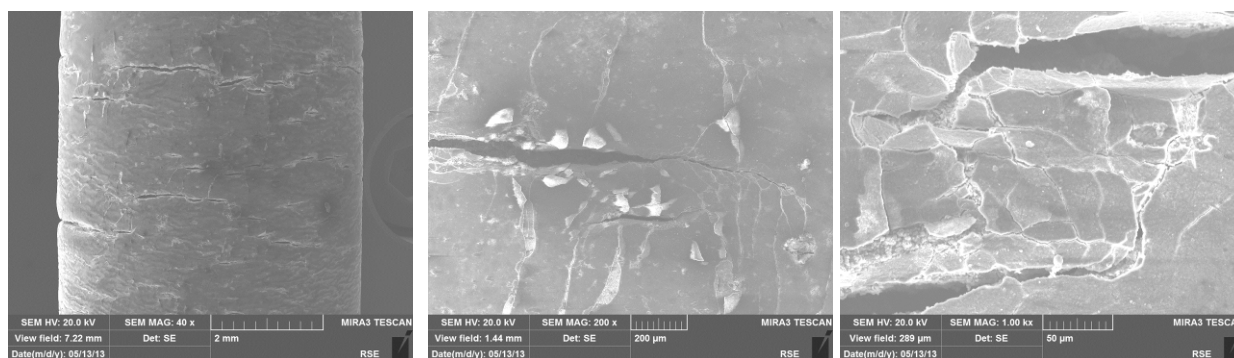

Figure 91 – Cracks on the surface of specimen R264-1 at the end of the TMF test

Two macro views of metallographic specimen prepared by longitudinal sectioning of tested specimen, in the center of biggest crack, show the presence of several cracks (see Figure 92); most of them limited to coating and some others extended to coating and base metal too (see Figure 93). A not perfect adhesion of bond coat to base metal and the inclusion of residual grit

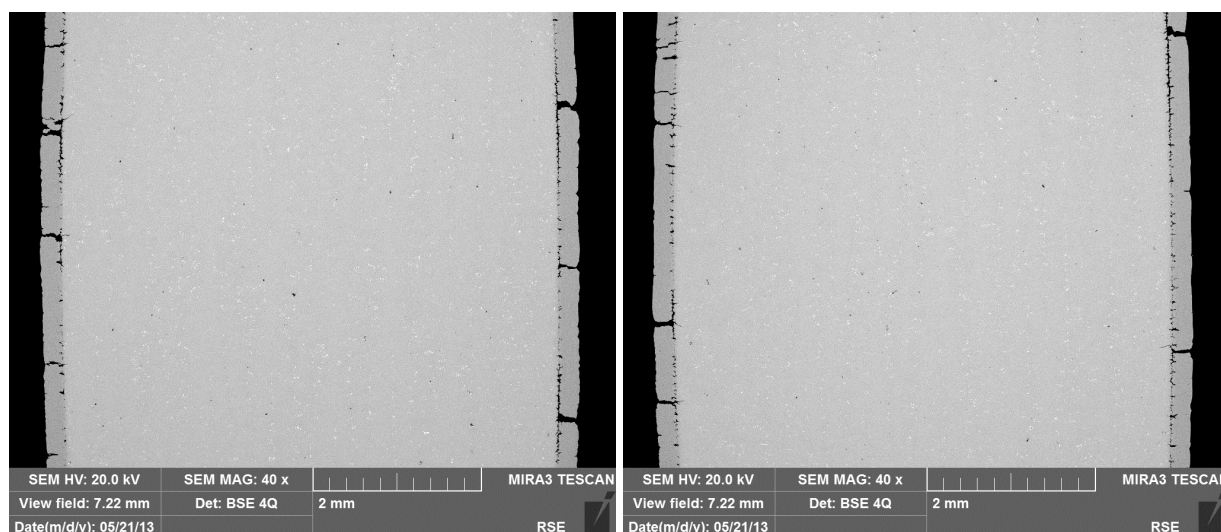blasting particles cam be observed, similarly to the situation discussed for Rene 80 coated specimens.

Figure 92 – Macro view of metallographic specimen prepared by R264-1 tested on TMF

Details at higher magnification of some cracks are presented in Figure 93
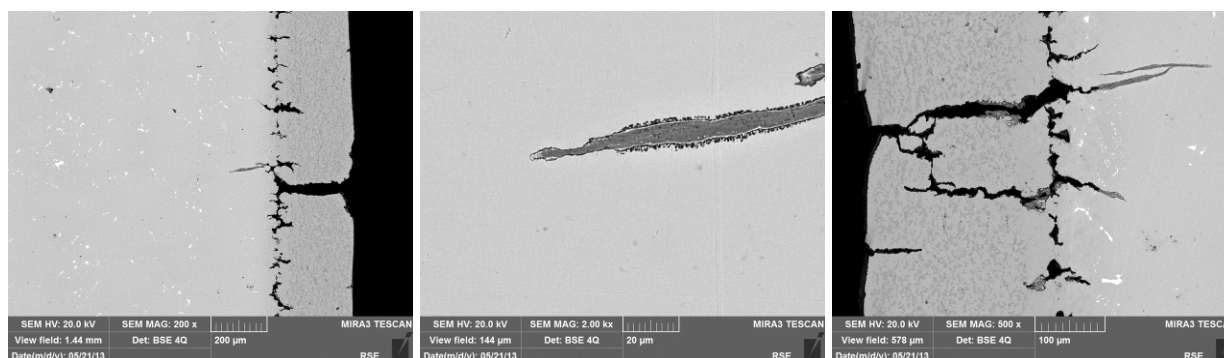

Figure 93 - The aspect of different cracks observed on metallographic section of specimen R264-1

2.4.6   PWA 1483 with SiCoat 2464 specimens aged in air with 20 % steam

Similarly to previous case other three PWA1483 specimens coated with SiCoat 2464 have been aged 1000 h at 1000°C in air with controlled content of added steam (20%).

2.4.6.1   Specimen R264-4

This specimen has been tested on TMF rig applying the same thermal and mechanical condition previously described for specimen R264-1. Test had a longer (than R264-1) duration and has been stopped after 3272 cycles; post-test analysis showed that end criteria (25 % drop load) has been matched after 2357 cycles based on the drop of delta stress (difference between maximum and minimum stress at each cycle).

Also in this case the presence of several cracks in gauge length has been confirmed by examination at SEM of specimen disassembled from TMF machine (see Figure 94).
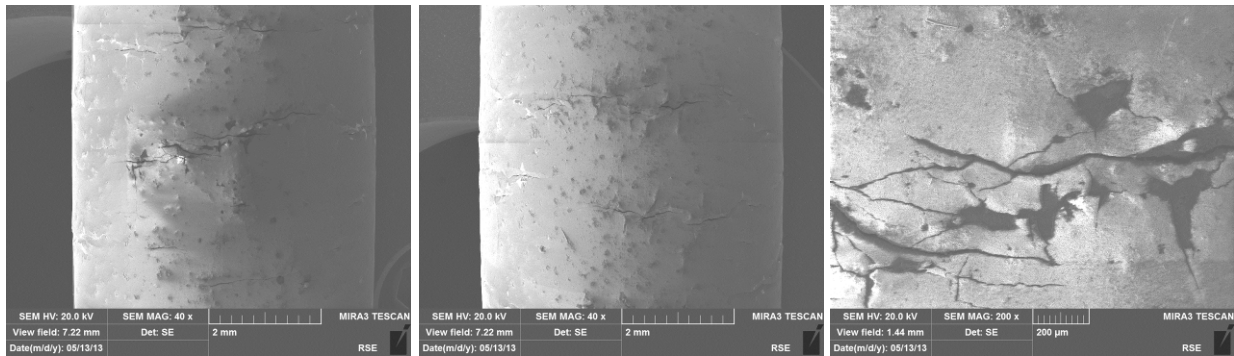
Figure 94 – Cracks on the surface of specimen R264-4 at the end of the TMF test

Examination of metallographic specimen by longitudinal section of the specimen confirms a situation very similar to that observed for specimen R264-1, as documented in Figure 95 and Figure 96.
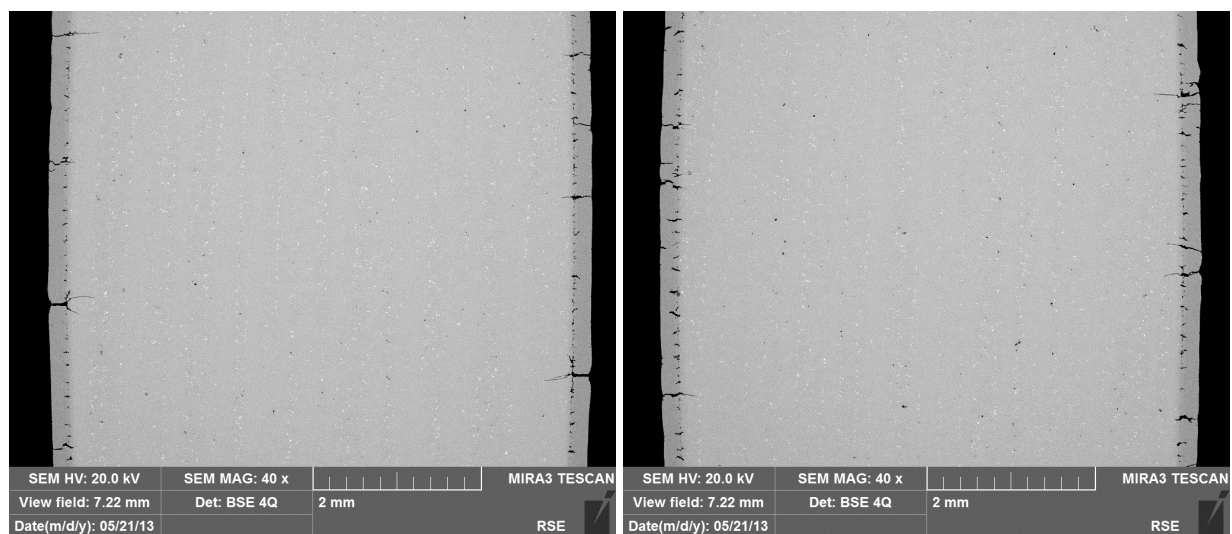

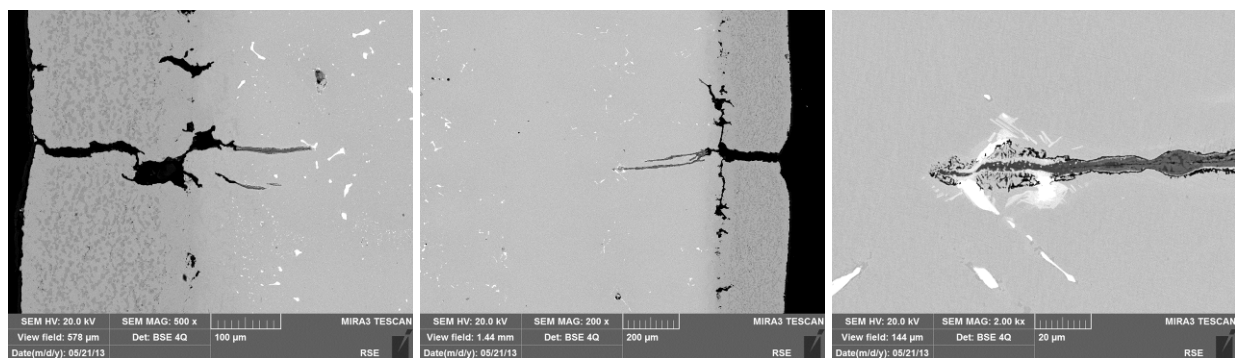**Figure 95 – Macro view of metallographic specimen prepared by R264-4 tested on TMF**

Figure 96 - The aspect of different cracks observed on metallographic section of specimen R264-4

3   Creep characterisation

Chapter 3.1 describes the test program and creep specimen preparation steps. Chapter 3.2 describes the Laborelec creep frames and obtained creep curves. Chapter 3.3 provides the metallurgical investigation of the samples while chapter 3.4 discusses all the results of the creep tests in order to come to the conclusion formulated in chapter 4.2. Chapter 3.5 describes results of small punch creep tests and comparison with uniaxial tests, while related metallurgical investigation results are collected in chapter 3.6. Finally additional tests results of small punch creep on Rene 80 fully heat treated are presented in chapter 3.7.

3.1   Creep specimens preparation

The creep characterisation has been performed on the cast nickel alloy Rene 80 in order to evaluate:
- the effect of exposure of material (coated or uncoated) to the aggressive environment of flue gas with high content of humidity
- compare the conventional technique of uniaxial macro test with miniaturised small punch creep test on an alloy not yet tested with this small size technique.

Some plates of cast material have been made available by Siemens with a partial preliminary heat treatment (not including the two final steps of heat treatment usually performed during coating application).

Specimens have been manufactured by Laborelec for uniaxial creep tests and some of them have been partially coated with HVOF SiCoat 2464 (bond coat) while other have been coated with SiCoat 2464 and standard thermal barrier coating. Some of the specimens were then tested as received while some other specimens have been aged in air at 1000°C for 1000 hours or in humidified (20 % H_2O) air for the same time and temperature of exposition. Table E shows all variables within the conventional creep testing program. The improved coatings form work package 2.4 are stated as well. The results will be provided in the deliverable of WP2.4.

Table E: Illustration of variables in the creep testing program

Base Metal	René 80
Coating	Uncoated
	HVOF SC2464 + TBC
	HVOF SC2464
	Improved MCrAlY + TBC (Code "AB" in WP2.4)
	Improved MCrAlY (Code "AA" in WP2.4)
Pre-ageing	No pre-ageing
	Air, 1000hrs, 1000°C
	Air + 20% water, 1000hrs, 1000°C
Test Conditions	950°C & 140 MPa
	950°C & 105 MPa
	1050°C & 50 MPa
	1050°C & 40 MPa

Figure 97 shows the typical heat treatment process René 80 blades and vanes receive during manufacturing. Step 1+2 are applied after casting. Step 3+4 are applied after application of the MCrAlY bond coat. The René 80 slabs provided received only step 1+2. This was only noticed in a later phase of the project after finalisation of all creep tests of the uncoated samples. Therefore it was decided to repeat one test on an uncoated sample which received additionally heat treatment step 3+4 in the Laborelec laboratory.

The uncoated René 80 samples with step 1 +2 are further labelled: "René 80 as received". The uncoated René 80 samples with step 1 +2 + 3+4 are further labelled "René 80 with completed heat treatment" or "Fully HT René 80".

Table F gives an overview of the coating specifications. The samples with coating are coated by Flamespray. The surface of the base material was grit blasted using 40 mesh brown corundum. The state of the art MCrAlY Bond-Coat is fully HVOF sprayed. The powder used is the SICOAT2464 commercialised by H.C. Starck. The TBC is applied by APS, the powder is Yttria stabilised Zirconia commercialised by H.C. Starck. Step 3+4 heat treatment was executed after the application of the Bond-Coat. The heat treatment was 1h at 1080°C followed by a cooling to less than 650°C at a cooling speed 10-60K/min then 12h at 870°C.

Table F: Coating specifications

Coating	Spraying equipment	Powder	Thickness (µm)
Bond-Coat	JP-5000	Amperit 429 (-45+22µm)	180-300
Top Coat	FSH Cascade torch	Amperit 827.006	300-350

The small punch test discs (8 mm diameter and 0.5 mm thickness) have been manufactured by RSE with the sampling disc axis parallel to the plate thickness. No coatings have been applied to small punch discs, while ageing in the same two different conditions as uniaxial creep specimens (air or humidified air) has been applied to some discs. A piece of René 80 has received additionally heat treatment step 3+4 in the RSE laboratory as used during coating application and additional small punch discs have been prepared.
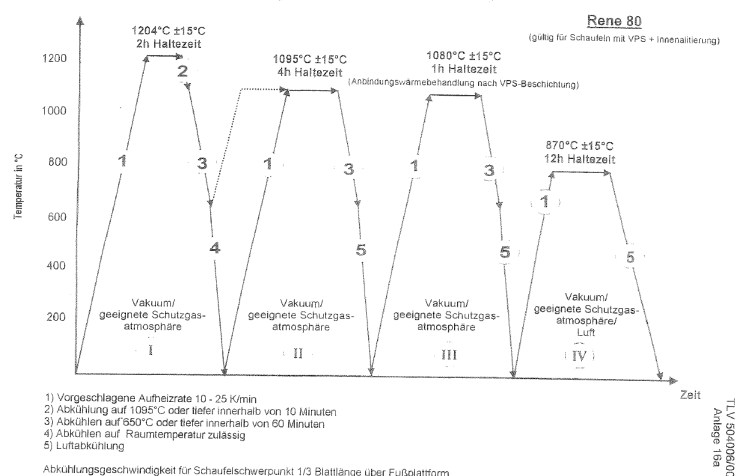

Figure 97: Overview of René 80 heat treatment: step 1-2-3-4.

Figure 98 represents the manufacturing, coating and ageing process of the creep samples before the samples are placed in the creep frame and the geometry of the creep samples. Table G and Table H represent the creep test program of Laborelec for the uncoated René 80 and the René 80 coated with the state of the art coatings.
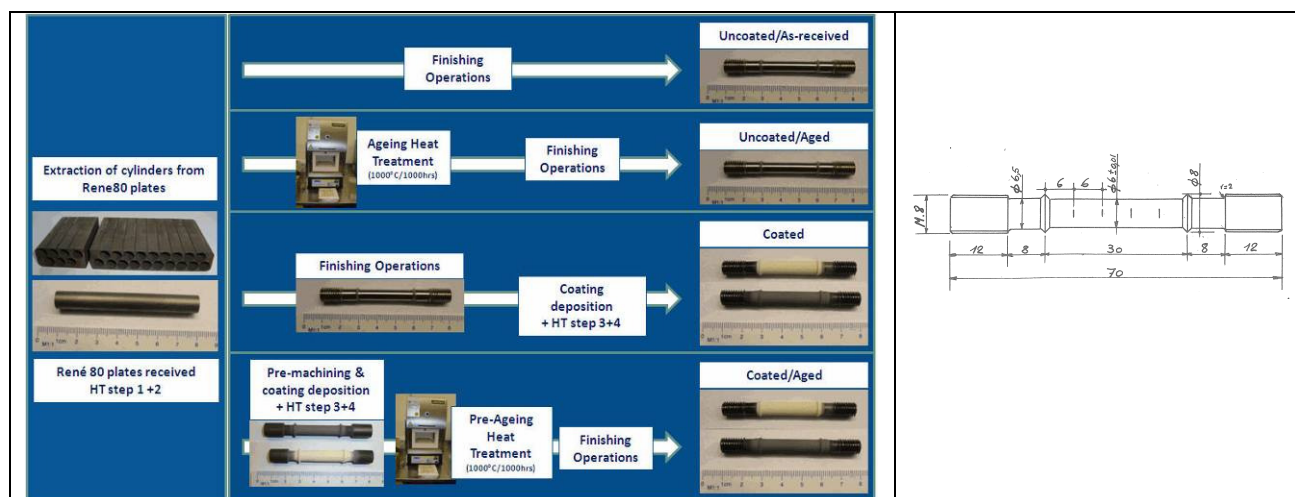
Figure 98: Left: Schematic view of preparation and pre-ageing of the non-coated and coated creep samples. Right: details of geometry creep sample

Table G: Test matrix creep testing at Laborelec of uncoated René 80

LBE reference sample	BM	Coating	Pre-ageing	Temp	Stress	Until rupture?
CT10-12-047T	René 80 HT	Uncoated	No HT Step 3+4	950	140	Y
CT10-04-028L	René 80	Uncoated	No	950	140	Y
CT10-04-028O	René 80	Uncoated	No	950	105	Y
CT10-04-028M	René 80	Uncoated	No	1050	50	
CT10-12-047K	René 80	Uncoated	No	1050	50	Y
CT10-12-047J	René 80	Uncoated	No	1050	40	Y
CT10-04-028S	René 80	Uncoated	In Air	950	140	Y
CT10-04-028T	René 80	Uncoated	In Air	950	105	Y
CT10-04-028U	René 80	Uncoated	In Air	1050	50	Y
CT10-04-028V	René 80	Uncoated	In Air	1050	40	Y
CT10-04-028X	René 80	Uncoated	In Air	950		SRT[1]
CT10-04-028P	René 80	Uncoated	In Air + 20%H_2O	1050	50	Y
CT10-04-028Q	René 80	Uncoated	In Air + 20%H_2O	1050	40	Y

Table H: Test matrix creep testing at Laborelec of René 80 coated with state-of-the-art coatings

LBE reference sample	Coating	Pre-ageing	Temp	Stress	Until rupture?
CT10-04-028F	SICoat2464 HVOF TBC	No	950	140	N - 0,8%
CT10-04-028H	SICoat2464 HVOF+ TBC	No	950	105	N - 0,8%
CT10-04-028K	SICoat2464 HVOF+ TBC	In Air (batch 04/2013)	950	105	N - 0,8%
CT10-12-047E	SICoat2464 HVOF+ TBC	In Air	950	140	N - 0,8%
CT10-12-047F	SICoat2464 HVOF+ TBC	In Air	950	105	N - 0,8%
CT10-12-047H	SICoat2464 HVOF+ TBC	In Air+ 20%H2O	950	140	N - 0,8%
CT10-04-028 A	SICoat2464 HVOF	No	1050	50	N - 0,8%
CT10-12-047B	SICoat2464 HVOF	In Air + 20%H2O	1050	50	Y
CT10-12-047D	SICoat2464 HVOF	In Air + 20%H2O	1050	50	Y
CT10-12-047C	SICoat2464 HVOF	In Air + 20%H2O	1050	50	N - 0,8%

---

[1] Stress Relaxation Test

3.2 Uniaxial creep results

3.2.1 Creep testers

Creep tests were carried out on ATS series 2320-MM dead weight single specimen lever arm creep testers with continuous strain monitoring (Figure 99). The calibrated load range of the frames is 1.11-11.1kN. Strain monitoring is done by means of series 4124 averaging extensometers type Heidenhain ST-12 (12mm range, 1µm accuracy). Furnaces are series 3210 split tube (three zone) type Kanthal A1 with a maximum temperature of 1100°C. Temperature is controlled and monitored by means of three N-type thermocouples attached to the specimen with quick tip connectors (Figure 100). These thermocouples are replaced for each test. For the creep samples coated with TBC all three thermocouples are attached on top of the TBC coating. Figure 101 shows a mounted creep sample inside the furnace.

Tests are carried out in an acclimatised room. The sample is heated to the test temperature and kept at that temperature for at least 2 hours in order to get a uniform temperature distribution. During this heating and soaking a small preload (<10% of the test force) is applied to keep the loading train well aligned. During the test, the temperature is controlled within ±5°C of the specified temperature for the test temperatures of 950°C and 1050°C.

All creep testers are equipped with a UPS to ensure unloading of the sample in case of a power interruption, to avoid overloading of the test piece due to contraction of the force assembly.

Figure 99 - ATS series 2320-MM dead weight single specimen lever arm creep testers with continuous strain monitoring.
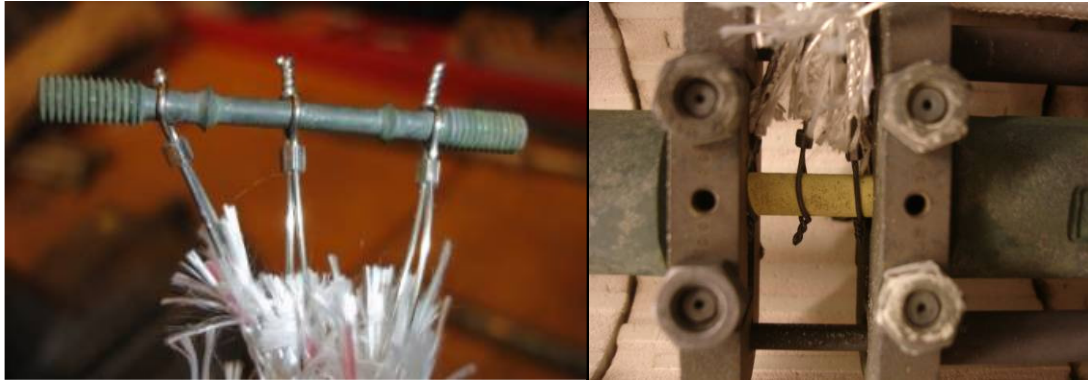
Figure 100 - Typical creep sample with the three attached N-type thermocouples used for temperature control. Left: uncoated sample, Right: coated sample in creep frame
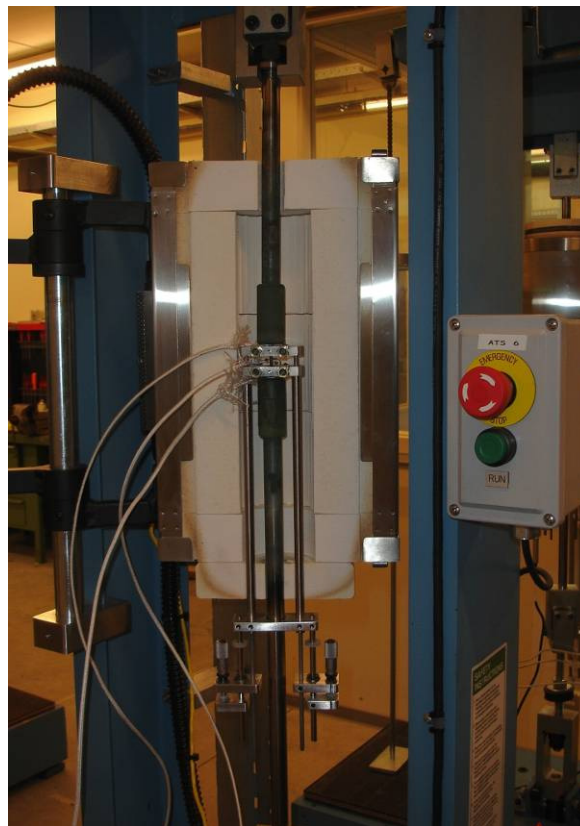

Figure 101 - Opened furnace showing a mounted creep sample with attached extensometer and thermocouples.

3.2.2   *René 80 with & without completed heat treatment*

As stated in chapter 3.1, the uncoated René 80 samples did not receive the full heat treatment as the coated samples or as the blades would receive. This means the gamma prime is different from the gamma prime as should be found in a gas turbine blade and therefore the mechanical properties will deviate as well. Therefore, Laborelec simulated the last two steps of the heat treatment in order to evaluate the effect of step 3+4. Figure 102 shows the creep curve of the fully heat treated sample together with the As Received René80 without pre-ageing and with the pre-ageing of 1000h at 1000°C in air.
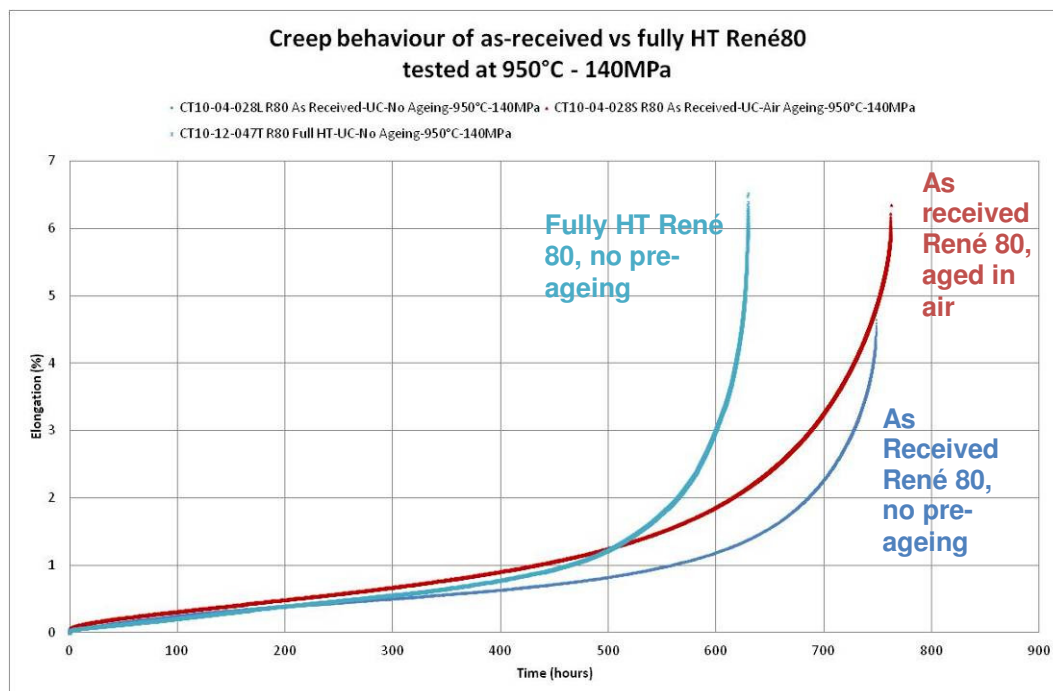
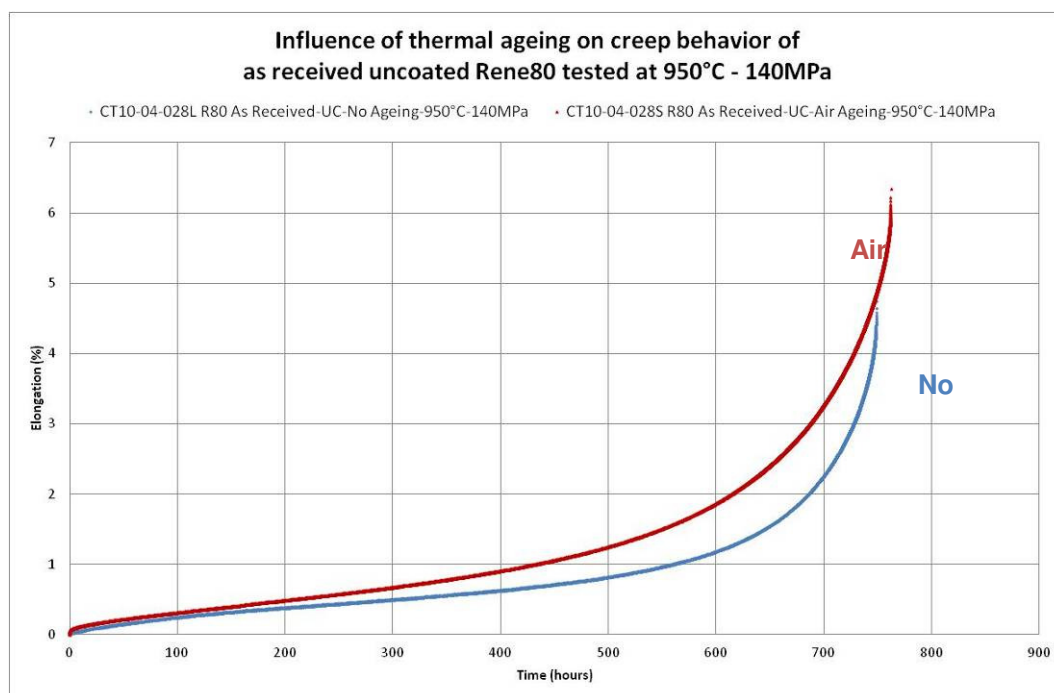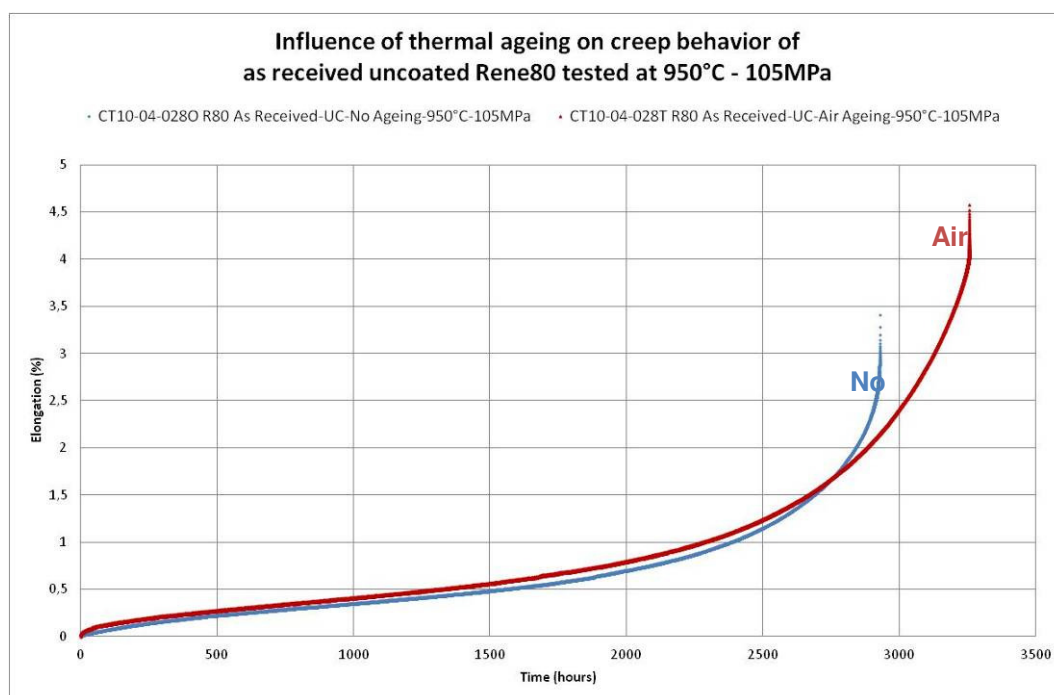**Figure 102 Creep curves of "as received uncoated René 80" without pre-ageing, with pre-ageing in air for 1000hrs at 1000°C and René 80 fully heat treaded without pre-ageing tested at 950°C and 140MPa.**

Figure 103 Graph representing minimum creep rate and time to rupture of "as received uncoated René 80" without pre-ageing, with pre-ageing in air for 1000hrs at 1000°C and René 80 fully heat treated without pre-ageing tested at 950°C and 140MPa

3.2.3 *Uncoated As received René 80*

Laborelec has creep tested "as received uncoated René 80" under 4 conditions: 950°C and 140MPa, 950°C and 105MPa, 1050°C and 50MPa, 1050°C and 40MPa. Figure 104 to Figure 108 represent the creep curves of all tests grouped for each condition. Figure 111 to Figure 112 summarize the minimum creep rate, time to rupture, time to 1% creep and elongation at rupture.

Figure 104 Creep curves of "as received uncoated René 80" without pre-ageing and with pre-ageing in air for 1000hrs at 1000°C tested at 950°C and 140MPa.

Figure 105 Creep curves after testing of "as received uncoated René 80" without pre-ageing and with pre-ageing in air for 1000hrs at 1000°C tested at 950°C and 105MPa.
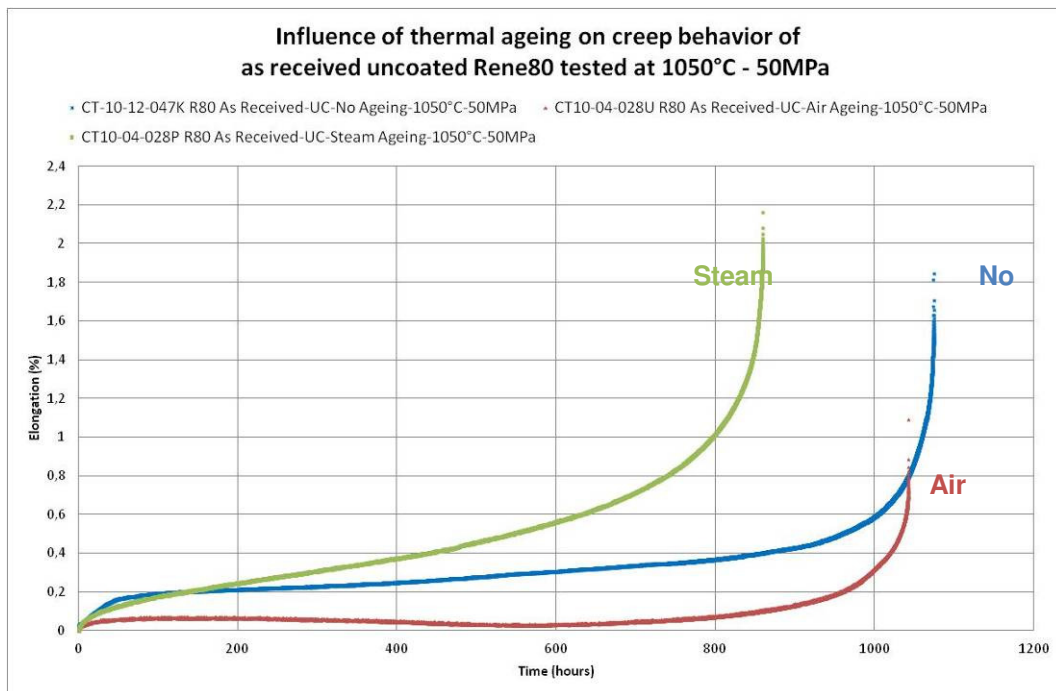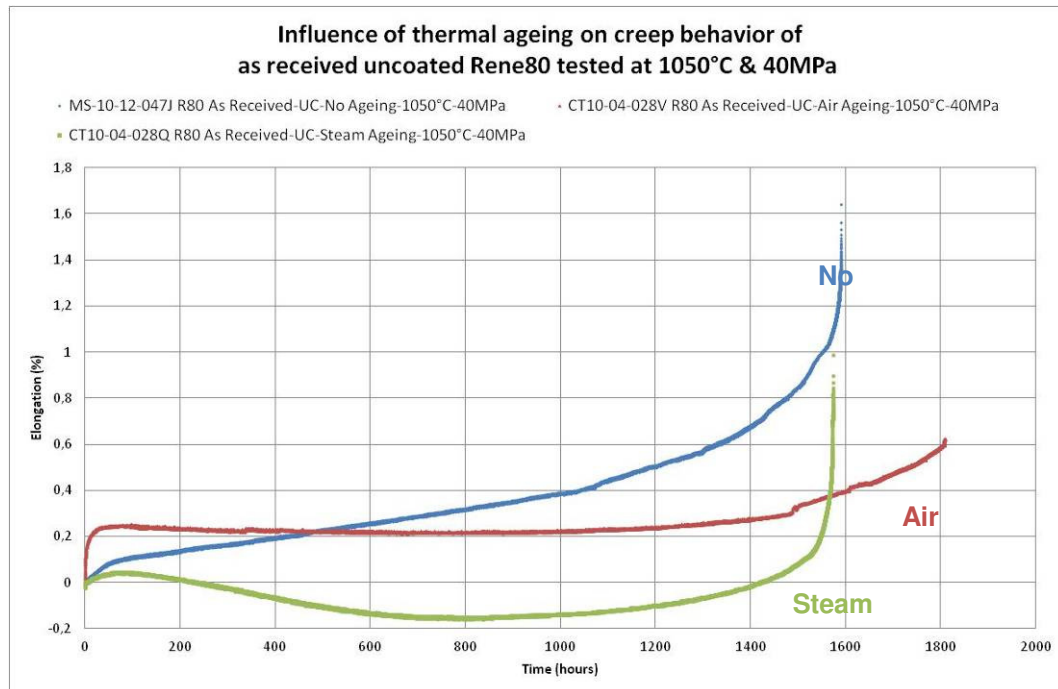
Figure 106 Creep curves after testing at 1050°C and 50Mpa of "as received uncoated René 80" without pre-ageing, with pre-ageing in air for 1000hrs at 1000°C, with pre-ageing in air + 20% steam for 1000hrs at 1000°C tested at 1050°C and 50MPa.
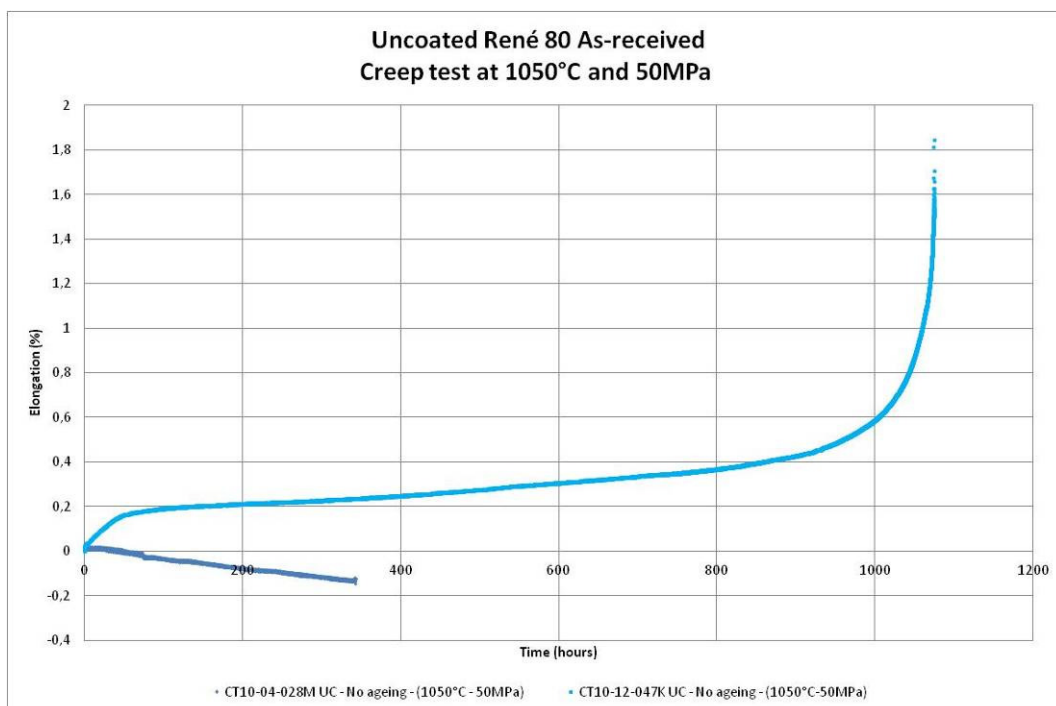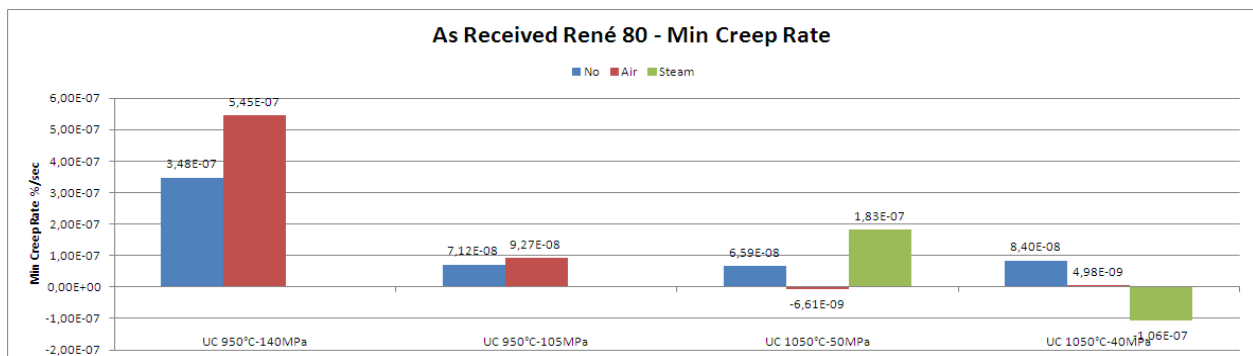

Figure 107 Creep curves of 2 samples "René 80" without pre-ageing, tested at 1050°C and 50MPa.

Figure 108 Creep curves after testing at 1050°C and 40MPa of "as received uncoated René 80" without pre-ageing, with pre-ageing in air for 1000hrs at 1000°C, with pre-ageing in air + 20% steam for 1000hrs at 1000°C tested at 1050°C and 40MPa.

Figure 109 Graph representing <u>minimum creep rate</u> for all creep tests of as-received uncoated René80
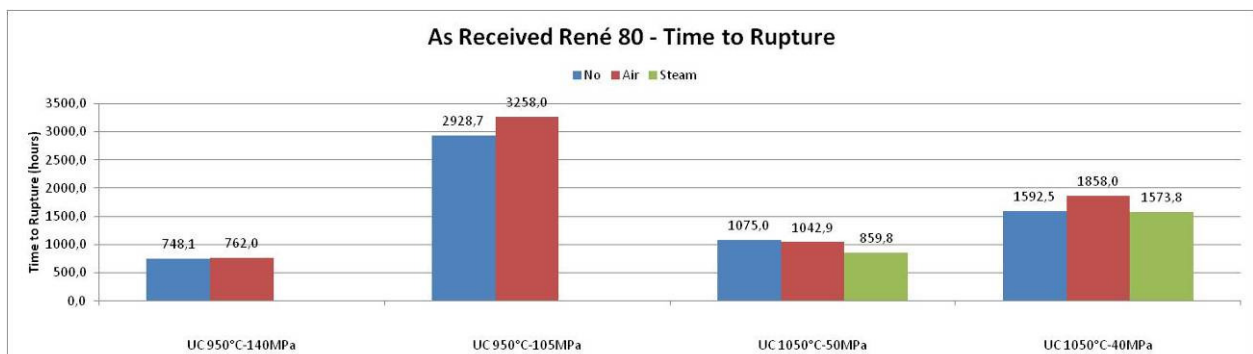
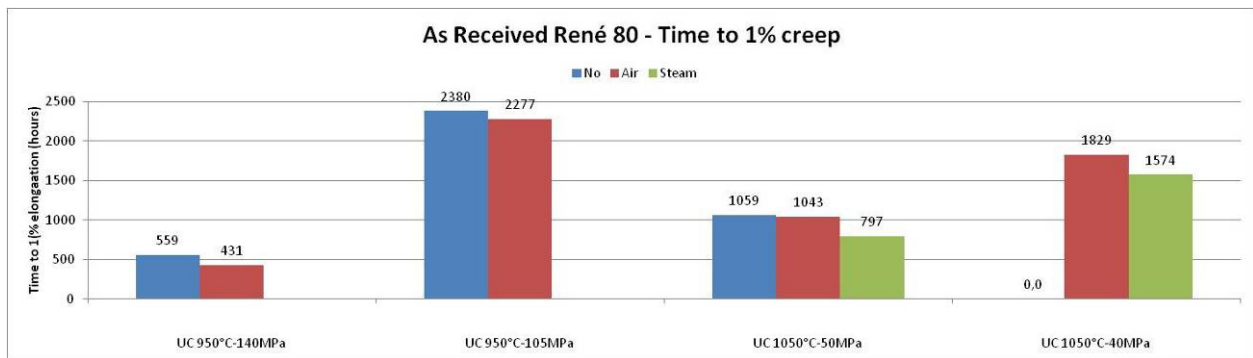**Figure 110 Graph representing <u>time to rupture</u> for all creep tests of as-received uncoated René80**

Figure 111 Graph representing <u>time to 1% creep</u> for all creep tests of as-received uncoated René80
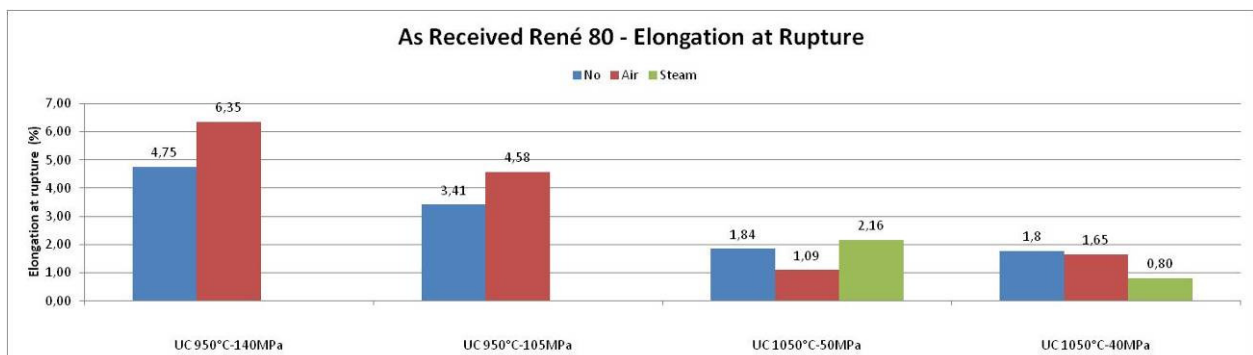

Figure 112 Graph representing <u>elongation at rupture</u> for all creep tests of as-received uncoated René80

3.2.4 *René 80 with SC2464 +TBC and SC2464*

The samples coated with Sicoat 2464 + standard TBC are tested under 2 conditions: 950°C and 140MPa and 950°C and 105MPa. The results are shown in Figure 113 to Figure 114. Test CT10-04-047F runned uptil 0.8% but data were loss due to a power cut. CT10-04-028K is still running to repeat test CT10-04-047F.
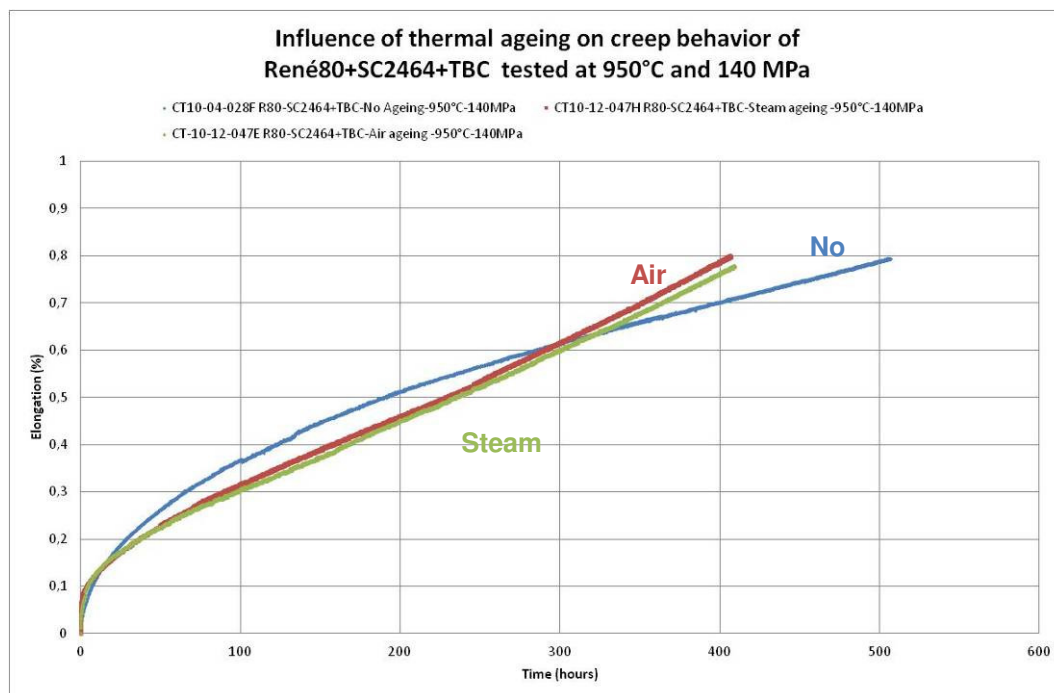

Figure 113 Creep curves of "René 80 + SC2464 + TBC" without pre-ageing, with pre-ageing in air and with pre-ageing in air + 20% steam, both for 1000hrs at 1000°C and tested at 950°C and 140MPa.
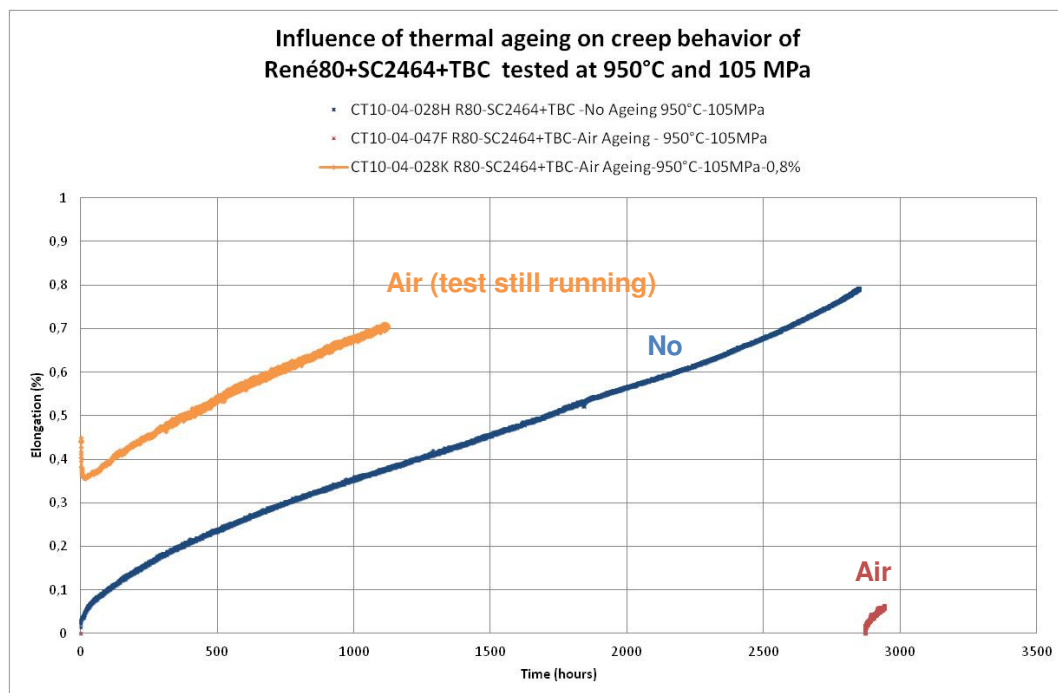
Figure 114 Creep curves of "René 80 + SC2464 + TBC" without pre-ageing and with pre-ageing in air for 1000hrs at 1000°C tested at 950°C and 105MPa.

Two test conditions were chosen to test the René 80 with only a SC2464 coating. One sample was not pre-aged, while the other samples were aged in air + 20% steam for 1000h at 1000°C. Figure 115 shows the creep curves for the tests performed. Two tests, blue and red curve, were performed until 0,8% elongation, while two other tests were performed till rupture (pink & orange curve). The tests until rupture both broke outside the shoulders of the specimen. Figure 116 summarizes the secondary creep rate. The secondary creep rate for the 3 specimens pre-aged in steam were nearly identical.
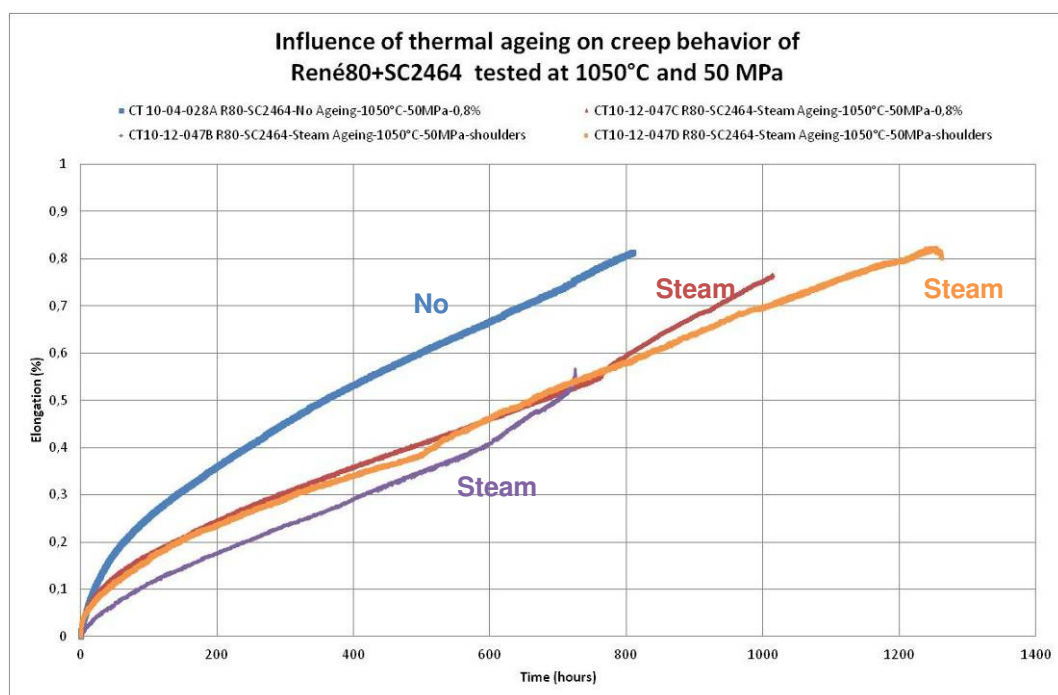

Figure 115 Creep curves of "René 80 + SC2464" without pre-ageing and with pre-ageing in air + 20% steam for 1000hrs at 1000°C tested at 950°C and 105MPa
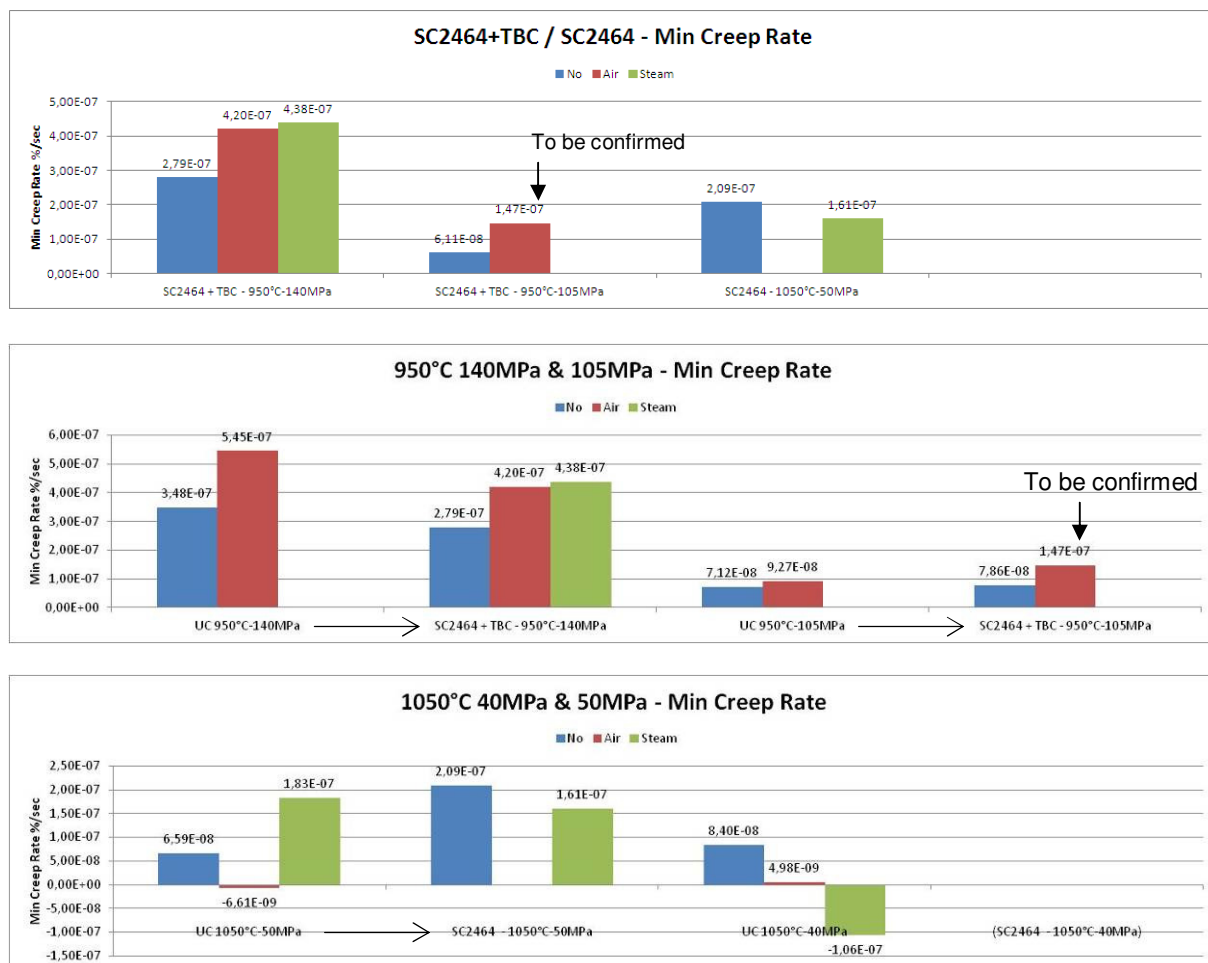
Figure 116 Graph representing <u>minimum creep rate</u> for all creep tests of "René 80 + SC2464 + TBC" and René80+SC2464 with comparison to uncoated samples.

3.3 Metallography related to uniaxial creep

Samples are electochemically etched in a mixture of 92 ml H_3PO_4, 5 ml H_2SO_4, 10 g CrO_3. A voltage of 3.6-4 V is applied for 10 to 30 seconds.

3.3.1 René 80 with completed heat treatment

Figure 117 compares the gamma prime microstructure of the plate material (René 80 as-received condition), root material of a first stage Si3D blade of a Siemens V94.2 unit. The primary gamma prime has a star shaped form and no secondary gamma prime is present. The microstructure in the root shows the presence of cubic primary gamma prime together with the secondary gamma prime.

Figure 118 compares the gamma prime microstructure after application of the step 3+4 (See Figure 97) heat treatment performed by Laborelec and Flamespray. Heat treatment at Laborelec and Flamespray followed heating procedures as provided in Figure 97 in a furnace in air. Samples are cooled in air. Flamespray carried out the heat treatment in a vacuum surface.

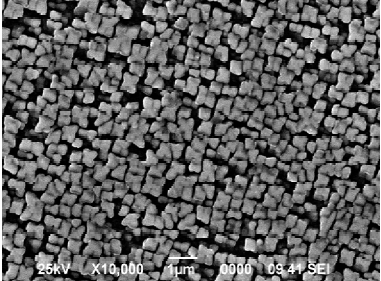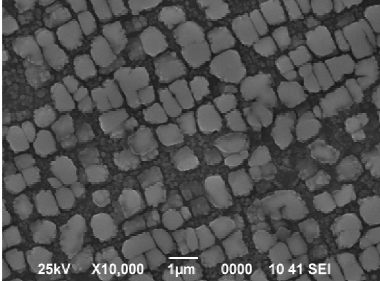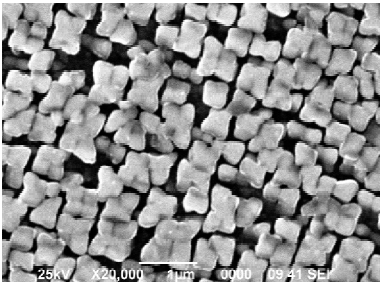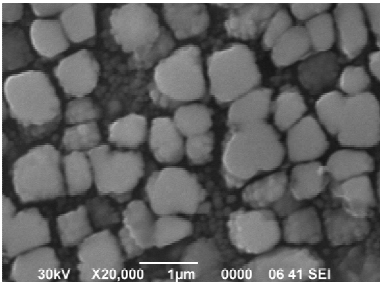Table I summarises the comparison of the microstructural features of the 4 samples.

As Received René 80 Plate material	René 80 Root material from a first stage Si3D blade of a Siemens V94.2
MS10-12-047V	MS09-12-014
HV20: 394±4	

Figure 117: Comparison of as received René 80 and root material of a Siemens V94.2 Si3D first stage blade.

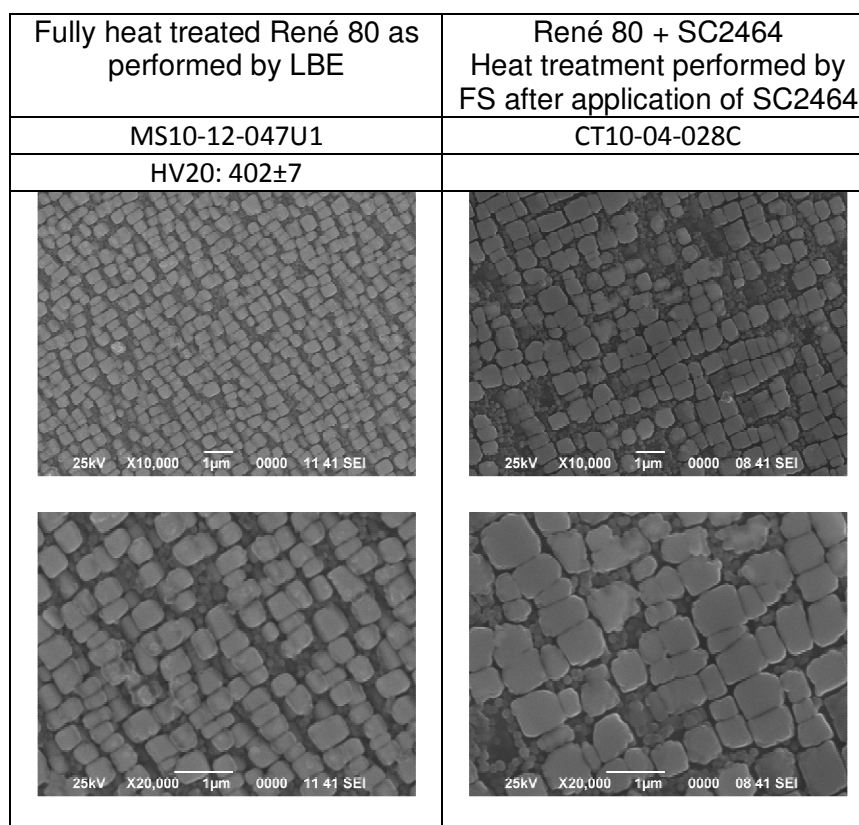| Fully heat treated René 80 as performed by LBE	René 80 + SC2464 Heat treatment performed by FS after application of SC2464
MS10-12-047U1	CT10-04-028C
HV20: 402±7	

Figure 118: Comparison of fully heat treated René 80 by LBE and fully heat treated René 80 by Flamespray after application of SC2464.

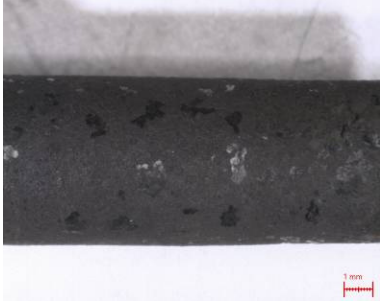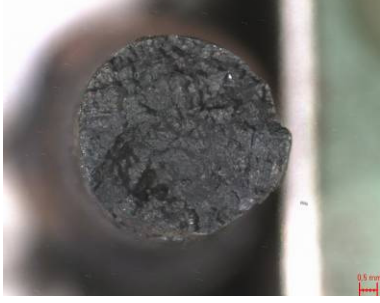**Table I: Microstructural features of as received René 80 and fully heat treated René 80 (heat treatment simulated by LBE) and root material of a Siemens V94.2 Si3D first stage blade**

Sample:	As Received René 80 Plate material	René 80 Root material from a first stage Si3D blade of a Siemens V94.2 GT	Fully heat treated René 80 as performed by LBE	René 80 + SC2464 Heat treatment performed by FS after application of SC2464
Sample ID:	MS10-12-047V	MS09-12-014	CT10-12-047U1	CT10-04-028C
Format Prim γ'	Star-shaped	cubical	cubical	cubical
Presence of Sec γ' size	No	Yes	Yes	Yes

Figure 119 and Figure 122 show the broken samples of René 80 as received (CT10-04-028L) and René 80 fully heat treated (CT10-12-047T) after the creep test at 950°C and 140MPa. Figure 120 shows the embedded samples, the visual aspect of the surface of the samples, the fracture surface, LOM microstructures near the fracture surface and at the surface and SEM images of the gamma prime morphology. The oxide layer formed on base material is thicker on the Fully HT sample and has partly spalled as can be noticed both on the external surface as on the LOM pictures. Creep voids are present in both samples, but the As Received sample showed more secondary cracks. No clear signs of secondary gamma prime are observed in the As Received sample, while signs of grown secondary gamma prime are still visible in the Fully heat treated sample. The rafting of the star shaped gamma prime is shown in Figure 120n. In the fully heat treated sample, still some signs of star-shape gamma prime can be seen with more pronounced near the fracture surface. Table J summarises the comparison of the microstructural features of the 4 samples.

Figure 119: Creep SAMPLE CT10-12-047T René 80 fully heat treated by Laborelec, tested at 950°C and 140MPa

CT10-04-028L R80 As Received-UC-No Ageing-950°C-140MPa	CT10-12-047T R80 Full HT-UC-No Ageing-950°C-140Mpa
CT10-04-028L	CT10-12-047T

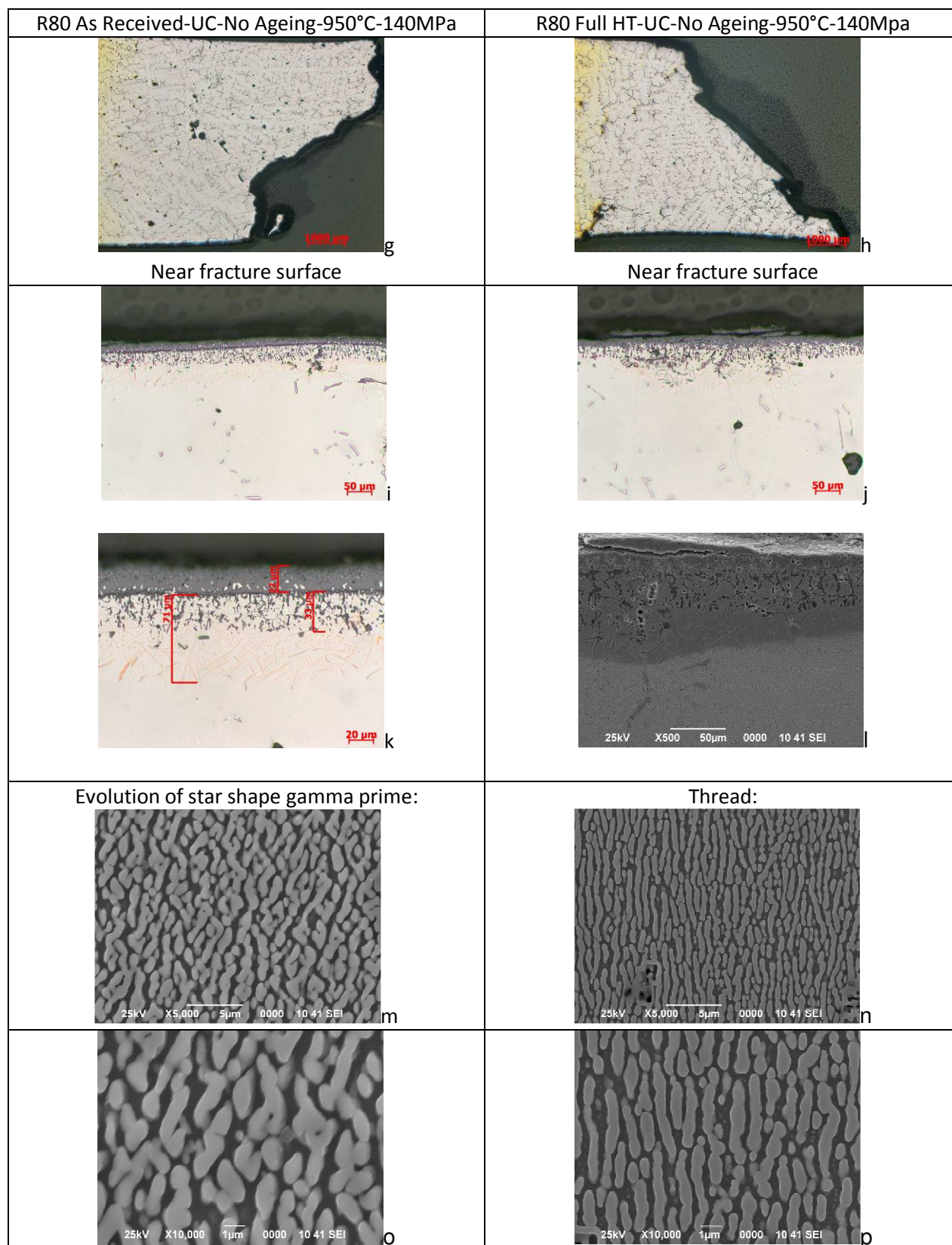| R80 As Received-UC-No Ageing-950°C-140MPa	R80 Full HT-UC-No Ageing-950°C-140Mpa
g	h
Near fracture surface	Near fracture surface
i	j
k	l
Evolution of star shape gamma prime:	Thread:
m	n
o	p

Figure 120: Metallurgical analyses of creep samples René 80 as received and René 80 fully heat treated after creep test at 950°C and 140MPa

Table J: Microstructural features of creep samples René 80 as received and René 80 fully heat treated after creep test at 950°C and 140MPa

Sample:	R80 As Received-UC-No Ageing-950°C-140MPa	R80 Full HT-UC-No Ageing-950°C-140Mpa	R80 As Received-UC-No Ageing-950°C-140MPa	R80 Full HT-UC-No Ageing-950°C-140Mpa
Sample ID:	CT10-04-028L	CT10-12-047T	CT10-04-028L	CT10-12-047T
Location	Mid thread	Mid thread	Fracture	Fracture
Format Prim γ'	Rafted with signs of star shaped gamma prime	Rafted, less signs of star shaped gamma prime	Rafted with signs of star shaped gamma prime	Rafted with signs of star shaped gamma prime
Presence of Sec γ' size	No	Yes	No	Yes

3.3.2   Uncoated as received René 80 with 3 pre-aging conditions

Figure 122, Figure 123 and Figure 124 show the visual appearance of the uncoated as received René80 samples after the creep tests at various parameters. The appearance of the external surface can be linked to the temperature and the time of the creep test. Figure 121 shows the time to rupture for all tests. The test at 950°C and 140 MPa with a test duration of approximately 800 hours still have a smooth surface, while the surface of the tests at 950°C and 105MPa with a test duration of approximately 3000hrs is oxidated. The tests at 1050°C are more heavily oxidised with a green oxide layer. The tests with the longest duration have the roughest surface appearance.
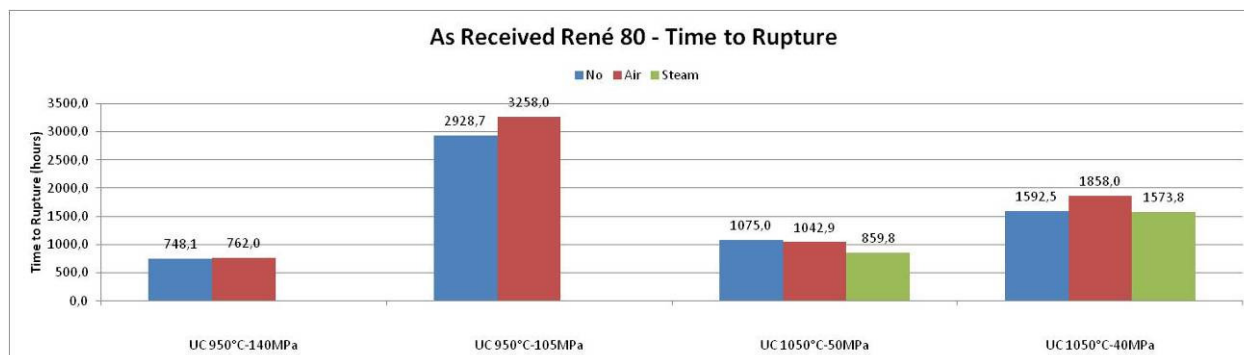

Figure 121: Time to rupture of creep tests on uncoated as received René 80 at different test parameters.

Figure 122: Creep samples of Uncoated as received René 80 after creep test till rupture at different test parameters.

Figure 123: Creep samples of "Uncoated as received René 80 pre-aged in air (1000hr, 1000°C) after creep test till rupture at different test parameters.

Figure 124: Creep samples of "Uncoated as received René 80 pre-aged in air+20% steam (1000hrs at 1000°C) after creep test till rupture at different test parameters. Sample on the right is not tested.

Figure 125 compares the metallographic investigation of the Uncoated René 80 samples tested at 1050°C and 40MPa. The samples without pre-ageing and pre-aged in air are broken close to the end of the section, while the sample pre-aged in air + 20% steam has broken in the middle of the section. Time to rupture of the three samples is between 1550 and 1900 hours. The visual aspect of the oxides at the surface of the mid-section of the samples is similar. The base metal is oxidised up to a depth of about 190µm. The oxide scale thickness on the analysed sections is up to 30µm. Creep porosities can be observed in the three samples as well as secondary creep cracks.
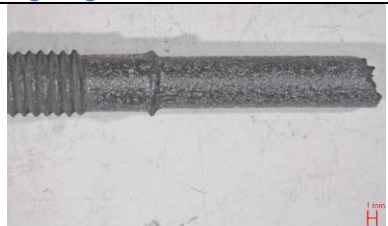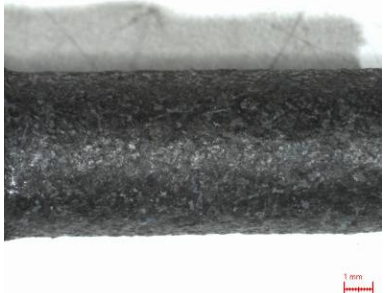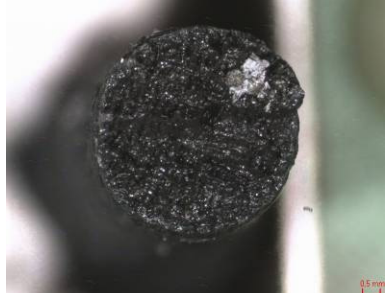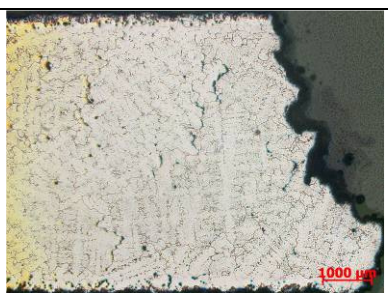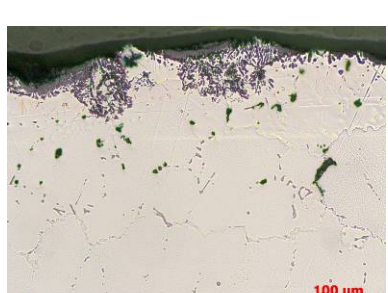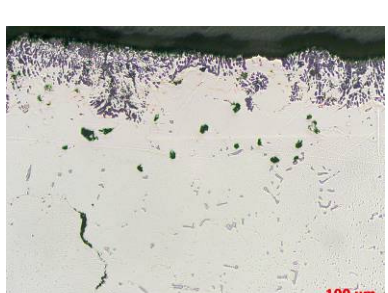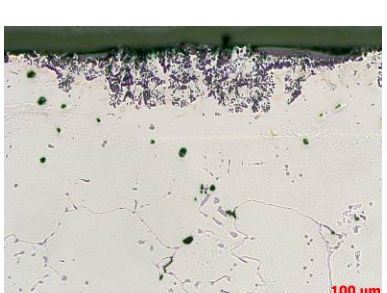
CT10-12-047J R80 As Received-UC-No Ageing-1050°C-40MPa	CT10-04-028V R80 As Received-UC-Air Ageing-1050°C-40MPa	CT10-04-028Q R80 As Received-UC-Steam Ageing-1050°C-40MPa
Fracture close to end of section	Fracture close to end of section	Fracture in middle of section
		Gamma prime see Figure 126

Figure 125: Metallurgical analyses of creep tests at 1050°C and 40MPa for uncoated René 80.

Figure 126 shows the gamma prime of 2 René 80 samples tested at 1050°C and 50MPa for 350h and at 1050°C and 40MPa for 1574h. Sample CT10-12-028M has a nearly cubic gamma prime shape with the presence of secondary gamma prime. The gamma prime of sample CT10-04-028Q starts to raft from a nearly cubic gamma prime. A lot of secondary gamma prime is present.

CT10-12-028M R80 As Received-UC-No Ageing-1050°C-50MPa stopped after 350h of creep test	CT10-04-028Q R80 As Received-UC-Steam Aged-1050°C-40MPa After rupture at 1574h
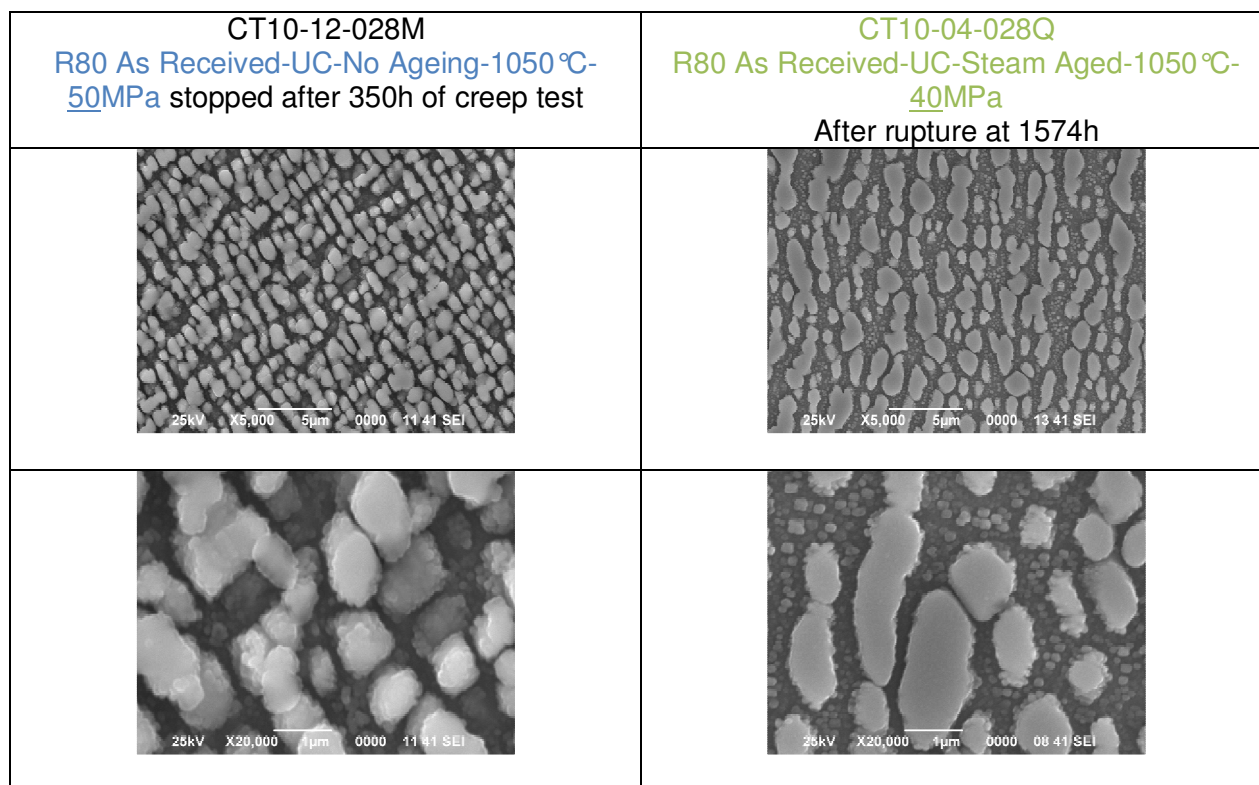
Figure 126: Metallographic structure of 2 René 80 samples tested 350h at 1050°C and 50Mpa and tested for 1574h at 1050°C and 40MPa.

Table K: Microstructural features of uncoated René 80 tested 350h at 1050°C and 50Mpa and tested for 1574h at 1050°C and 40MPa.

Sample:	R80 As Received-UC-No Ageing-1050°C-50MPa after 350h of creep test	R80 As Received-UC-Steam Aged-1050°C-40MPa After rupture at 1574h
Sample ID:	CT10-12-028M	CT10-04-028Q
Location	Mid	Near fracture surface
Format Prim γ'	Cubic	Cubic to start of rafting
Presence of Sec γ' size	Yes	Yes

3.3.3 René 80 + SC2464 + TBC

Figure 127 shows the optical image of the TBC coated samples in the 3 pre-ageing conditions. There are little porosities in the interface between the base material and MCrAlY for the non-pre-aged sample while there are many in both the aged samples. There is still a good bonding for the sample without pre-ageing and pre-aged in air while the TBC seems to come loose for the sample aged in steam. The beta aluminium zone of the SC2464 has depleted for the pre-aged samples.

CT10-04-028I R80-SC2464+TBC-No Ageing- No creep test	CT10-04-028J R80-SC2464+TBC-Air Ageing- No creep test	CT10-12-047I R80-SC2464+TBC-Steam Age- No creep test

Figure 127: Microstructural features of "René 80 + SC2464 + TBC" without pre-ageing, with pre-ageing in air for 1000hrs at 1000°C and with pre-ageing in air + 20% steam for 1000hrs at 1000°C before creep test.

Figure 128 shows the result of the metallographic investigations of the samples after creep testing at 950°C and 140MPa. Kirkendall porosities are present in between the base metal and SC2464 with increasing amount for the samples pre-aged in air and pre-aged in steam. The TBC coating spalled for the test aged in air at dismantling. The TBC is nearly spalled as well after steam ageing but not without pre-aging. The gamma prime evolution is less evolved for the sample without pre-ageing and more evolved for both pre-aged samples. Gamma prime start to raft for the 3 samples. Some secondary gamma prime is still present. Table L summarises the microstructural features as observed on the 3 samples.
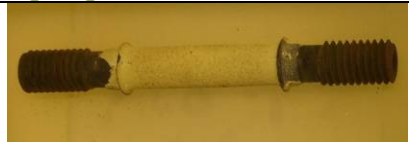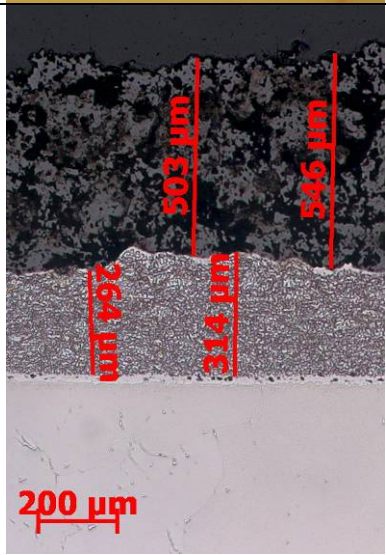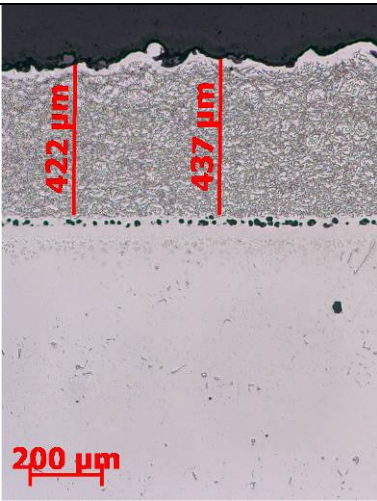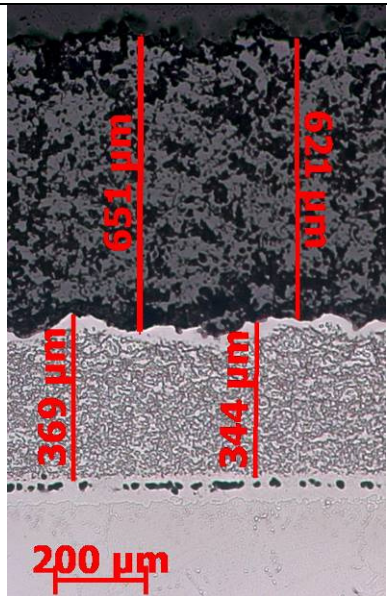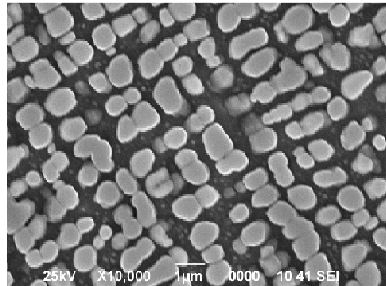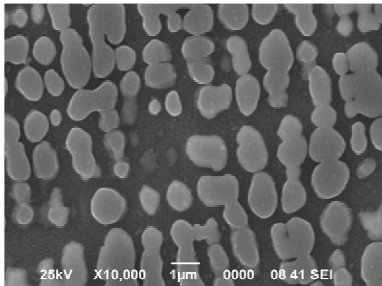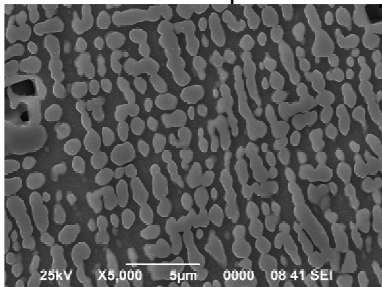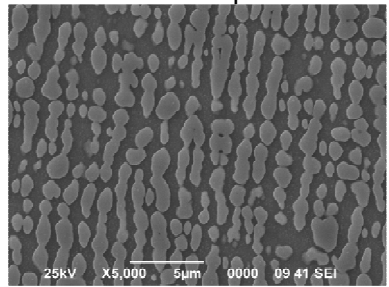
CT10-04-028F R80-SC2464+TBC-No Ageing-950°C-140MPa-0,8%	CT10-12-047E R80-SC2464+TBC-Air Ageing-950°C-140MPa-0,8%	CT10-12-047H R80-SC2464+TBC-Steam Ageing-950°C-140MPa-0,8%
Thread	Thread	Thread
Mid Sample	Mid sample	Mid sample

Figure 128: Microstructural features of "René 80 + SC2464 + TBC" without pre-ageing, with pre-ageing in air for 1000hrs at 1000°C and with pre-ageing in air + 20% steam for 1000hrs at 1000°C tested at 950°C and 140MPa.

Table L: Microstructural features of "René 80 + SC2464 + TBC" without pre-ageing, with pre-ageing in air for 1000hrs at 1000°C and with pre-ageing in air + 20% steam for 1000hrs at 1000°C tested at 950°C and 140MPa.

Sample:	CT10-04-028F R80-SC2464+TBC-No Ageing-950°C-140MPa-0,8%	CT10-12-047E R80-SC2464+TBC-Air Ageing-950°C-140MPa-0,8%	CT10-12-047H R80-SC2464+TBC-Steam Ageing-950°C-140MPa-0,8%
Sample ID:	CT10-04-028F	CT10-12-047E	CT10-12-047H
Location:	Mid sample	Mid sample	Mid sample
Format Prim γ'	Start of rafting from cubic gamma prime	Start of rafting from cubic gamma prime	Start of rafting from cubic gamma prime
Presence of Sec γ' size	Yes	Yes, Little amount	Yes

3.3.4 René 80 + SC2464

Figure 129 shows the René 80+ SC2464 samples without pre-ageing and pre-aged in air+20% steam (1000hrs at 1000°C) after creep testing. As in the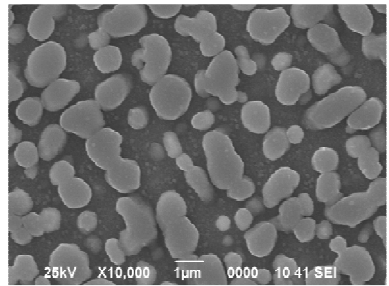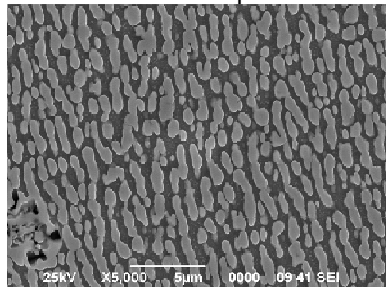 TBC coated samples, porosities are present in between the base metal and SC2464 with increasing amount for the samples pre-aged in air and pre-aged in steam.

Figure 129: Creep samples of "René 80+sc2464 without pre-ageing and pre-aged in air+20% steam (1000hrs at 1000°C) after creep test.

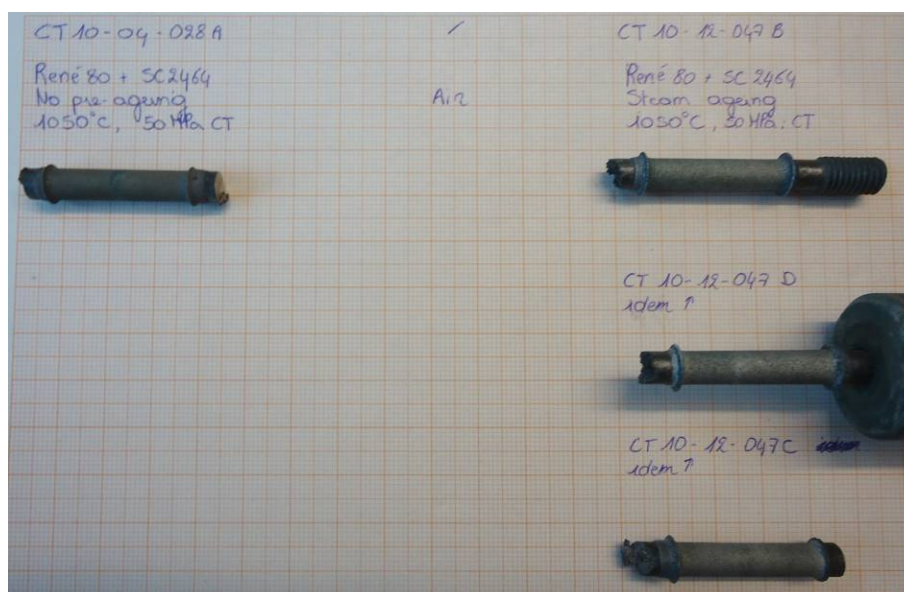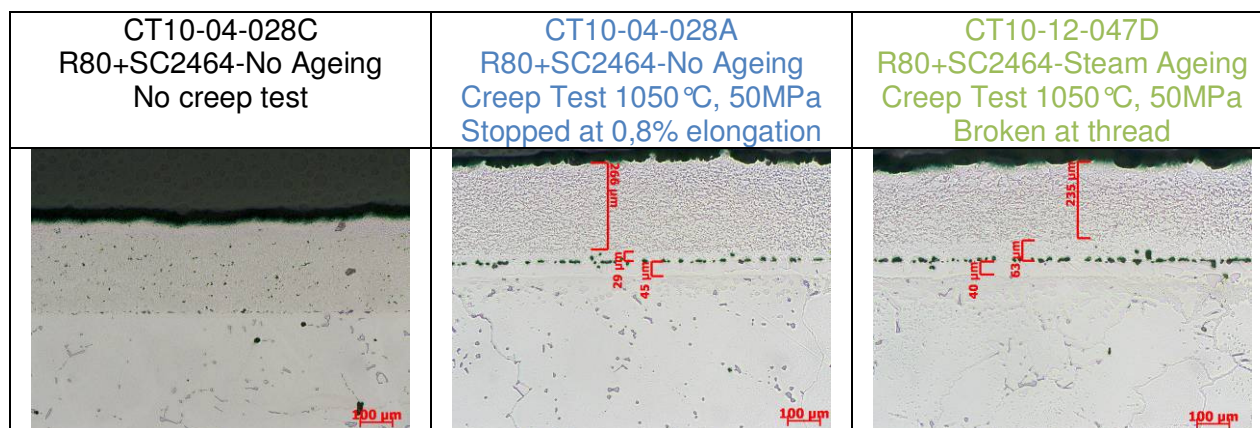| CT10-04-028C R80+SC2464-No Ageing No creep test	CT10-04-028A R80+SC2464-No Ageing Creep Test 1050°C, 50MPa Stopped at 0,8% elongation	CT10-12-047D R80+SC2464-Steam Ageing Creep Test 1050°C, 50MPa Broken at thread

Figure 130: Microstructural features of "René 80 + SC2464" without pre-ageing before and after creep task at 1050°C and 50MPa. After steam ageing and creep test at 1050°C and 50MPa.

3.4 Discussion on uniaxial creep results

3.4.1 René 80 with & without completed heat treatment

As discussed in previous chapters, René 80 with the fully heat treated condition, has been tested additional to the initial agreed work program in order to check the influence of the missing heat treatment on uncoated René 80 compared to the coated samples. The heat treatment needed on René 80 blades after casting are represented in Figure 97. Step 1 is the solution heat treatment. Step 2 is the stabilisation of the gamma prime. Step 3 is performed to further stabilize the gamma prime and to achieve a good bonding quality of MCrAlY coating. During step 4, the secondary gamma prime is formed. The uncoated samples (As Received) received HT step 1+2. The coated samples received HT step 1 to 4.

The microstructural analyses confirmed that the microstructure of the "As Received" material is not conform with the microstructure as found in a blade. The γ' morphology of the as-received René 80 has a star-shaped morphology. The primary gamma prime is formed, but not yet stabilized. No secondary gamma prime is present. The sample with the completed heat treatment have cubical primary γ' and secondary gamma prime. The microstructure is comparable to the microstructure observed in the root material. The samples that received a coating have similar microstructure as the fully heat treated samples at Laborelec, although the primary gamma prime is slightly larger for the coated samples.

In contrary with the expectations, the fully heat treated sample has a slightly higher secondary creep rate as the "As Received René 80" tested at 950°C and 140MPa. The microstructure of the "As Received" René 80 shows clearly signs of the initial star-shaped gamma prime and the evolution towards rafting. The "fully heat treated sample" still show some signs of initial star shaped gamma prime. Therefore it is assumed that the gamma prime was not fully stabilized after the heat treatment.

The influence of 1000h pre-ageing at 1000°C is barely visible for the tests at 950°C and 140MPa and 105MPa.

Some of the tests performed at 1050°C show first a shrinkage of the sample before the sample starts to elongate. This behaviour is unusual. Therefore, microstructural analyses are made afterwards in order to understand the phenomena and evaluate if the test results can be used as such.

Sample CT10-04-028M was tested at 1050 °C and 50MPa. The test was first stopped after 70h, then restarted and stopped at 350 hours since a negative trend was observed (Figure 107) which is unusual. Figure 126 shows the metallurgical investigation of sample CT10-04-028M. The initial microstructure, the star shaped gamma prime (Figure 117) has evolved towards cubic gamma prime of comparable size. Additionally the presence of secondary gamma prime is clearly visible. Sample CT10-12-047K, supposed to be in identical state as sample CT10-04-028M was tested under similar conditions, whereby no negative elongation was observed.

Sample CT10-04-028Q was pre-aged in air + 20% steam and broke after 1574h. This sample had a large negative elongation of almost -0.2% up to 800h. The presence of the large amount of secondary gamma prime is remarkable. This is again a sign that a remarkable transformation of the microstructure took place.

The "as-received René 80" is an unstable microstructure when exposed to temperatures of 1050 °C. The transformation in microstructure seems to be a contributing factor for the negative elongation of the samples. Therefore, the absolute results of the creep tests of "As-Received René 80" cannot be used.

But more research would be needed to study in detail this phenomena and the effect on the long term mechanical properties at 1050 °C.

3.4.2 *Literature data on René 80*

A literature search was performed in order to find reference creep data of René 80 material. In total 6 relevant sources [Ref 1 to 6] with in total 34 data points were found. The literature data was fitted by different creep models among others: Larson Miller, Manson Brown, Sherby Dorn and Soviet Model. The literature data were fitted most accurately following the Larson Miller model with N=4. This model plot the applied stress vs the time to rupture for different temperatures.

$$f(\sigma) = T(\log t_r + C)$$
$$\text{For N= 4: } f(\sigma) = B_0 + B_1 * \sigma + B_2 * \sigma^2 + B_3 * \sigma^3 + B_4 * \sigma^4$$

The C is calculated for the model and is found to be 13.75 which is low compared to the value of 20 which is commonly used for Ni-base superalloys. R^2 is 0.95. Additionally to the literature data (round dots), 5 data points of LBE creep tests are added as well (square dots). Literature data with time to rupture below 10 hours are not taken into account in the model.
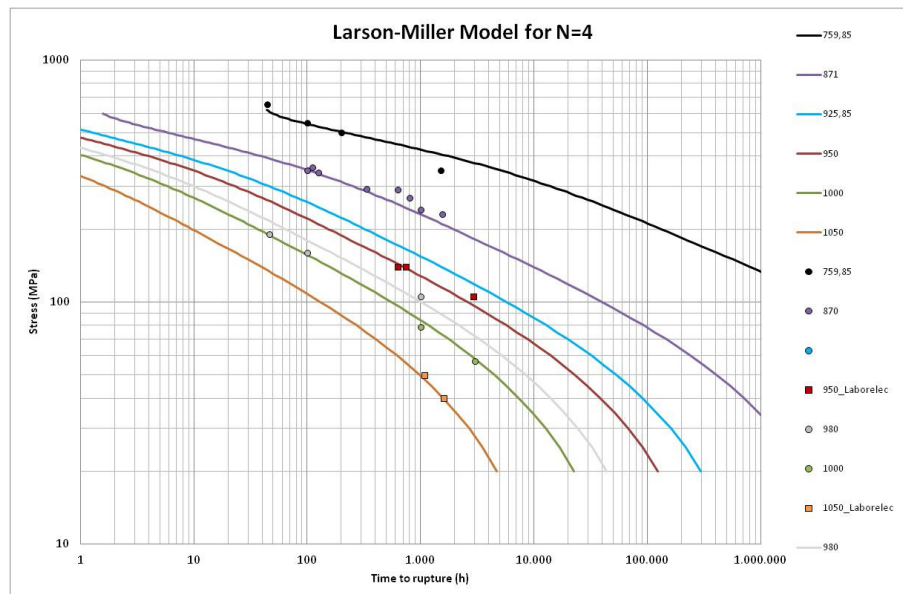
Figure 131: Larson miller model for N=4 for uncoated René 80 based on literature data and Laborelec test results

3.4.3 Influence of pre-aging on creep resistance of uncoated as received René 80

Figure 132 shows in detail the test results of uncoated René 80 aged in different environments vs Larson-Miller Model for N=4 of virgin René 80 material.

The test at 950°C show nearly no influence of thermal ageing in air. This is not abnormal since 1000 hours ageing is not a lot compared to the time a blade is placed in a gas turbine, which is 24000 to 30000 OH before the blade is extracted and repaired or declared scrap. The samples aged in air show even a slightly better creep resistance, although the results of the creep tests are within an acceptable scatterband both for tests at 105MPa and 140MPa. As discussed previously, the creep resistance of the fully heat treated René 80 is slightly lower as well. This can be due to a transformation in microstructure.

At 1050°C, negative creep is observed for 1 out of 3 samples without pre-ageing, for all 2 samples pre-aged in air and for 1 sample out of 2 pre-aged in steam. Some samples with the similar initial state tested at the same conditions show not always negative creep. At 1050°C, the steam ageing compared to the air ageing has a negative influence on the creep strength of the material. Ageing in steam lowers the time to rupture for the applied stresses.
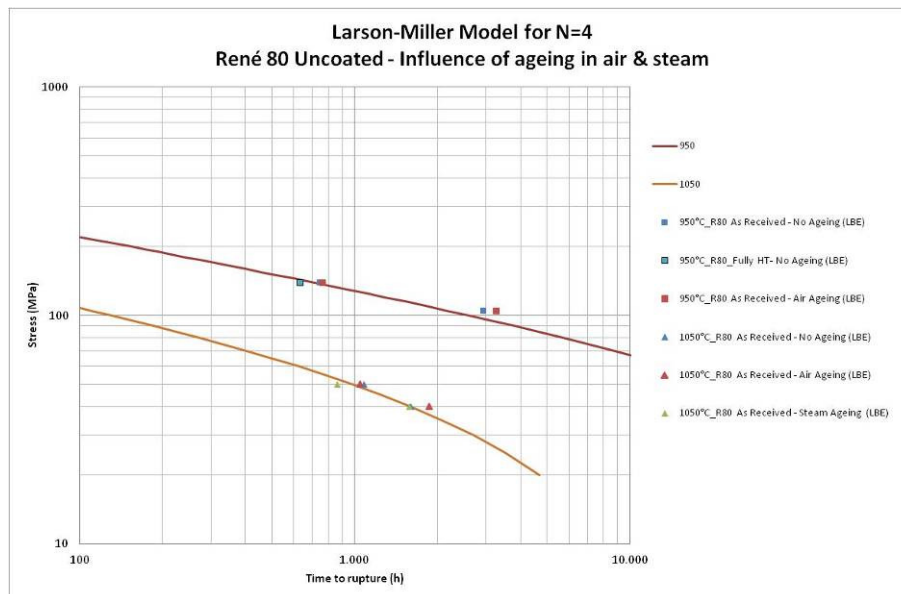
Figure 132: Test results of uncoated René 80 aged in different environments vs Larson-Miller Model for N=4 of virgin René 80 material.

3.4.4 Influence of pre-aging on creep resistance of René 80 + SC2464 + TBC

The creep curves, as shown in Figure 113, of the samples tested at 950°C and 140MPa show an identical behaviour for the samples aged in air and in air + 20% steam. The secondary creep strength of the samples without pre-aging is lower as for the aged samples. This is confirmed by the analyses of the microstructures as well as seen in Figure 128. The gamma prime evolution is less evolved for the sample without pre-ageing and more evolved for both pre-aged samples. The TBC coating spalled for the test aged in air at dismantling. The TBC is nearly spalled as well as shown in Figure 128 after steam ageing but not without pre-aging.

No confirmative interpretation can be provided currently for the tests at 950°C and 105MPa since the test at 105MPa must be repeated due to data loss. The test is still running at the time of writing this report, but the curve is added as well. Up to 400h, a secondary creep rate of 1,02 E-7 %/sec is measured. No explanation can be found why the elongation starts at 0.4% instead of 0%. Based on the current status of the test, the same trend is observed as for the test at 140MPa.

The ageing of steam on TBC coated samples has no influence compared to ageing in air. Secondary creep rate is identical. The ageing in air or air+20%steam for 1000 hours at 1000°C has a small negative influence compared to the samples without pre-ageing.

3.4.5 Influence of pre-aging on creep resistance of René 80 + SC2464

In contrast to TBC coated samples, the secondary creep rate decreased for samples aged in air + 20% steam compared to samples without pre-aging. But 1 sample pre-aged in steam, broke earlier after about 750 hours.
Although the tests are carried out at 1050°C, no negative creep was observed. Therefore it is assumed that the fully heat treated René 80 is more stable than the As-Received René 80.

3.4.6 Influence of coating on creep resistance of René 80

The influence of the application of a coating on the secondary creep rate is presented in Figure 116. Since the microstructures of the as-received René 80 samples are not in the same initial state as the coated samples, no conclusions can be made.

The state of initial microstructure of the René 80 base material determines the creep strength of the material. No cracks were observed in the SC2464 or TBC that could possibly lead to preliminary crack initiation in the base metal.

3.5 Small punch creep

The life assessment and potential for possible failure of in service components is a critical issue in the safety and reliability analysis of industrial plants operating at elevated temperature for long times, when mechanical properties of their structural elements, in particular the creep resistance, can be severely impaired. The component integrity can be rarely evaluated with the traditional and well-standardised mechanical test techniques, such as the uniaxial creep test, because there is insufficient material to sample non-invasively from the component. Hence, the need for evaluating the residual mechanical properties of structural components by direct testing methods has led to innovative techniques based on miniaturised specimens: among these, a technique called the Small Punch Creep (SPC) test can be considered as effectively a non-destructive technique because of the very limited amount of material to be sampled, as an efficient and cost-effective technique having the potential to enable measurement of the realistic material properties for the specific component, identifying the present state of damage and focusing on the more critical (more stressed, more damaged) locations in the component.

A Code of Practice (CoP) standardising Small Punch test was developed by a CEN Workshop Agreement in 2006: Part A concerned the time dependent SP, also called Small Punch Creep, which is the object of this report, when Part B defined the time independent SP, by which tensile and fracture material properties can be inferred.

SPC test is performed at constant temperature, above creep threshold, on a small specimen, typically a disk ø8 mm diameter, 0.5 mm thick, constantly loaded by means of a hemispherical punch, which displacement is measured and plotted versus test time.

1. SP disc test-piece
2. Hemispherical ended punch
3. Lower die
4. Upper die
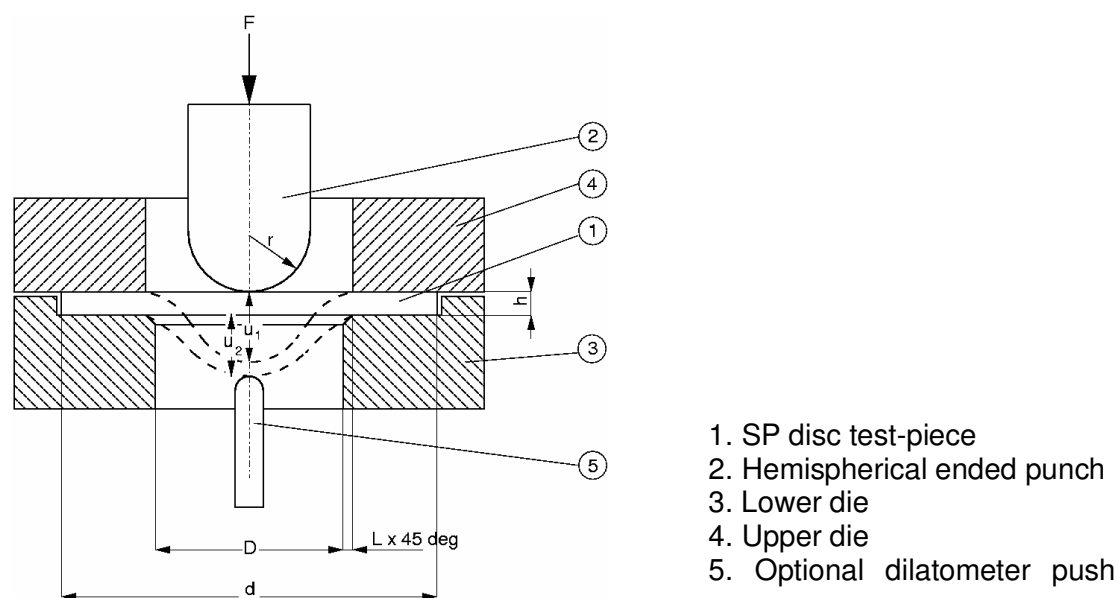5. Optional dilatometer push

Figure 133 – Small Punch Test schematics

The applied load has to be determined from geometrical factors and material properties in order that creep failure in the Small Punch Creep test will occur at the same time as that in a conventional uniaxial creep test at the same temperature. For the case where there is no prior

information on expected behaviour, the ratio of SP test load (F) to the uniaxial creep stress (σ), according to stretching membrane theory, is given by:

$$F/σ = 3.33k_{SP} R^{-0.2} r^{1.2} h_0$$

r: punch indenter radius (1.25 mm at RSE rig)
h_0: test-piece thickness (0.5 mm standard value)
R: receiving hole radius (2 mm at RSE rig)

The SP creep test correlation factor, k_{SP} has first to be determined empirically for the particular material under test but, where k_{SP} is not known, the first tests should be set up assuming $k_{SP}=1$ and a subsequent series of a minimum of 5 tests are needed to tune k_{SP} parameter at one particular temperature.

3.5.1 As received Rene 80

3.5.1.1 As received Rene 80 without ageing

A first series of SPC tests on as received Rene 80 (partially heat treated excluding final steps applied during coating) has been performed at 950 °C and 1050 °C with the aim to have at both temperature tests with 1000 h and 3000 h duration, similarly to tests performed by Laborelec with standard uniaxial specimens. According to literature, data on Rene 80 and to H₂-IGCC Partners' experience, stress for the assumed target time in uniaxial creep should be considered 140 and 105 MPa at 950 °C and 50 and 40 MPa at 1050 °C.

Past experience at RSE on wrought nickel alloy, as Udimet 520 and cast nickel alloy IN939, suggested the possibility to apply a K_{SP} factor in the range 0.75-0.85 in the equation proposed by CEN Small punch Code of Practice, for estimating the correspondent load to be applied in small punch creep. Based on the choice of testing this kind of nickel alloy at the maximum temperatures from those available in RSE database a conservative initial assumption of K_{SP} = 0.78 has been adopted.

For the geometry of RSE small punch rig and the assumed correlation factor, the 140 MPa and 105 MPa (stress defined for 950 °C uniaxial creep) should have been correspondent respectively to 200 N and 150 N in SPC. SPC tests performed in these conditions showed a duration shorter than that expected as it can be seen from the displacement vs. time graphs in Figure 134 and in Figure 135.
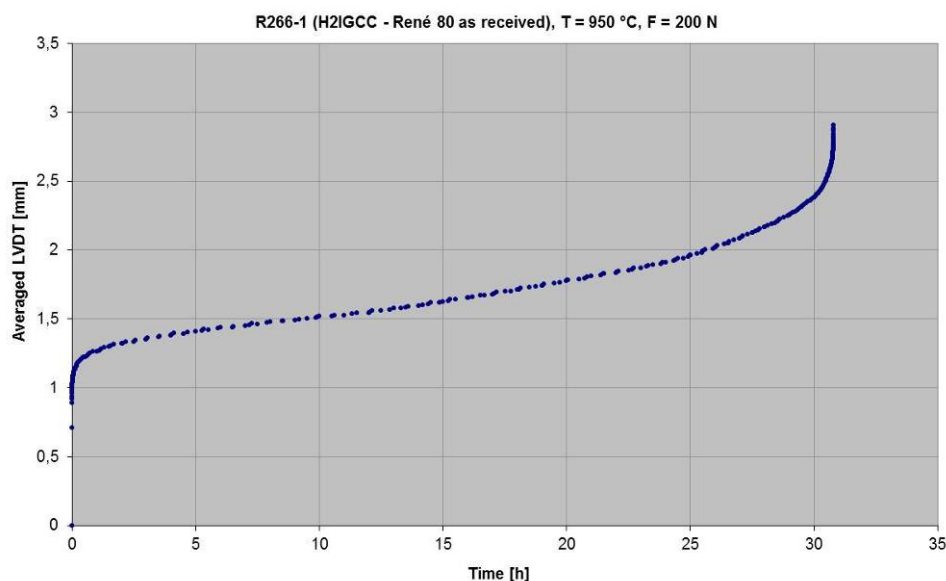

Figure 134 – SPC displacement vs. time curve of specimen R266-1

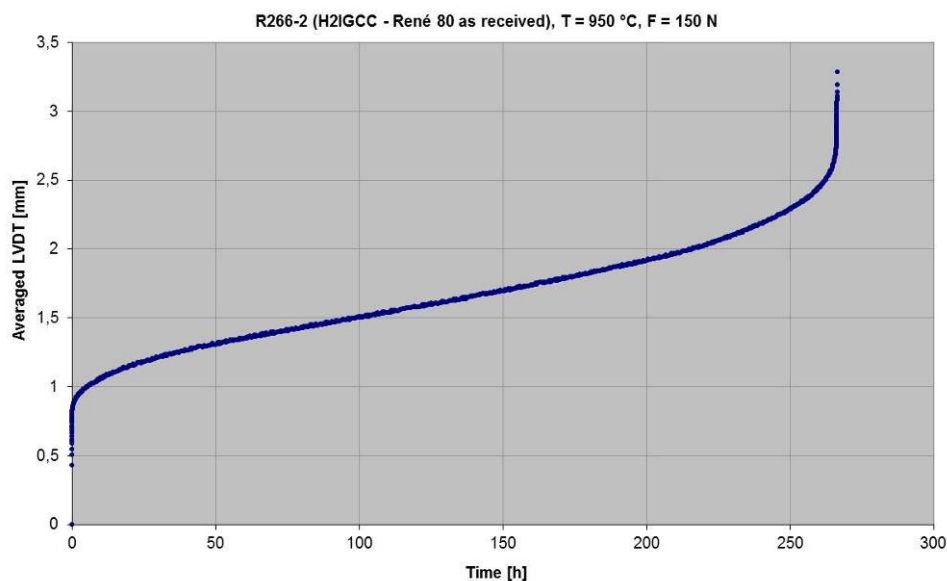R266-2 (H2IGCC - René 80 as received), T = 950 °C, F = 150 N

Figure 135 – SPC displacement vs. time curve of specimen R266-2

Additional tests at the same temperature with strongly reduced loads have been performed in order to get longest duration close to target time scheduled for uniaxial creep tests. Based on a Larson-Miller analysis of the first tests results, load conditions of 120 N and 90 N have been set. The displacement vs. time curve for these tests are presented in Figure 136 and Figure 137.
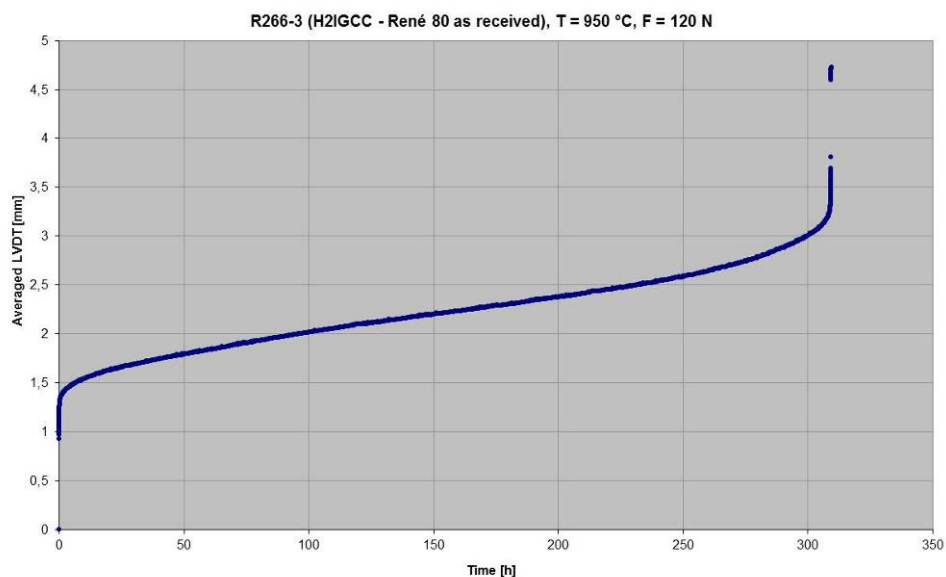
R266-3 (H2IGCC - René 80 as received), T = 950 °C, F = 120 N

Figure 136 - SPC displacement vs. time curve of specimen R266-3
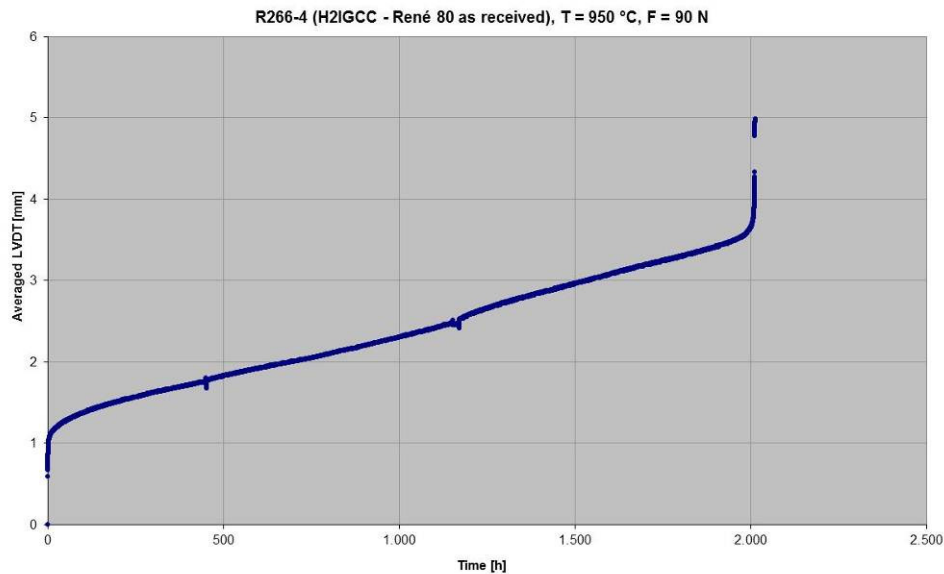
Figure 137 - SPC displacement vs. time curve of specimen R266-4

A good correlation of small punch creep experimental data of rupture time, with an isothermal (950°C) creep rupture time curve, calculated by literature data with Manson-Roberts-Mendelson approach, can be obtained assuming a reduced K_{SP} = 0.45 as shown in Figure 138.
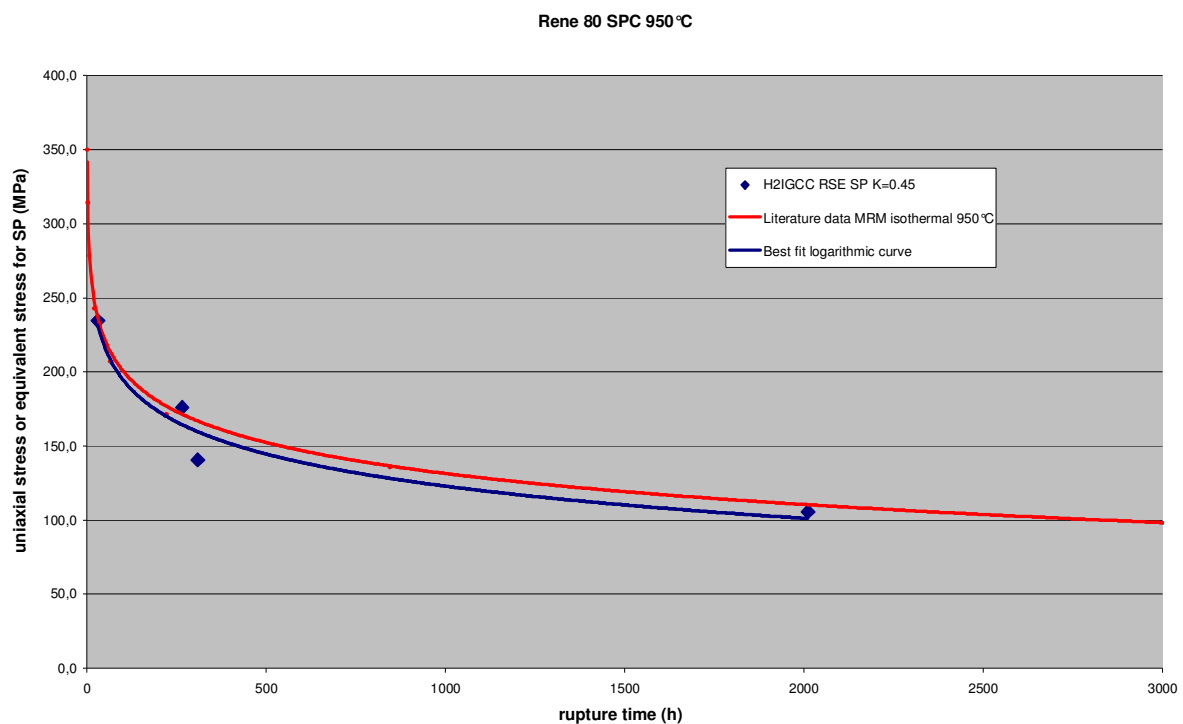

Figure 138 – Creep rupture time vs. stress at 950°C: small punch creep results compared to curve from literature uniaxial data

Based on the SPC tests performed at 950°C and considering the Larson-Miller approach, SPC tests at 1050°C have been performed by applying 43 N and 34 N loads.
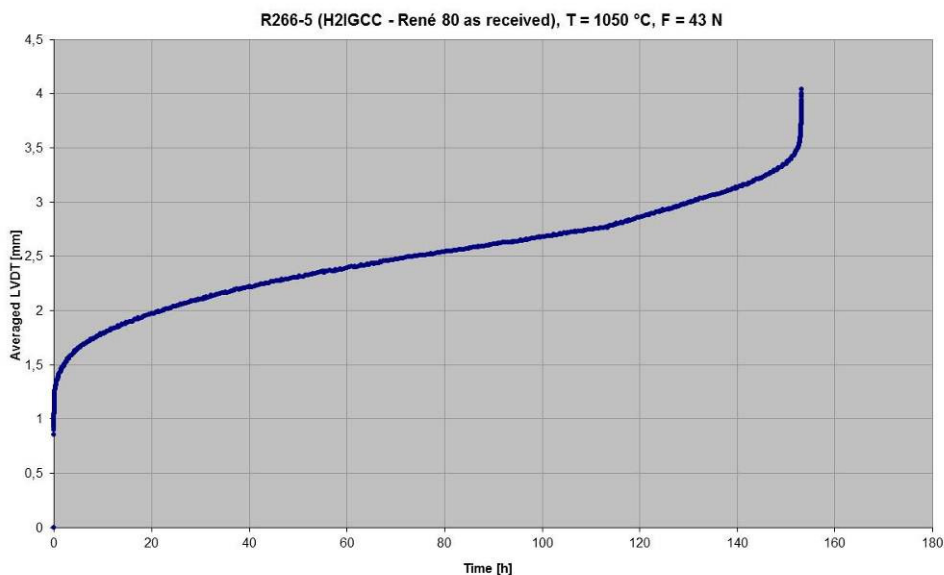Displacement vs. time curve for these two tests are presented in Figure 139 and Figure 140.

Figure 139 – SPC displacement vs. time curve of specimen R266-5
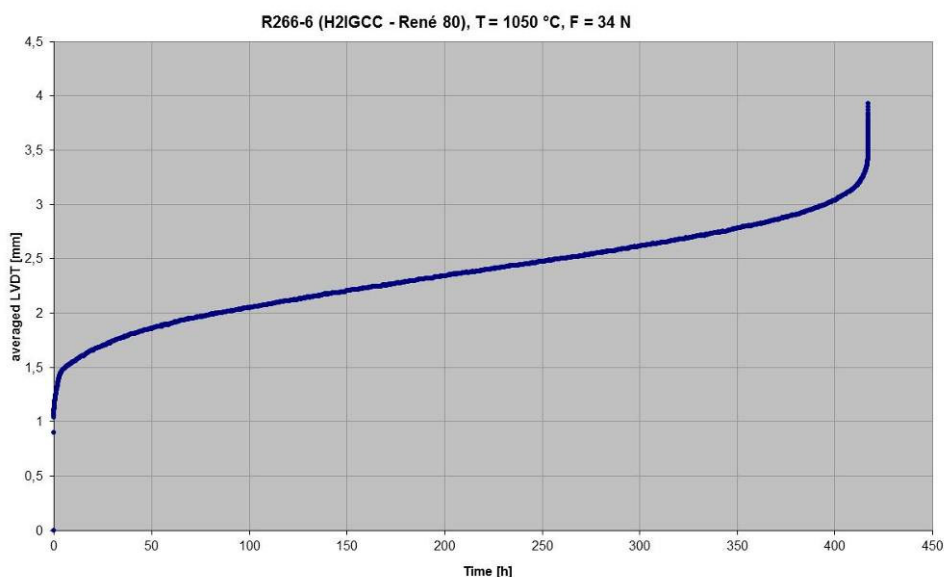

Figure 140 – SPC displacement vs. time curve of specimen R266-6

These results suggests that in order to have a good correspondence for rupture times with literature data from uniaxial creep tests, a K_{SP} value even lower than 0.45 should be considered in the empirical correlation of CEN Code of Practice.

Rupture time results performed on as received Rene 80 are summarised in Table M.

Table M - Small punch creep tests on as received Rene 80

Specimen	Temperature (°C)	Load (N)	Rupture time (h)
R266/1	950	200	31
R266/2	950	150	266
R266/3	950	120	309
R266/4	950	90	2011
R266/5	1050	43	153
R266/6	1050	34	417

The whole set of small punch creep test results is graphically presented in a Larson-Miller analysis in Figure 141 assuming for both SPC test temperatures the previously mentioned value K_{SP} =0.45.
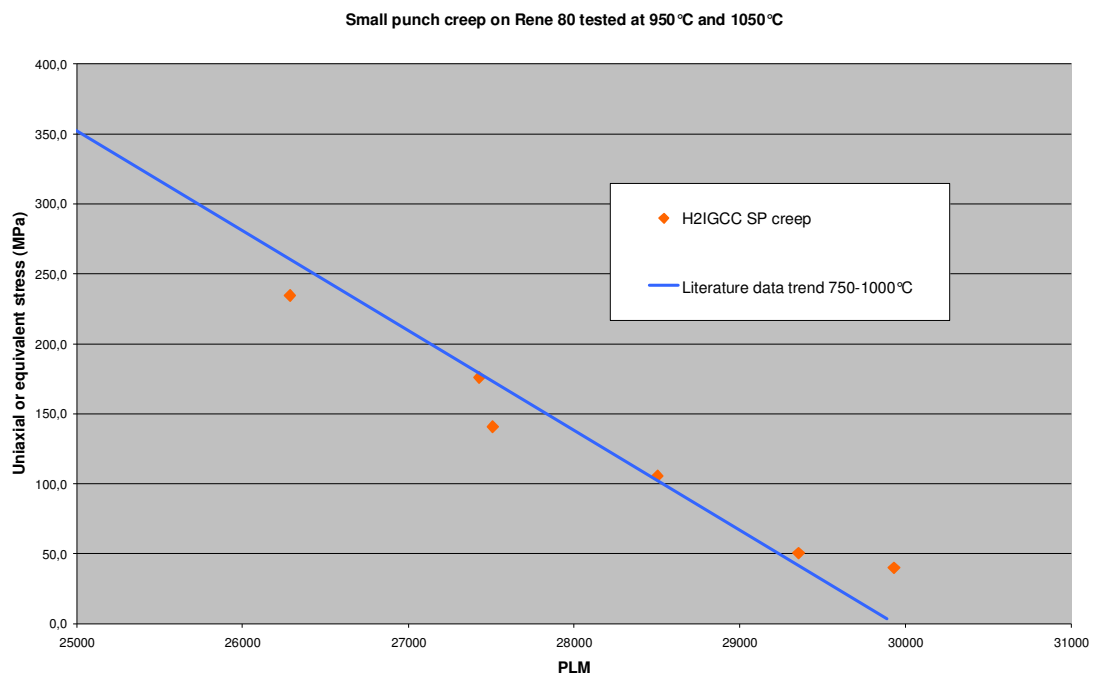

Figure 141– Larson Miller parameter vs. stress: small punch creep results at 950 and 1050°C compared to curve from literature uniaxial data in the range 750-1000°C.

3.5.1.2 As received Rene 80 aged in air

Some discs with standard thickness 0.5 mm have been aged in air with exposure to 1000°C for 1000 hours. After this ageing, discs show a significant oxidation of external surface leading to an increase of disc thickness as shown in Figure 142, where some measurements of local thickness are reported.
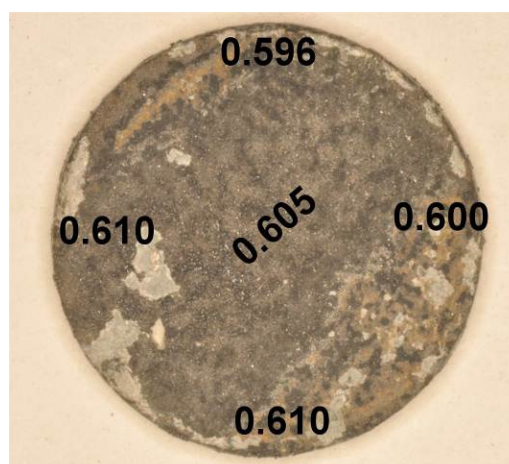

Figure 142 - Aspect of a small punch disc aged in air at 1000°C for 1000 h with local measurement of total (metal and oxides) thickness

One of these aged discs has been sectioned transversally to disc thickness in order to estimate oxide and base metal thickness. The undamaged base metal thickness in this disc results approximately close to 80% of standard value (0.5 mm); results of this evaluation are described with more details in the successive paragraphs related to metallographic investigation for SPC.

Aged discs have been tested without any removal of oxide layer and results are summarised in Table N.

Table N - Small punch creep tests on aged in air (1000°C 1000 h) Rene 80

Specimen	Temperature (°C)	Load (N)	Rupture time (h)
R266/7	950	120	160
R266/8	950	90	798
R266/9	1050	34	909
R266/10	1050	43	860

The experimental displacement vs. time curves for the tests performed on discs aged in air are presented in Figure 143 and Figure 144 for tests performed at 950°C, and in Figure 145 and Figure 146 for tests performed at 1050°C.
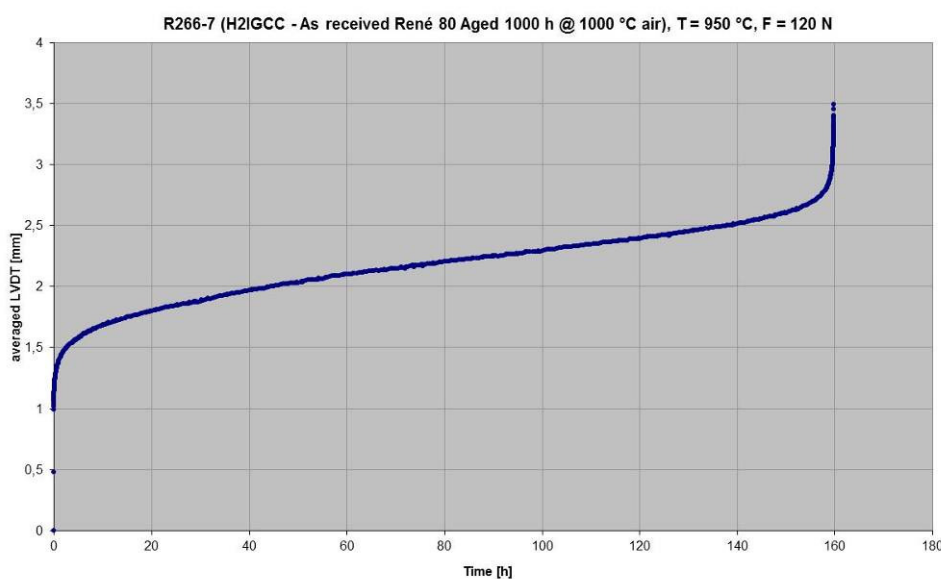

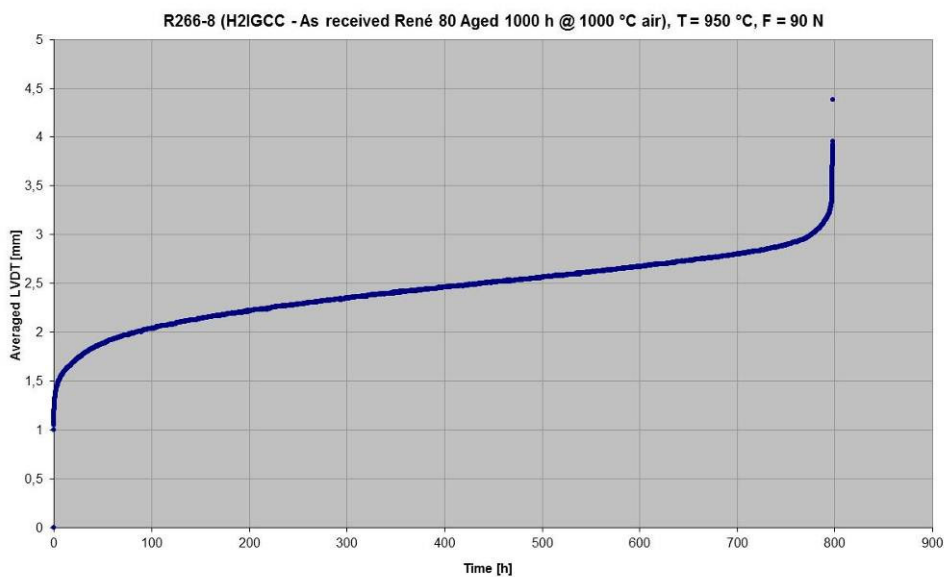**Figure 143 – SPC displacement vs. time curve of specimen R266-7 (aged in air)**

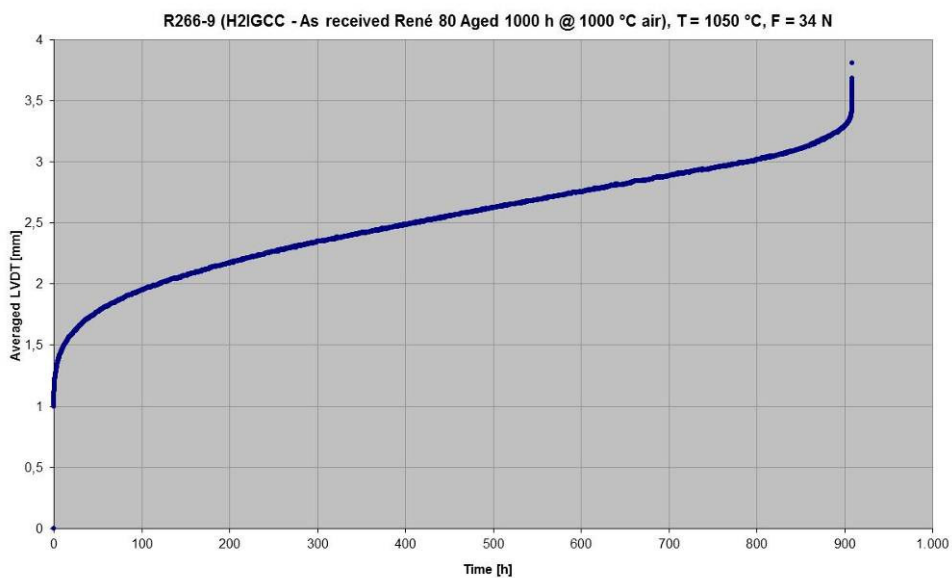**Figure 144 – SPC displacement vs. time curve of specimen R266-8 (aged in air)**

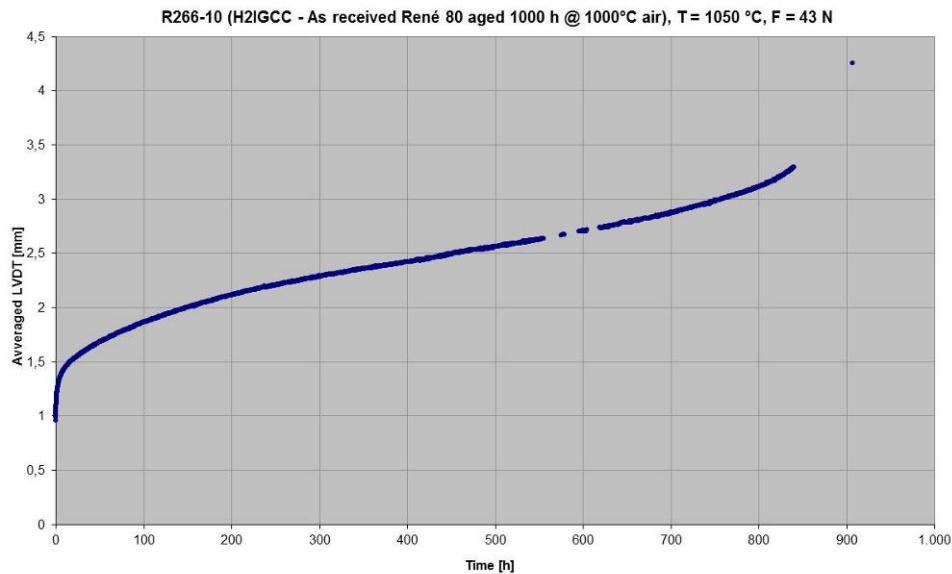**Figure 145 – SPC displacement vs. time curve of specimen R266-9 (aged in air)**

Figure 146 – SPC displacement vs. time curve of specimen R266-10 (aged in air)

Assuming no creep resistance contribution for oxide layers and basing on the residual metal thickness estimation (approx. 0.4 mm), it's possible to estimate equivalent stresses (calculated by means of CEN CoP equation with the same $K_{SP}=0.45$ but with reduced disc thickness); this assumption for tests performed at 950 °C give results approaching the curve of uniaxial data as shown in Figure 147 while tests performed at 1050 °C are out of trend with a higher resistance.
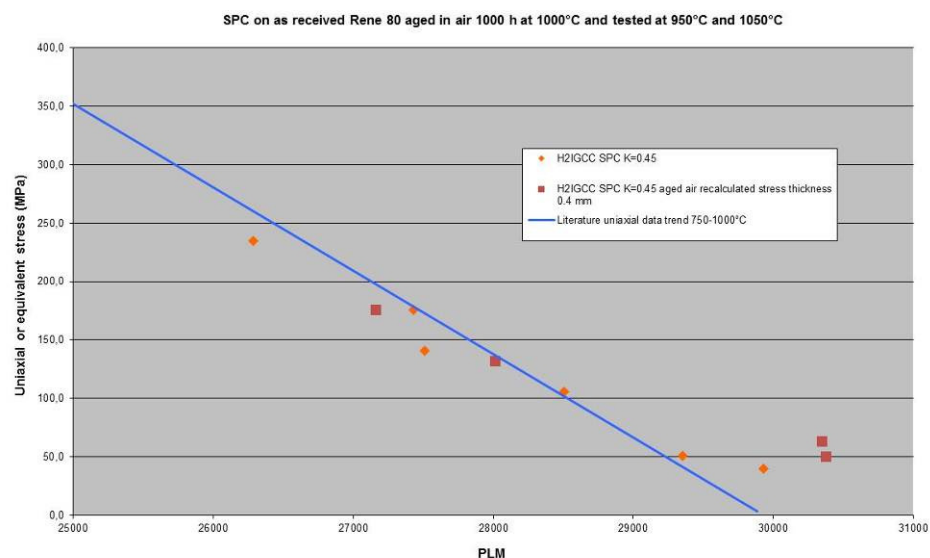

Figure 147– Larson Miller parameter vs. stress: small punch creep results (recalculated with reduced thickness for aged specimens) at 950 and 1050°C compared to curve from literature uniaxial data in the range 750-1000°C.

3.5.1.3   As received Rene 80 aged in air with 20 % steam

Similarly to previous case, some discs with standard thickness 0.5 mm have been aged in humid air (steam content controlled to 20%) with exposure to 1000 °C for 1000 hours.

One of these specimens has been tested in SPC, setting the temperature to 950 °C and applying a 120 N load; displacement vs. time curve is showed in Figure 148; the rupture time for this test is 396 h, longer than those obtained, in the equivalent conditions for the specimen aged in air and for the as received material, too.
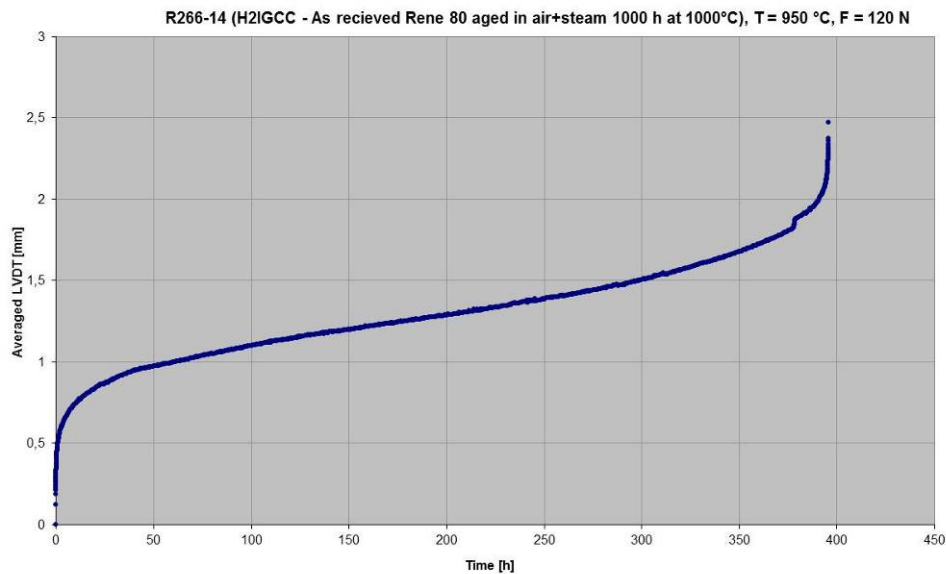
R266-14 (H2IGCC - As recieved Rene 80 aged in air+steam 1000 h at 1000°C), T = 950 °C, F = 120 N

Figure 148 – SPC displacement vs. time curve of specimen R266-14 (aged in air+steam)

3.6 Metallography related to small punch creep characterization

Specimens have been electrochemically etched with oxalic acid 0.5% solution for generic microstructure examination or Kallin II solution for γ' examination, unless otherwise indicated in the singular reported micrograph.

3.6.1 As received Rene 80

A piece of as received Rene 80 has been sectioned in order to prepare a metallographic specimen for the evaluation of material microstructure. The optical microscope documentation on this specimen shows the presence of significantly large grains with precipitates at grain boundary (see micrographs with different magnification in Figure 149).
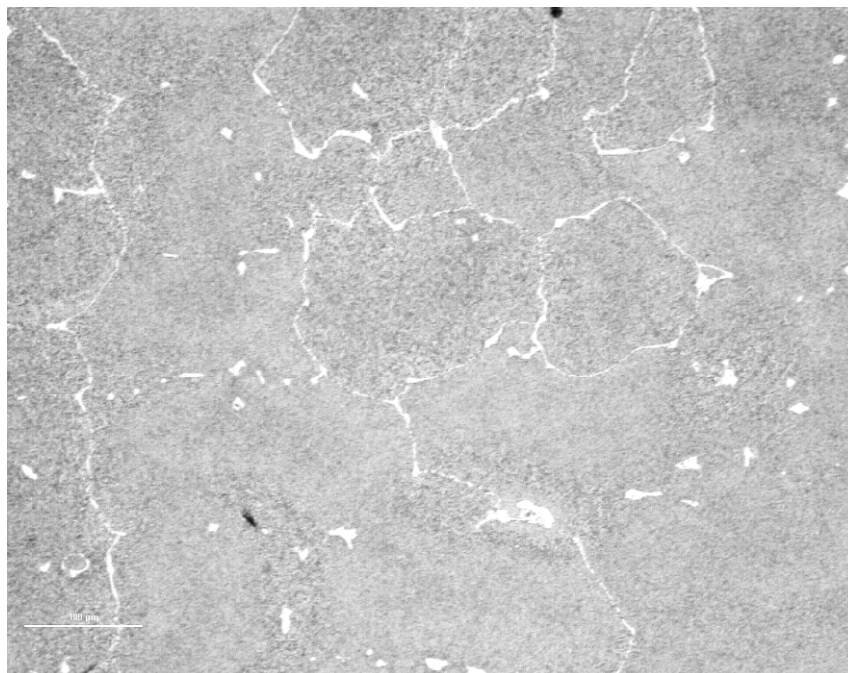
Figure 149 – LO micrographs of as received Rene 80

After etching of metallographic specimen is possible to detect on SEM the γ' phase with nearly cuboidal shape (see Figure 150), unless a not completely regular shape of this phase is evident (some coarsening of cuboid and irregular shape are evident); no evidence of secondary γ'.
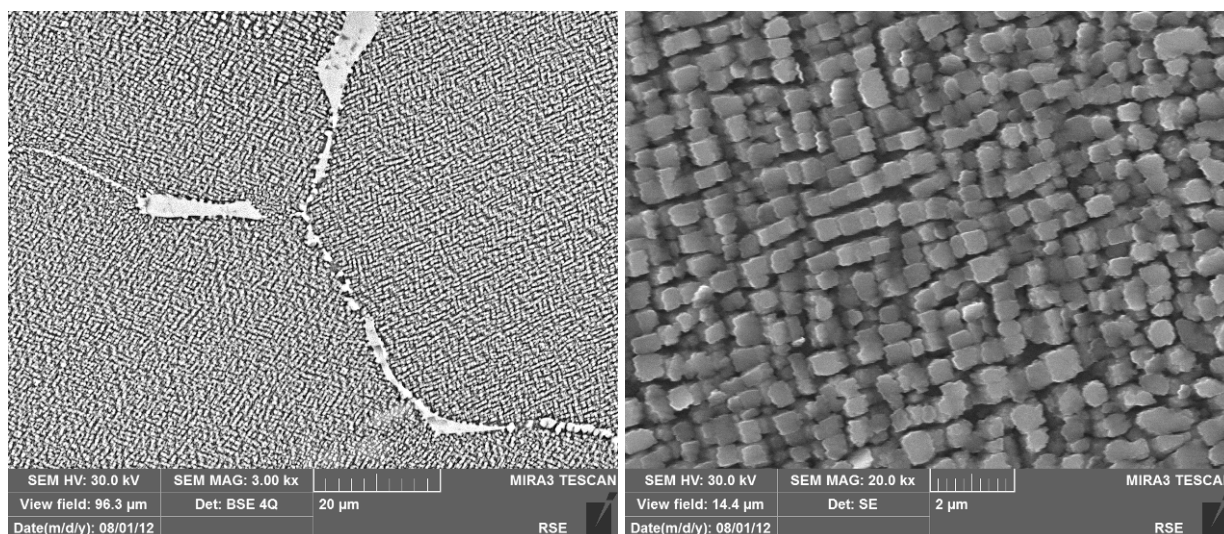

Figure 150 – As received Rene 80 etched in order to detect γ' phase

Rene 80 in this condition has a Vickers Hardness of 428±3 HV that can be considered as a high value, compared to standard condition of component manufacturing.

3.6.1.1   As received Rene 80 tested SPC at 950°C

Specimen R262-4 has been tested in small punch creep by applying a 90 N load; the disc went to rupture after 2011 h. The aspect of the specimen at the end of the test is reported in Figure 151, while some details of fracture surface observed on SEM are collected in Figure 152, where it's possible to detect the fracture developed along detachment of metal grains.
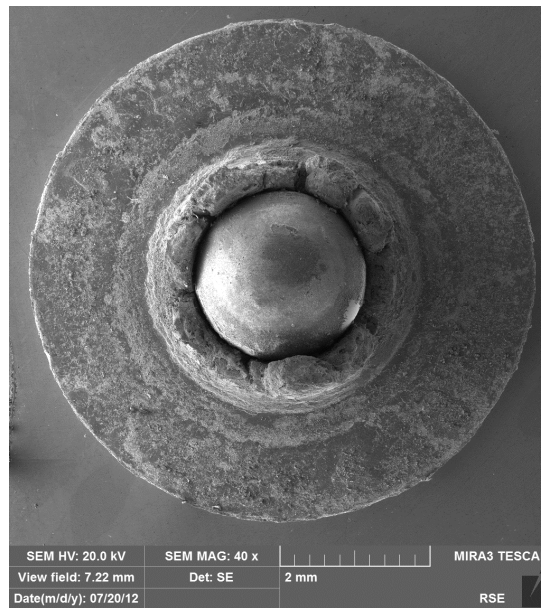
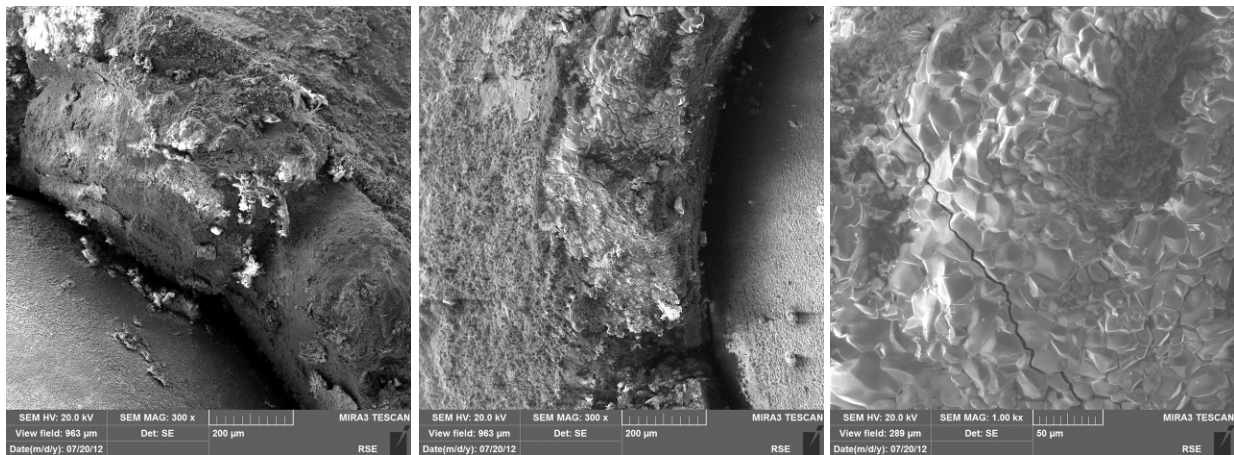**Figure 151 – Aspect of R266-4 tested SPC 950°C 90N**

Figure 152 – Details observed on SEM of fracture surface for specimen R266-4

By sectioning the disc along a plane perpendicular to original disc plane, it has been prepared a metallographic specimen, whose half section is in Figure 153. An external layer of oxide products and damaged material is clearly detectable.
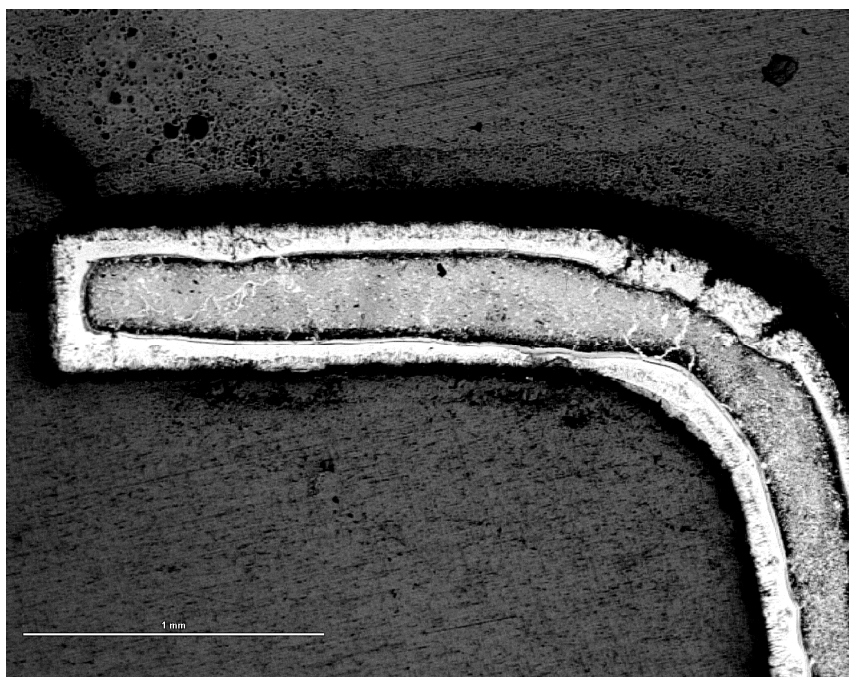
Figure 153 – Half section of metallographic specimen prepared by R266-4

The characterisation of different layers observed in the disc section is presented in Figure 154 where for each area delimited and labelled, an EDS spectrum has been collected. Spectra are then reported in the following figures (from Figure 155 to Figure 161). The distribution of chemical elements along the different layers can be observed also from the EDS-line characterisation reported in Figure 162. In general it can be observed the formation of a thin layer of external oxide, while more thick is the layer of depleted zone (no γ') under the external oxide. The internal part of metal area, where γ' presence is still evident, shows anyway a significant rafting and coarsening of cuboidal strengthening phase and the coarsening of grain boundaries precipitates as demonstrated in Figure 163.
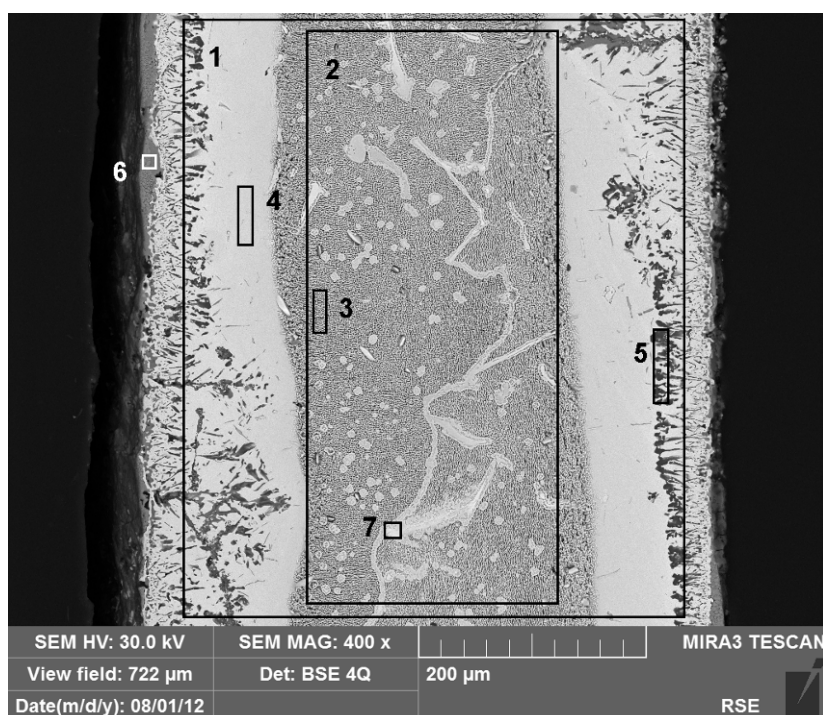

Figure 154 – Metallographic section of disc R266-4 with indication of the areas where EDS spectra have been collected
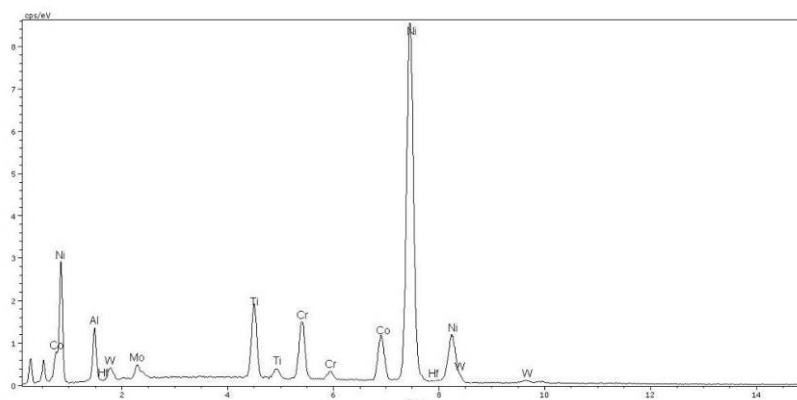
Figure 155 – EDS specturm of Zone 1 in Figure 154: mixed total area
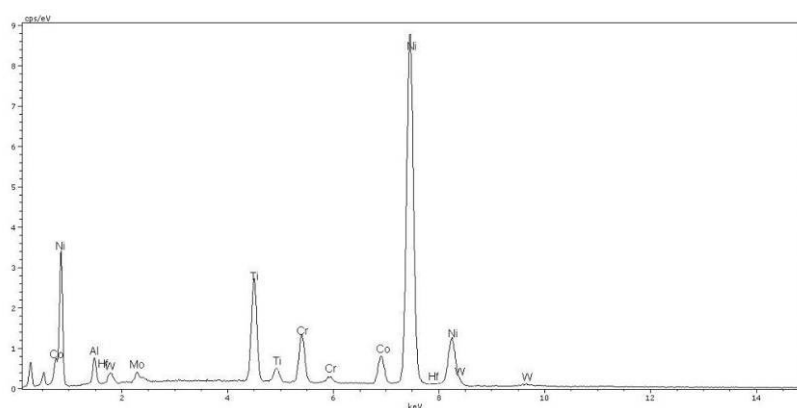

Figure 156 – EDS spectrum of Zone 2 in Figure 154: metallic matrix with γ' including grain boundaries precipitates
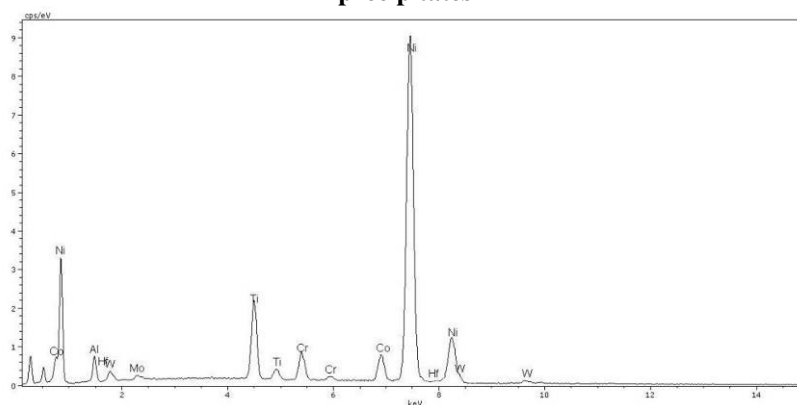

Figure 157 – EDS spectrum of Zone 3 in Figure 154: metallic matrix with γ' excluding grain boundaries precipitates
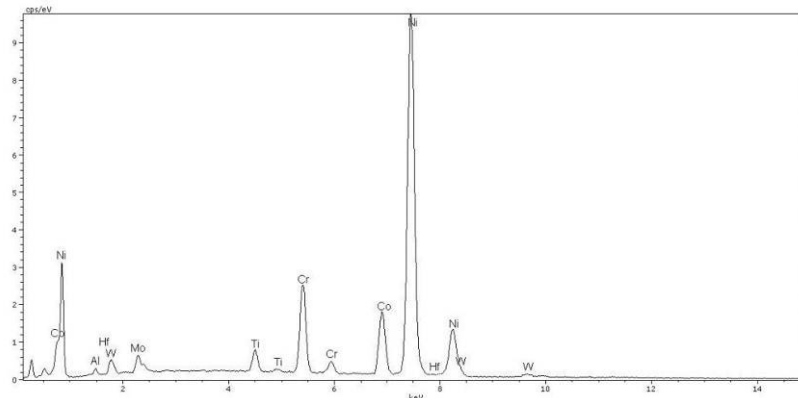
Figure 158 – EDS spectrum of Zone 4 in Figure 154: metallic depleted layers (no γ') with reduced content of Al and Ti
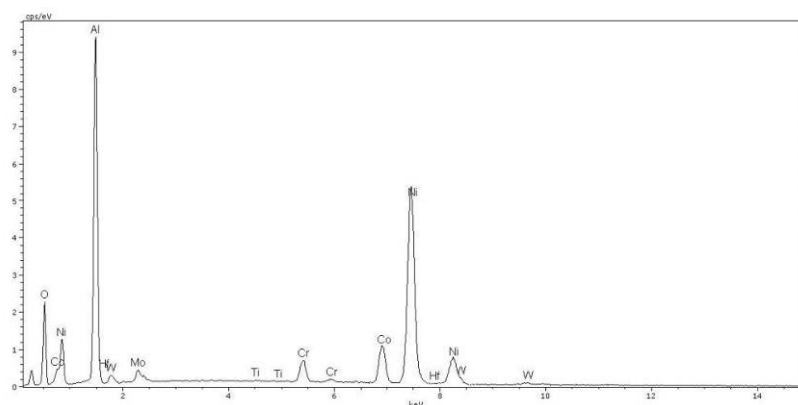

Figure 159 – EDS spectrum of Zone 5 in Figure 154: Al precipitates (detectable oxygen presence)
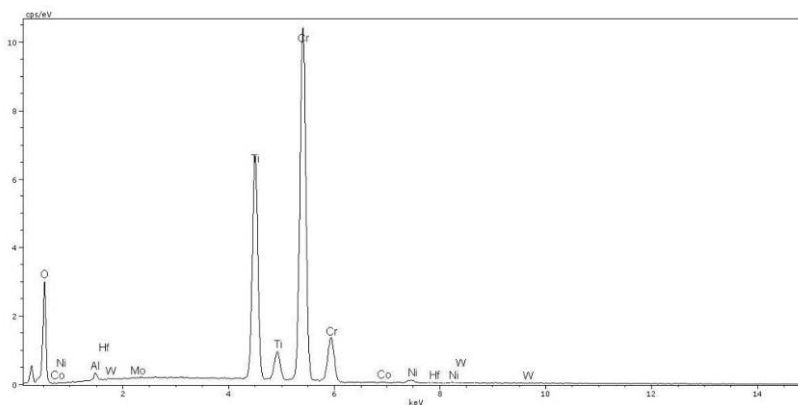

Figure 160 – EDS spectrum of Zone 6 in Figure 154: external oxide layer (Cr and Ti enriched)
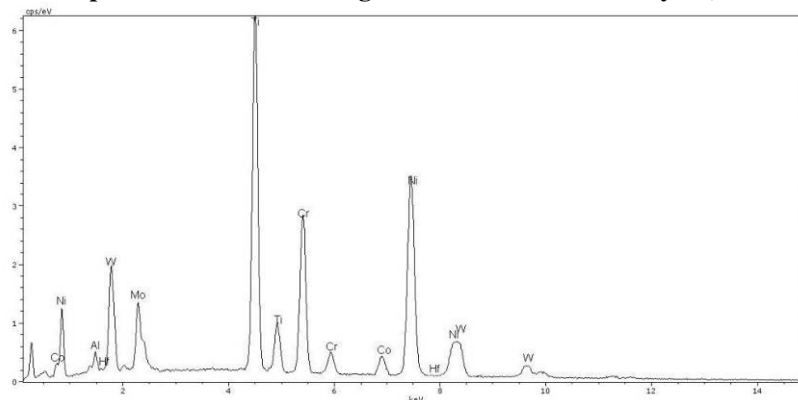
Figure 161- EDS spectrum of Zone 7 in Figure 154: grain boundaries precipitates (internal to γ' matrix) Ti rich
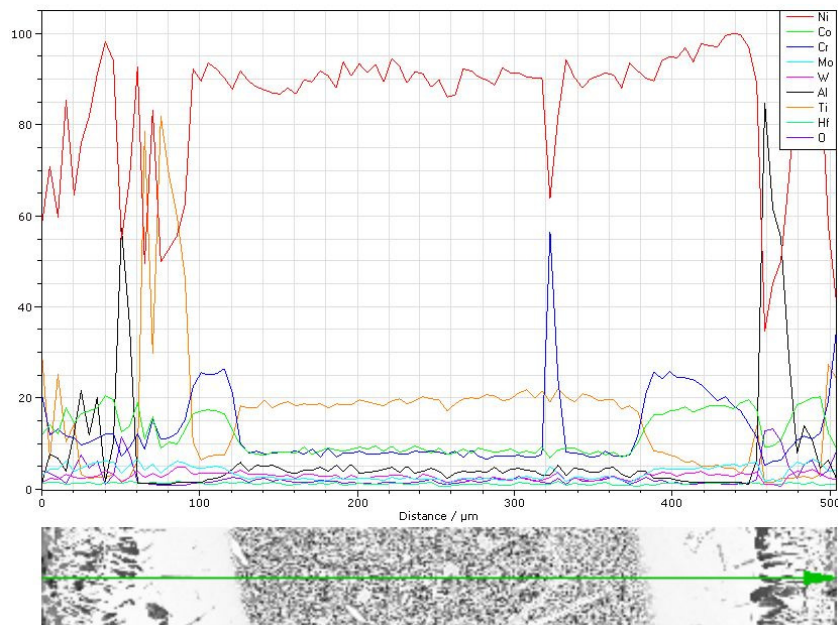
Figure 162 – EDS-line on the section of metallographic specimen from R262-4
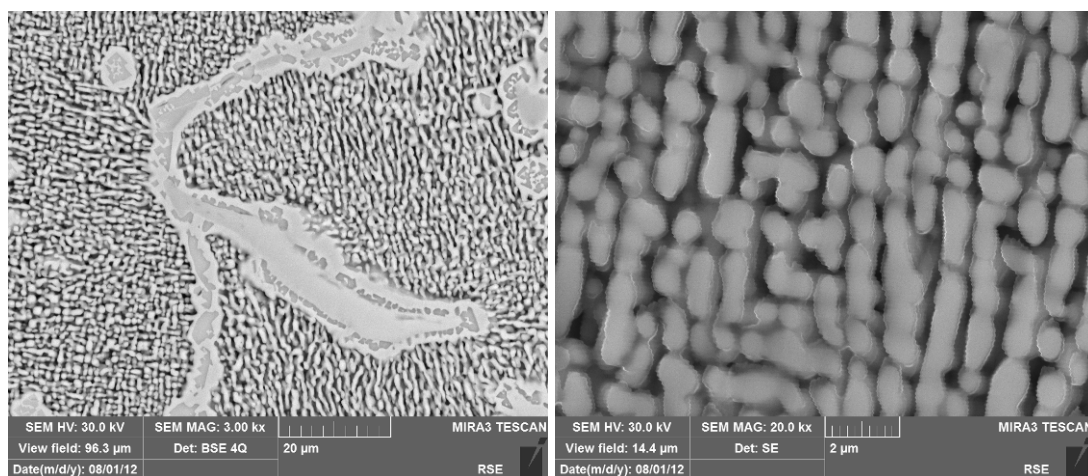

Figure 163 – Aspect of γ' and grain boundaries precipitates in the central part of metallographic specimen from R266-4

3.6.1.2 As received Rene 80 tested SPC at 1050°C

Specimen R262-6 has been tested in small punch creep by applying a 34 N load; the disc went to rupture after 417 h. The aspect of the specimen at the end of the test is reported in Figure 164.
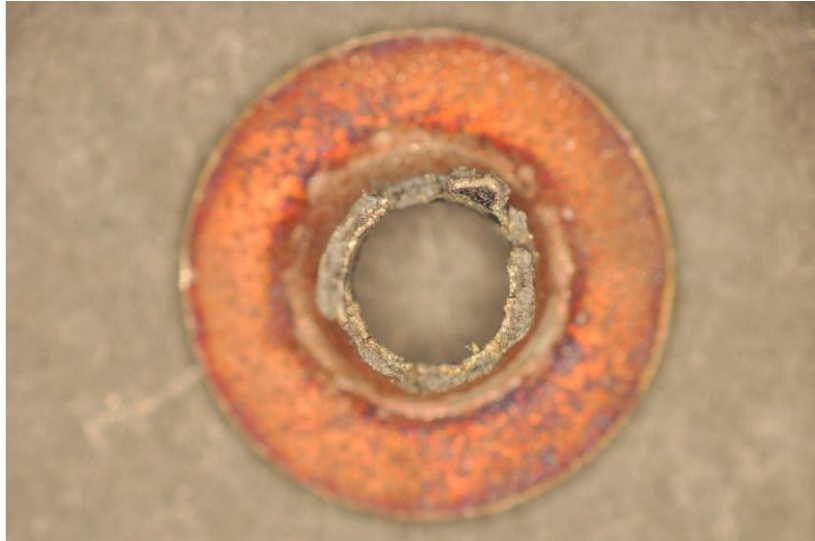
Figure 164 - Aspect of R266-6 tested SPC 1050°C 34N

The metallographic specimen obtained by sectioning the disc along a plane perpendicular to original disc plane, show a situation of external degradation similar to that observed in the disc tested at lower temperature; unless the oxidation and depletion layer appear to be less symmetric and more evident on punch contact side compared to opposite, as shown in Figure 165 and Figure 166.

The γ′ phase in the central part of the discs shows a coarsening of cuboidal strengthening phase as reported in Figure 167.

Figure 165 - Metallographic section of disc R266-6

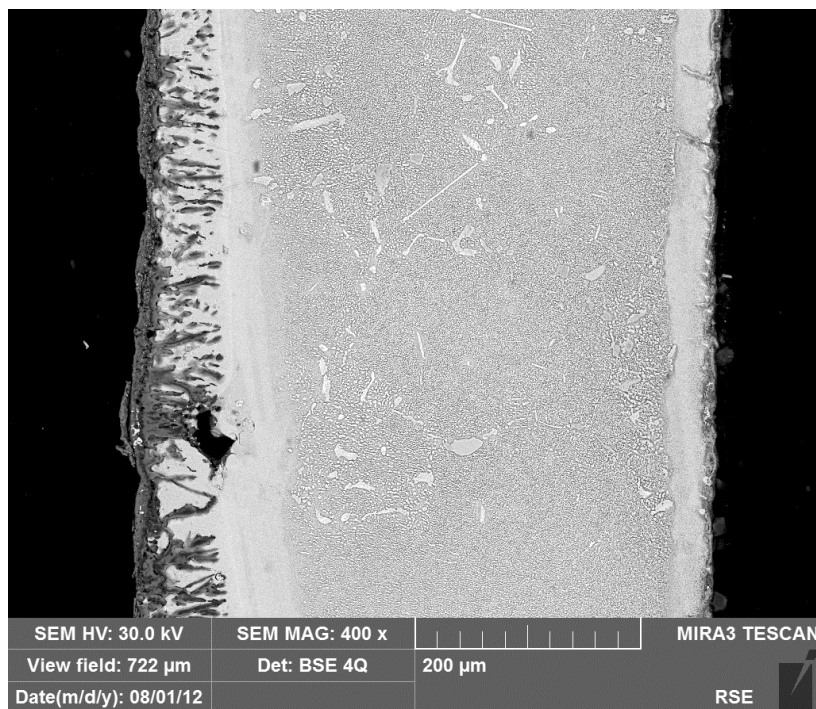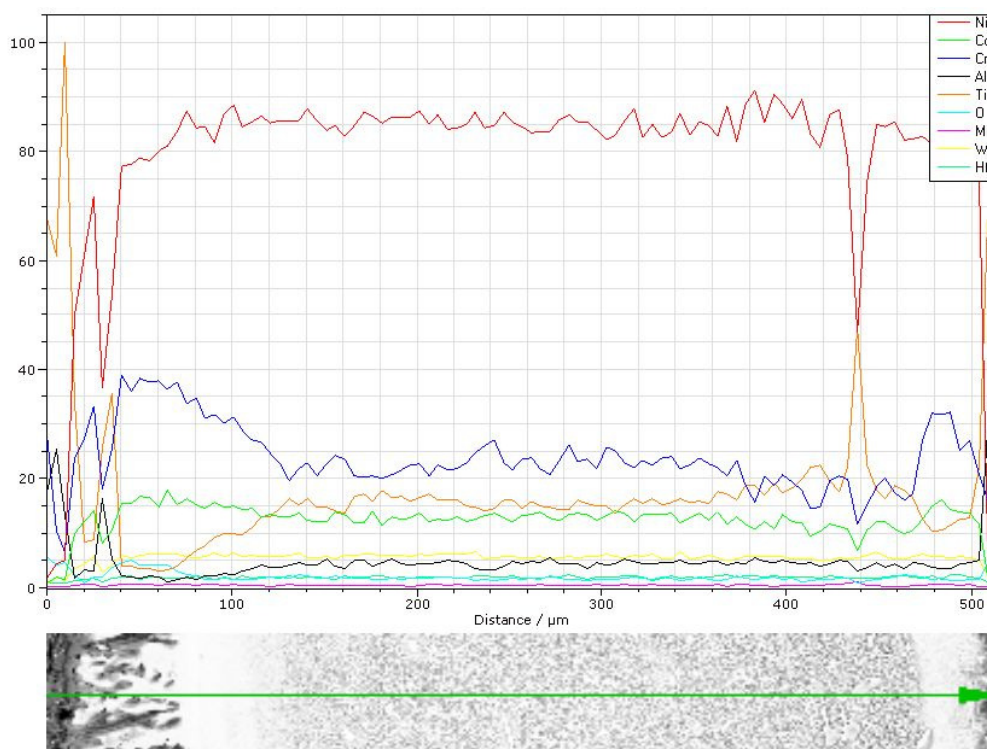**Figure 166 - EDS-line on the section of metallographic specimen from R262-6**
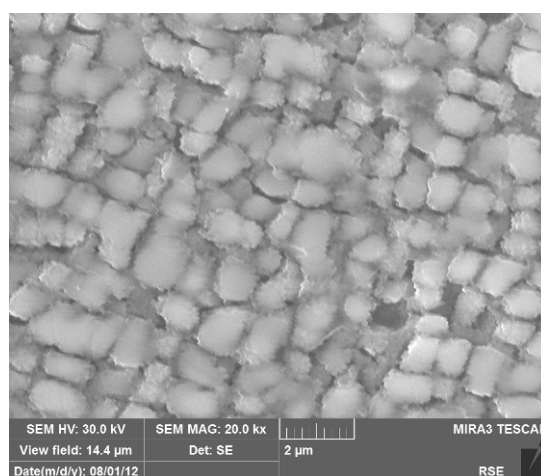
Figure 167 – Aspect of γ' in the central part of metallographic specimen from R266-6

3.6.2   As received Rene 80 aged in air

As previously mentioned one of the Rene 80 disc aged in air for 1000 h at 1000°C has been sectioned for the preparation of a metallographic specimen in order to evaluate the effect of thermal ageing prior to testing in SPC.

This specimen shows a situation very similar to that observed for the as received Rene 80 disc tested in SPC, as shown in Figure 168. The external layer of oxidation products is thicker than in the tested discs (SPC tests are performed in inert argon atmosphere). Also in this case in the metallic layer, the evidence of a central layer still strengthened by γ' and of external depleted (no γ') layers can be observed; some large voids are included in base metal, too.

Figure 168 – Metallographic specimen of a disc aged in air

Grain boundaries precipitates appear coarsened compared to virgin material (see Figure 169) and γ' cuboid are coarsened and coalesced without a preferential direction (see Figure 170).

Figure 169 – Grain boundaries precipitates of a disc aged in air
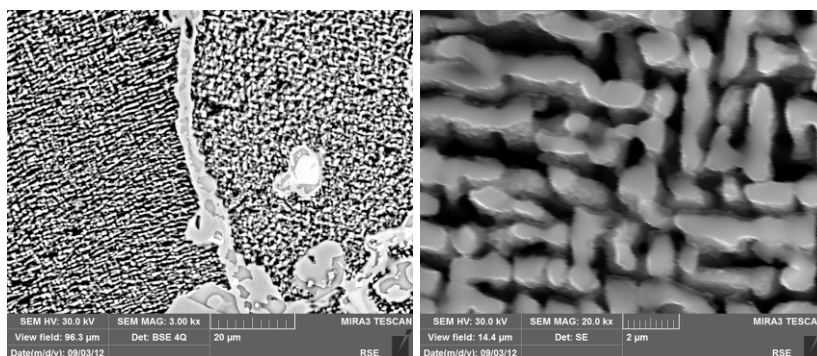
Figure 170 - Aspect of γ' and grain boundaries precipitates in the central part of metallographic specimen from a disc aged in air

3.6.2.1 As received Rene 80 aged in air (1000 h 1000°C) and tested at 950°C

Specimen R266-8 has been tested in small punch creep by applying a 90 N load; the disc went to rupture after 798 h. The specimen prepared by sectioning the disc after test shows a situation similar to previously described specimens (see Figure 171) with an even stronger effect of coarsening and rafting for γ' phase, as shown in Figure 172.

Figure 171 – Metallographic section of disc R266-8

Figure 172 - Aspect of γ' in the central part of metallographic specimen from R266-8

3.7 Rene 80 with completed heat treatment

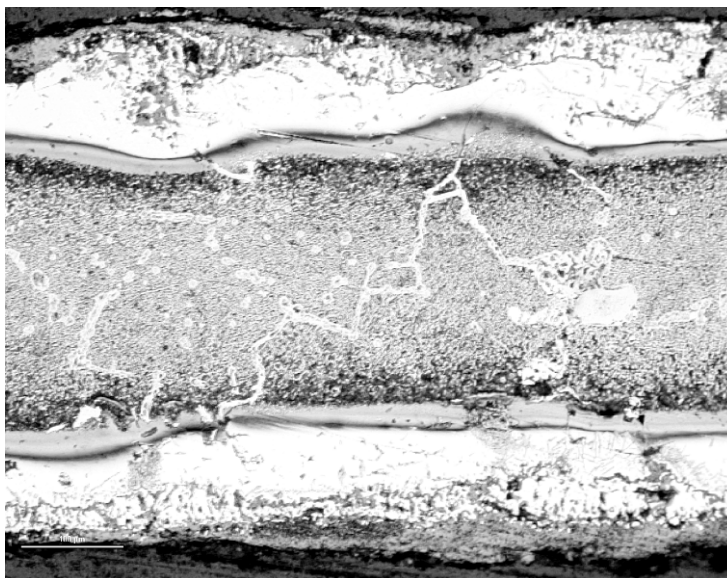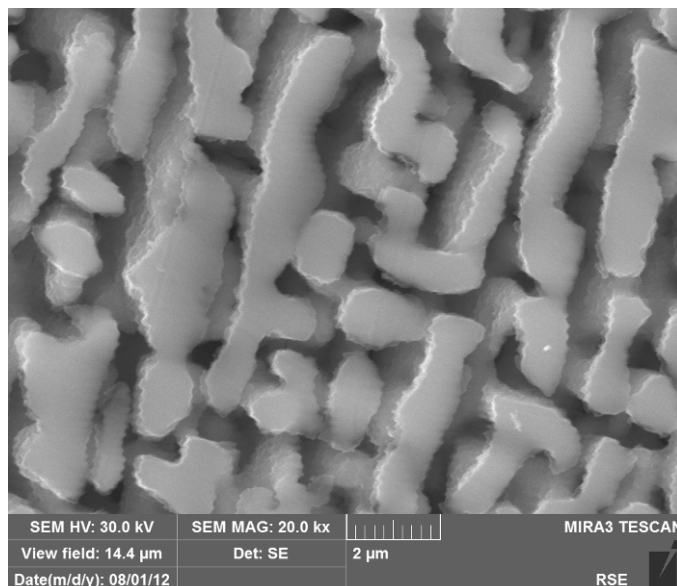Although results of uniaxial standard creep tests showed creep rupture times in good agreement with literature data also for the Rene 80 characterized in the as received conditions (lack of the two final heat treatment steps usually applied during coating application), in order to verify the behavior of this material in small punch creep tests, it has been decided among WP2 Partners to repeat some small punch tests on a piece of Rene 80 uncoated, but completely heat treated (adding final steps of industrial procedure for manufacturing actual components). The material after a first heat treatment step (1080 °C) showed a significant hardness reduction to 380±3 HV; this value was confirmed (HV 382±2) also at the end of the second heat treatment step (870 °C).

The microstructure of Rene 80 CHT (completely heat treated) observed in optical microscopy is showed in Figure 173 with two different magnifications. The presence of large grains and precipitates at grain boundaries is similar to that observed in the as received material.
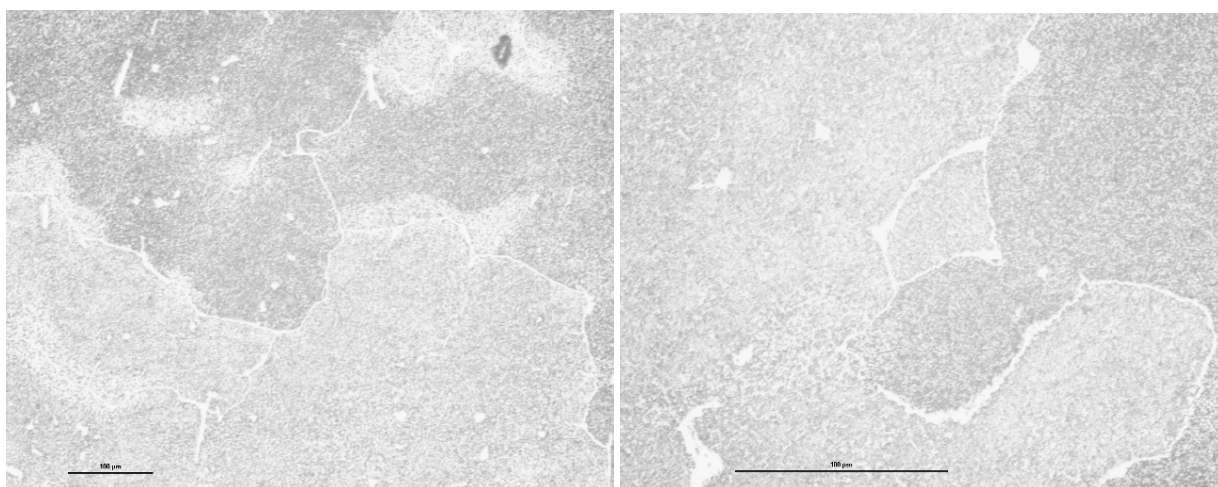
Figure 173 – LO micrographs of Rene 80 completely heat treated

Shape and size of cuboidal γ' strengthening phase appears more regular than that in as received material, as it can be observed in Figure 174.
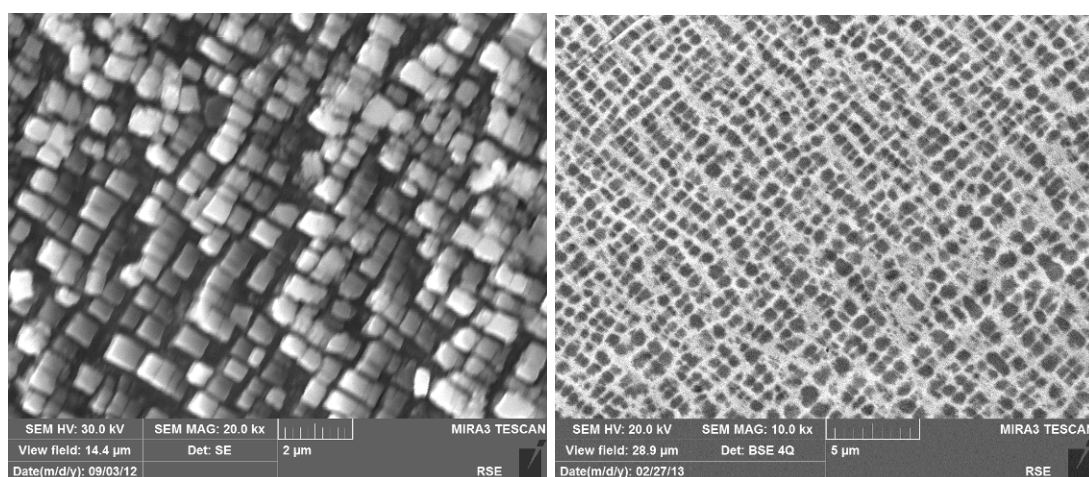
Figure 174 - Rene 80 CHT γ' phase (on the left matrix etched specimen 20k magnification, on the right matrix un-etched specimen 10k magnification)

3.7.1 Small punch creep tests on Rene 80 CHT

This piece of Rene 80 with completed heat treatment has then been machined for the preparation of 15 additional small punch discs. Among them, 5 discs have then been aged in air for 1000 h at 1000 °C and 5 others have been aged in the same conditions but with the addition of 20% steam to air, the remaining ones have been tested in virgin condition.

3.7.1.1 Rene 80 CHT without ageing

Some of the tests conditions applied to as received Rene 80 has then been used for Rene 80 CHT too.

At the temperature 950°C the test with 120 N applied load went to rupture with a longer time than as received material; the displacement vs. time graphs for this test is presented in Figure 175.
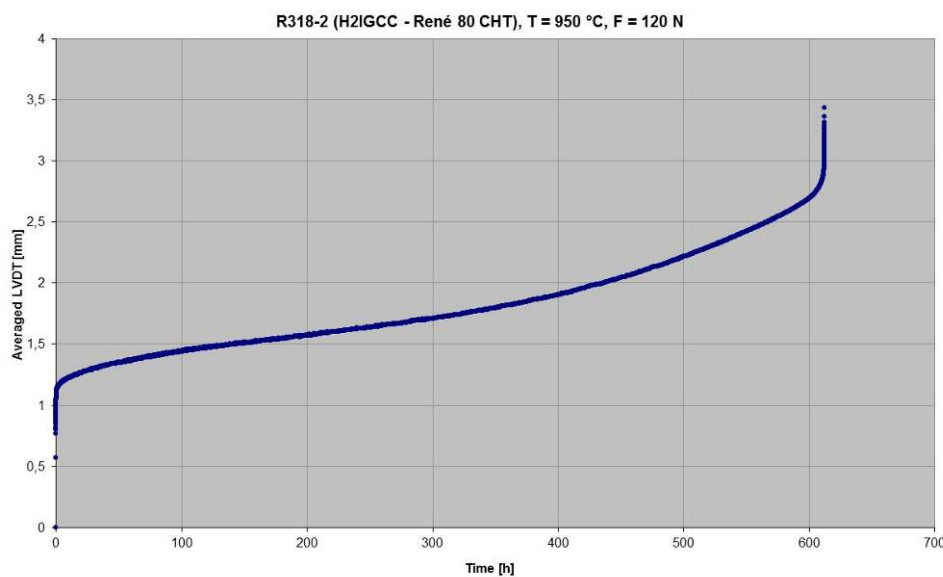
Figure 175 - SPC displacement vs. time curve of specimen R318-2

At the temperature 1050°C both tests (43 N and 34 N loads) have been repeated on Rene 80 CHT, showing also in this case longer rupture times, compared to as received material.

Displacement vs. time curve for these two tests are presented in Figure 176 and Figure 177.

These results for Rene 80 CHT confirmed the influence on creep resistance of the final heat treatment steps, enhancing the correct precipitation of γ' phase; the creep resistance improvement for this "second batch" of Rene 80 is more evident for the higher temperature of testing (1050°C), as represented by Larson-Miller analysis in Figure 178, where the estimated stresses are calculated keeping for both materials $K_{SP}=0.45$.
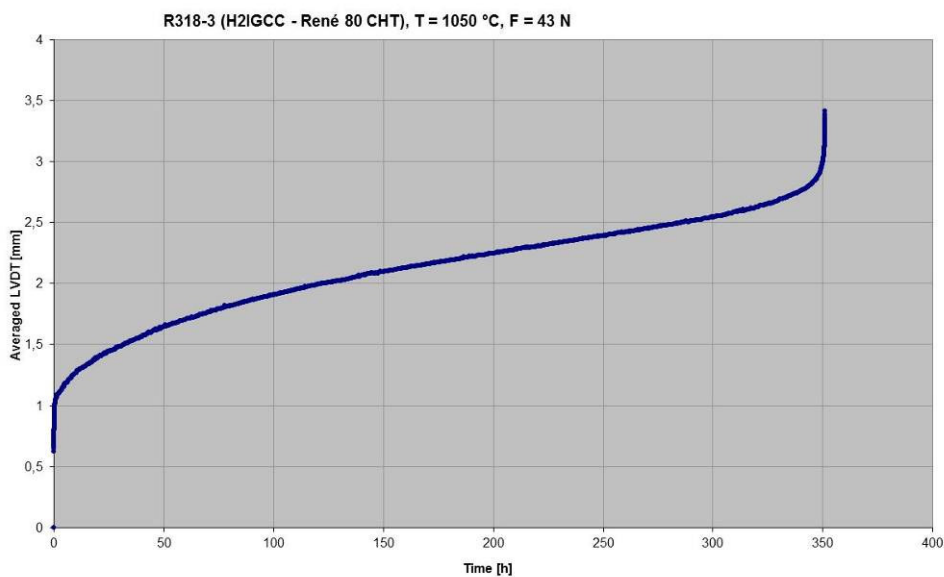
Figure 176 – SPC displacement vs. time curve of specimen R318-3
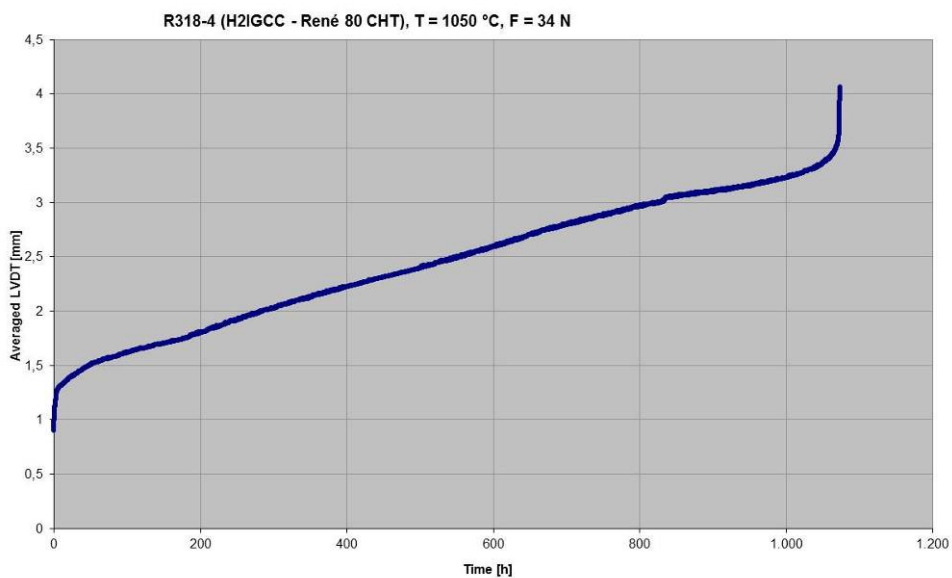
Figure 177 – SPC displacement vs. time curve of specimen R318-4
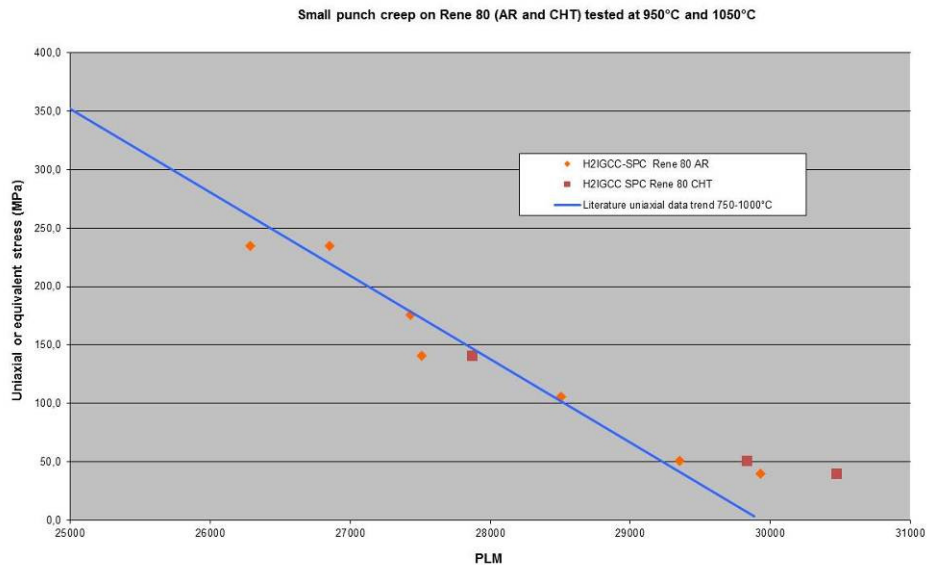
Figure 178 - Larson Miller parameter vs. stress: small punch creep results at 950 and 1050°C for both Rene 80 (as received and completely heat treated) compared to curve from literature uniaxial data in the range 750-1000°C.

3.7.1.2   Rene 80 CHT aged in air

One test on aged in air disc of Rene 80 completely heat treated, performed at 950°C with 120 N applied load showed an extremely higher resistance overcoming 2000 h duration instead of the equivalent test performed on the Rene 80 without completed heat treatment that went to rupture after 160 hours.

4 Final considerations on mechanical testing results

4.1 Thermomechanical fatigue

From the tests performed on Rene 80 with the same thermal and mechanical cycle, the uncoated material in the as received conditions (partially heat treated without final steps) gives the longest duration in TMF tests. The material in actual component conditions (completely heat treated CHT) shows an increase in TMF resistance for coated specimens compared to uncoated one, while no significant differences can be observed for coated materials aged in air or in air with additional content of 20% steam. An overview of these results is graphically presented in Figure 179 in terms of maximum and minimum stress at each cycle up to end life criteria for each test.
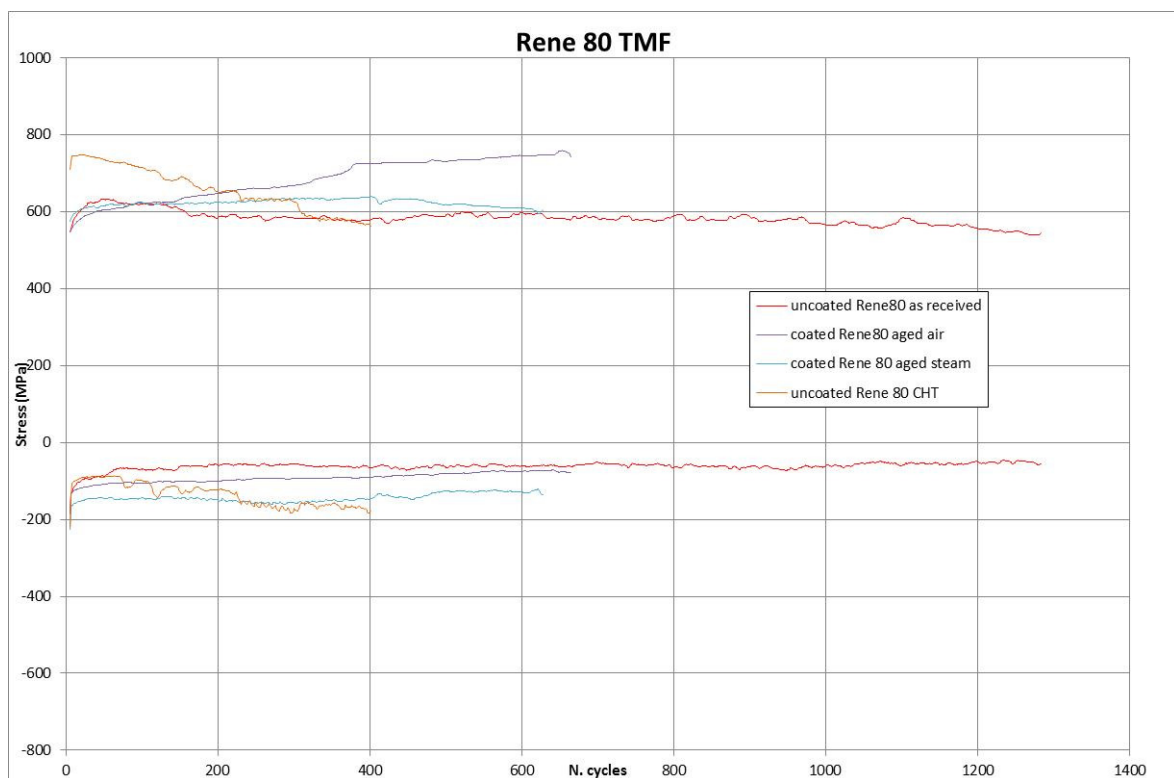
Figure 179 – Summary of TMF tests on Rene 80 performed with an OP mechanical strain -0.4 %

For the PWA 1483 the difficulties observed for a stable welding of thermocouple with single crystal bare alloy, doesn't allow to make any comparison of coated vs. uncoated material. Anyway in this case it appears that the coated material after ageing in air with additional content of 20% steam has a longer life than the equivalent specimen aged only in air. Figure 180 shows the summary of results in terms of stress variation during TMF up to the end of each test.
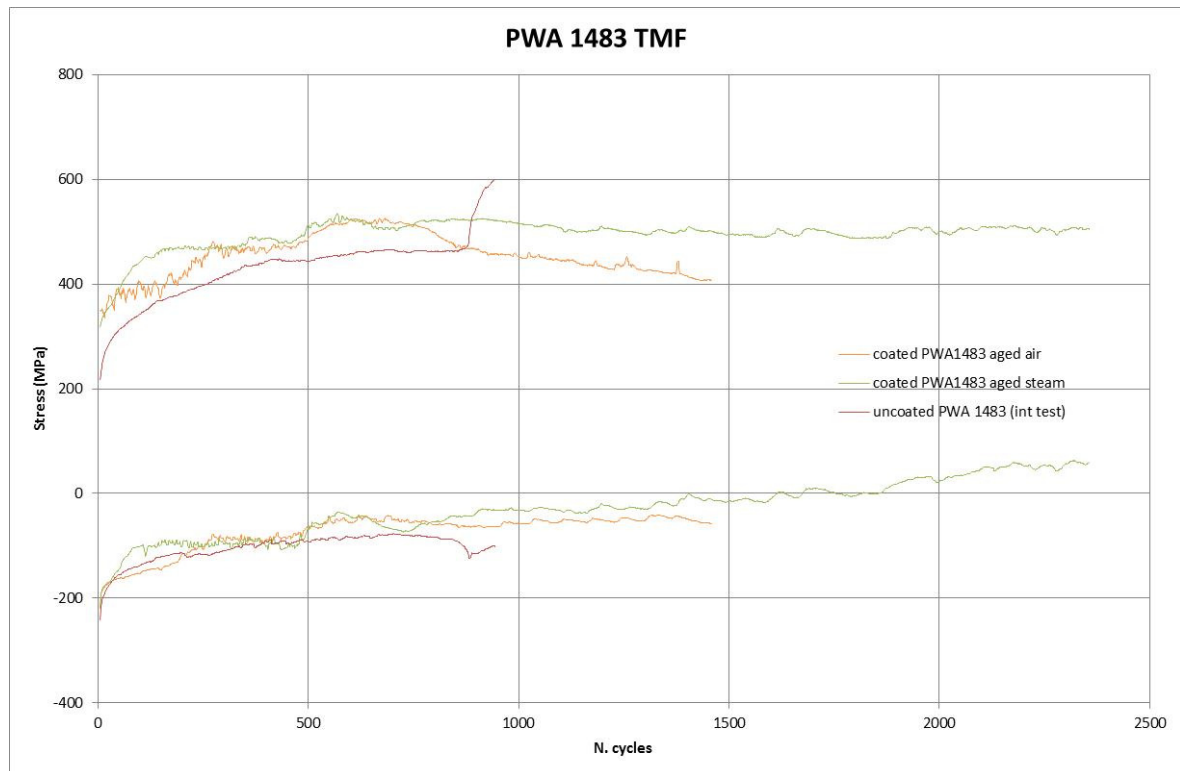
Figure 180 - Summary of TMF tests on PWA 1483 performed with an OP mechanical strain -0.4 %

The summary of all the tests performed with the same thermal cycle and out of phase different mechanical strains is presented in Figure 181 and gives evidence of the higher resistance for the single crystal alloy (PWA1483) compared to the cast one (Rene 80).
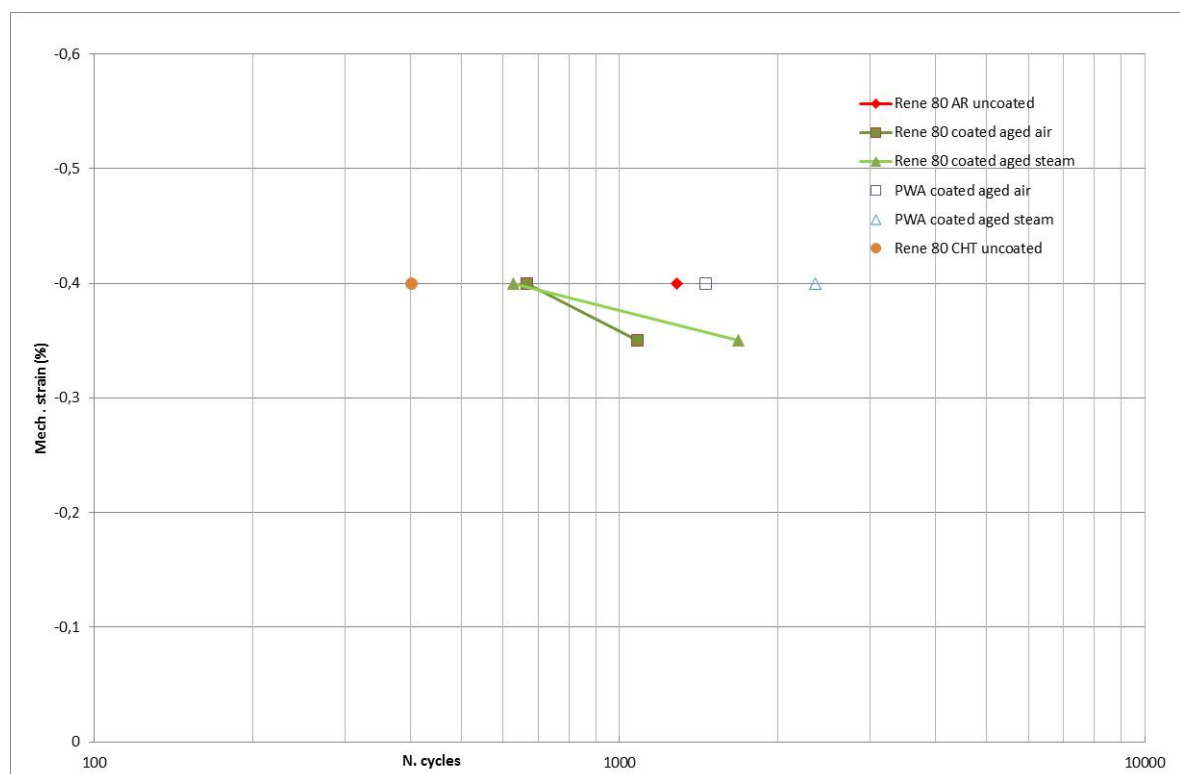

Figure 181 – Summary of TMF life as function of applied OP mechanical strain with the same thermal cycle

The results of image analysis for detection of first cracks appearing in the gauge length of coated specimens, showed that the first detected crack is not always the responsible for the final failure. First cracks in gauge length can be detected generally after 20-30 % of spent life and in some cases only after the half-life; no correlation can be observed on first crack to end of life ratio with pre-ageing conditions or combined out of phase mechanical strain (see Table O).

Table O – TMF summary data for coated specimens (first crack and end of life)

Material	Pre-ageing	N_i	N_f	N_i/N_f	N_i	N_f	N_i/N_f
Coated Rene 80	Air	250	665	0.38	570	1079	0.53
	Steam	350	627	0.56	480	1685	0.28
Coated PWA 1483	Air	350	1458	0.24			
	Steam	820	2357	0.35			
OP ε_m (%)		0.40			0.35		

4.2 Creep

The literature data on René 80 are fit the most accurately in the Larson Miller Model with N=4. C is calculated for the model and is found to be 13.75 which is low compared to the value of 20 which is commonly used for Ni-base superalloy.

The state of initial microstructure of the René 80 base material determines the creep strength of the material. The microstructural analyses of the "As Received" material showed that the microstructure is not conform with the microstructure as found in a blade, therefore the absolute values of the creep tests of the uncoated samples cannot be used as such.

Negative creep is observed on some uncoated As-Received René 80 samples when tested at 1050°C. During the creep tests at 1050°C, the initial microstructure with star-shaped gamma prime seems to evolve towards a cubic gamma prime with the formation of secondary gamma prime. The extensometer measures a shrinkage of the test samples.

Relatively seen, there is little influence observed of ageing in air of uncoated as received René 80 when tested at 950°C. At 1050°C, the steam ageing compared to the air ageing has a negative influence on the creep strength of the material. This can be due to the higher oxidation rate. Ageing in steam lowers the time to rupture for the applied stresses.

The creep curves of René 80 + SC2464 + TBC show an identical behaviour for the samples pre-aged in air and in air + 20% steam. The secondary creep rate of the samples without pre-aging is lower as for the aged samples.

The difference in initial microstructure between the uncoated and coated samples make it also impossible to quantitatively compare the coated with uncoated samples. No cracks were observed in the SC2464 or in the TBC that could possibly lead to preliminary crack initiation & premature failure of the coated samples.

It is recommended to study further the stability of René 80, in fully heat treated condition, at 1050°C in order to check the long term properties of René 80 when exposed to temperatures of 1050°C.

As far as concern the application of small punch tests for determination of creep properties of Rene 80, activity performed show the necessity to consider a reduced k_{SP} factor in the empirical correlation proposed by CEN Code of Practice compared to previously characterized nickel alloys. This reduced factor allows to define creep trend curve reasonably acceptable for

material characterization with limited quantity of material available. The relevant tendency of Rene 80 to have a γ′ depletion on the external surface under exposure at temperatures as high as those used for ageing and or testing suggests to restrict however the application of small size technique to the temperatures lower than 1000 °C.

5 Reference list

Ref 1. ASM Specialty Handbook, Heat resistant materials; DAVIS J.R.; p 243

Ref 2. Creep Life Prediction of Thermally Exposed Rene 80 Superalloy; M. Aghaie-Khafri and S. Farahany; Journal of Materials Engineering and Performance; Volume 19(7) October 2010—1065; JMEPEG (2010) 19:1065–1070 - DOI: 10.1007/s11665-009-9584-6".

Ref 3. Microstructure evolution and its influence on deformation mechanisms during high temperature creep of a nickel base superalloy - J. Safari, S. Nategh / Materials Science and Engineering A 499 (2009) 445–453

Ref 4. Life prediction of Ni-base superalloy - Bull. Mater. Sci., Vol. 34, No. 2, April 2011, pp. 305–309. c Indian Academy of Sciences.

Ref 5. Creep Rupture in a Nickel-Based Superalloy - T.K. KIM, JIN YU, and J.Y. JEON; METALLURGICAL TRANSACTIONS A; VOLUME 23A, SEPTEMBER 1992—2581

Ref 6. Siemens test data provided by Werner Stamm